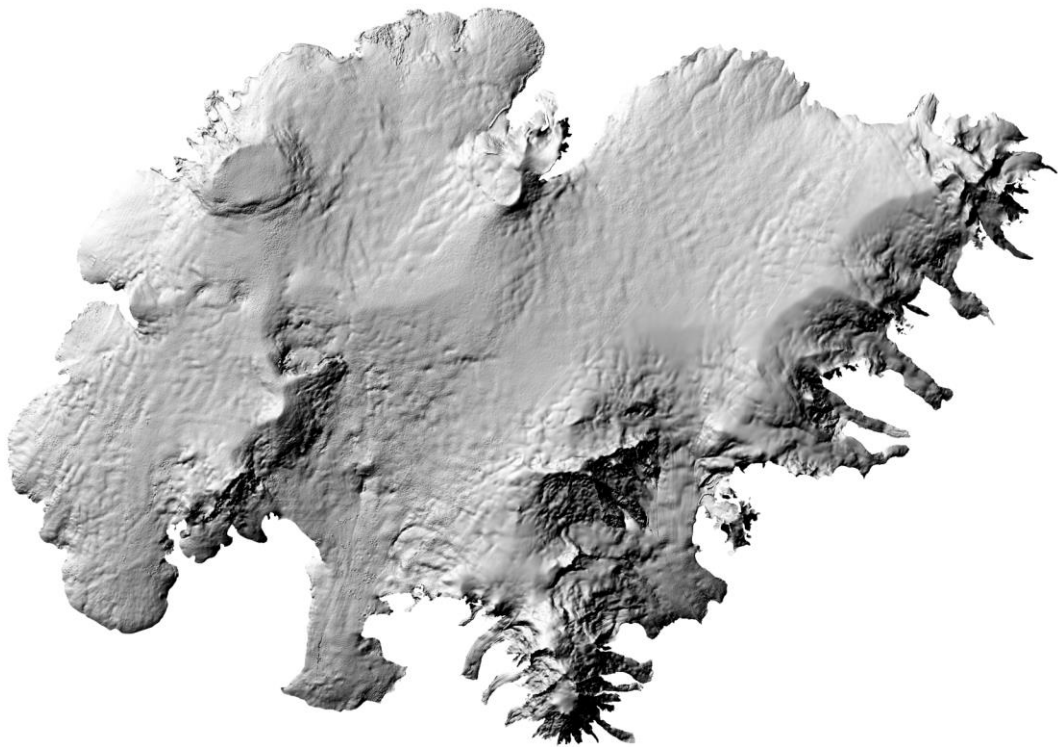


VATNAJÖKULL:
Mass balance, meltwater drainage
and surface velocity of
the glacial year 2016_17



Institute of Earth Sciences
University of Iceland
and
National Power Company

Finnur Pálsson
Andri Gunnarsson
Ágúst Þór Gunnlaugsson
Gestur Jónsson
Hlynur Skagfjörð Pálsson
Sveinbjörn Steinþórsson
Þorsteinn Jónsson

RH-07-2017

Contents:

1. Introduction	2
2. Diary	2
3. Mass balance measurements	3
3.1 Methods	3
3.2 Results of mass balance measurements	4
3.2.1. Tungnaárjökull	9
3.2.2. Köldukvíslarjökull	9
3.2.3. Dyngjujökull	10
3.2.4. Brúarjökull	11
3.2.5. Eyjabakkajökull	12
3.2.6. Breiðamerkurjökull	12
3.2.7. Síðujökull	13
3.2.8. Grímsvötn	14
3.3. The mass balance record for Vatnajökull	14
4. Surface velocity measurements	17
5. Melt water runoff	18
6. Conclusions	20
Figures:	
Figure 1. Outlets of Vatnajökull and location of mass balance sites in 2016_17.	4
Figure 2. Maps showing point values of specific in m water equivalent (m_{we}), 2016_17.	5
Figure 3. a. Specific mass balance (m_{we}), along all mass balance profiles 2016_17. b. Specific mass balance as a function of elevation on central flow lines on Vatnajökull outlets.	6
Figure 4. Specific mass balance of Vatnajökull (m_{we}) 2016_17. Top: winter, Centre: summer Bottom: net balance.	7
Figure 5. Top left: The difference between winter balance in 2016_17 and the average winter balance 1995_96 to 2015_16. Top right: The difference between summer balance in 2017 and the average summer balance 1996 to 2015. Lower left: The difference between net balance in 2016_17 and the average net balance 1995_96 to 2015_16.	8
Figure 6. Mass balance at a central flow line on Tungnaárjökull 2016_17, and average mass balance 1991_92 to 2015_16.	9
Figure 7. Specific mass balance at a central flow line on Köldukvíslarjökull 2016_17, and average mass balance 1991_92 to 2015_16.	9
Figure 8. Mass balance at a central flow line on Dyngjujökull 2016_17, and average mass balance 1992_93 to 2015_16.	10
Figure 9. Mass balance at two flow lines on Brúarjökull 2016_17, and average mass balance 1992_93 to 2015_16.	11
Figure 10. Mass balance at a central flow line on Eyjabakkajökull 2016_17, and average mass balance 1995_96 to 2015_16.	12
Figure 11. Mass balance at a central flow line on Breiðamerkurjökull 2016_17, and average mass balance 1995_96 to 2015_16.	12
Figure 12. Mass balance at a central flow line on Síðujökull 2016_17, and average mass balance 2004_05 to 2015_16.	13
Figure 13. Mass balance at a central flow line towards Grímsvötn 2016_17, and average mass balance 1991_92 to 2015_16.	13
Figure 14. Specific mass balance record of Vatnajökull 1991_92 – 2016_17.	14
Figure 15. Cumulative specific mass balance of Vatnajökull 1991_92 – 2016_17.	14
Figure 16. Specific mass balance for Vatnajökull outlets 1991_92 – 2016_17.	15
Figure 17. Cumulative specific mass balance of Vatnajökull outlets 1991_92 – 2016_17.	16
Figure 18. The relation between net annual balance (b_n) and accumulation area ratio (AAR) and b_n and equilibrium line altitude (ELA), for Vatnajökull outlets during the survey period.	16
Figure 19. Average surface velocity at survey sites in 2016_17.	17
Figure 20. Water divides and drainage basins of selected rivers draining water from Vatnajökull.	18
Figure 21. The temporal variation of the average annual meltwater runoff to selected river catchments.	18
Tables:	
Table I. Melt water drainage to selected rivers.	19
Appendixes:	
Appendix A: Mass balance at survey sites 2016_17.	21
Appendix B: Balance distribution by elevation in 2016_17.	23
Appendix C: Coordinates at velocity measurement sites, and overview of surface elevation profiles.	31
Appendix D: Measured surface velocity on Vatnajökull in 2016_17.	35
Appendix E: Melt water runoff to selected rivers in summer 2017 derived from summer ablation.	37
Appendix F: MODIS satellite images of Vatnajökull and vicinity 2016_17.	48

1. INTRODUCTION

In 1992 (glacial year 1991_92) a program of mass balance measurements was started for Vatnajökull by the Science Institute University of Iceland (now Institute of Earth Sciences, IES) in collaboration with the National Power Company (NPC). For the first year the program was limited to the western part of the glacier, but then expanded to include the northern outlets as well. In 1996 this study was further expanded to include southern outlets, with support from The European Union (Framework IV - Environment and Climate, TEMBA project 1996-1997). This program was extended 1998–2000 with further support from EU (Framework IV - Environment and Climate, ICEMASS project, 1998-2000). In 2000-2002 NPC and IES continued the program. In 2003-2005 IES participated in a multinational research project, which was financially supported by The European Union (EVK2-CT-2002-00152 SPICE). IES was responsible for obtaining data sets for calibration of models of the mass balance and dynamics of Vatnajökull. This work was also supported by The National Power Company of Iceland and The National Road Authority, and is a continuation of the TEMBA-project of 1996-97 and ICEMASS project 1998-2001.

In 2016_2017 IES and NPC continued a similar program. Mass balance measurements on the southeast outlets Breiðamerkurjökull and Hoffellsjökull is financially supported by the National Road Authority.

The aim of the collaborative work of NPC and IES is to improve our understanding of the mass balance and melt water runoff from glaciers. This work in combination with energy balance measurements by NPC and IES on Vatnajökull will be used for calibration of models of the energy and mass balance of Vatnajökull.

This report describes the field measurements, GPS survey, mass balance and melt water runoff for the glacial year 2016_17.

2. DIARY

Mars 2 - 3: installation of melt wires, maintenance of AWSs on Breiðamerkurjökull

May 3 - 7: measurements of the winter balance

June 4-9: measurements of the winter balance.

October 24 – 29: summer balance measurements, maintenance of AWSs on Breiðamerkurjökull.

December 14-15: summer balance measurements at lowest sites on Brúarjökull, maintenance of AWSs on Tungnaárjökull and Brúarjökull.

In all expeditions and short visits to the glacier the locations of mass balance stakes were measured with Kinematic GPS (or fast static GPS and a few with DGPS) for surface velocity calculation.

The following members of staff of the Institute of Earth Sciences, University of Iceland, carried out the fieldwork on Vatnajökull: Finnur Pálsson, Þorsteinn Jónsson, Sveinbjörn Steinþórsson and Ágúst Þór Gunnlaugsson also Andri Gunnarsson, Gestur Jónsson and Helgi Karl Guðmundsson (National Power Company) and Hlynur Skagfjörð Pálsson (Reykjavík Rescue Team).

Members of the Iceland Glaciological Society assisted in the June fieldwork.

3. MASS BALANCE MEASUREMENTS

The purpose of the mass balance measurements is to describe the temporal and spatial distribution of the components of the mass balance. The mean annual values of the components and their variation from year to year are analyzed and related to meteorological conditions and climatic variability. The results will be used in studies of changes in the glacier volume, estimates of meltwater contribution to glacial rivers, mass balance modeling, evaluation of altitudinal and regional variations of mass balance in response to climatic variations, and to assess the hydrometeorological and dynamic response of the ice cap to climate change.

The mass balance was determined by a stratigraphic method, measuring changes in thickness and density relative to the summer surface. The winter balance was estimated by drilling ice cores through the winter layer in the spring. Ablation was monitored from markers; snow stakes were put up on the glacier and wires were drilled down in the ablation area. The summer balance was measured in the autumn.

3.1 Methods

Measurements of the surface mass balance on a large ice cap like Vatnajökull are impractical in terms of cost with conventional techniques and sampling density that are typically used on small glaciers. The spatial variability of the mass balance may, however, be predictable on the flat large outlets of such an ice cap given data on several profiles extending over the elevation range of the glacier. The precipitation generally increases with elevation and decreases with the distance from the coast, but both the distribution of snowfall and

redistribution of snow by drift depend on the prevailing wind direction during the winter. The summer melting depends mainly on the altitude and the albedo of the glacier surface. Therefore, we have used observations along a limited number of flowlines, which span the elevation range of the outlets to assess aerial estimates of surface mass balance. Each profile describes the variation with elevation, but together they also describe the lateral variation of the mass balance. Recently, modern over-snow vehicles and helicopters have allowed fast traverses to ensure successful fieldwork in spite of frequently poor weather conditions. The error for individual point measurement is estimate $\sim 30 \text{ cm}_{\text{we}}$ for both summer and winter balance. The error for the area integral of mass balance is however considered smaller, since the error for individual survey sites is independent.

The winter mass balance (b_w) is defined as the mass of snow accumulated during the winter months, the summer balance (b_s) is the mass balance during the summer, and the net balance (b_n) is defined as their sum. The specific mass balance is expressed in terms of the equivalent thickness of water. All mass balance components apply to a time interval between given measurement dates, which are not fixed from one year to another. The dates in the autumn are separated by approximately one calendar year, which roughly coincides with the glaciological year defined as October 1st to September 30th. Snow cores are drilled in April-May through the winter layer and profiles of the density are measured. The summer balance is derived in the autumn from measurements of the changes in the snow core density during the summer in the accumulation area and from readings at stakes and wires drilled into the ice in the ablation areas.

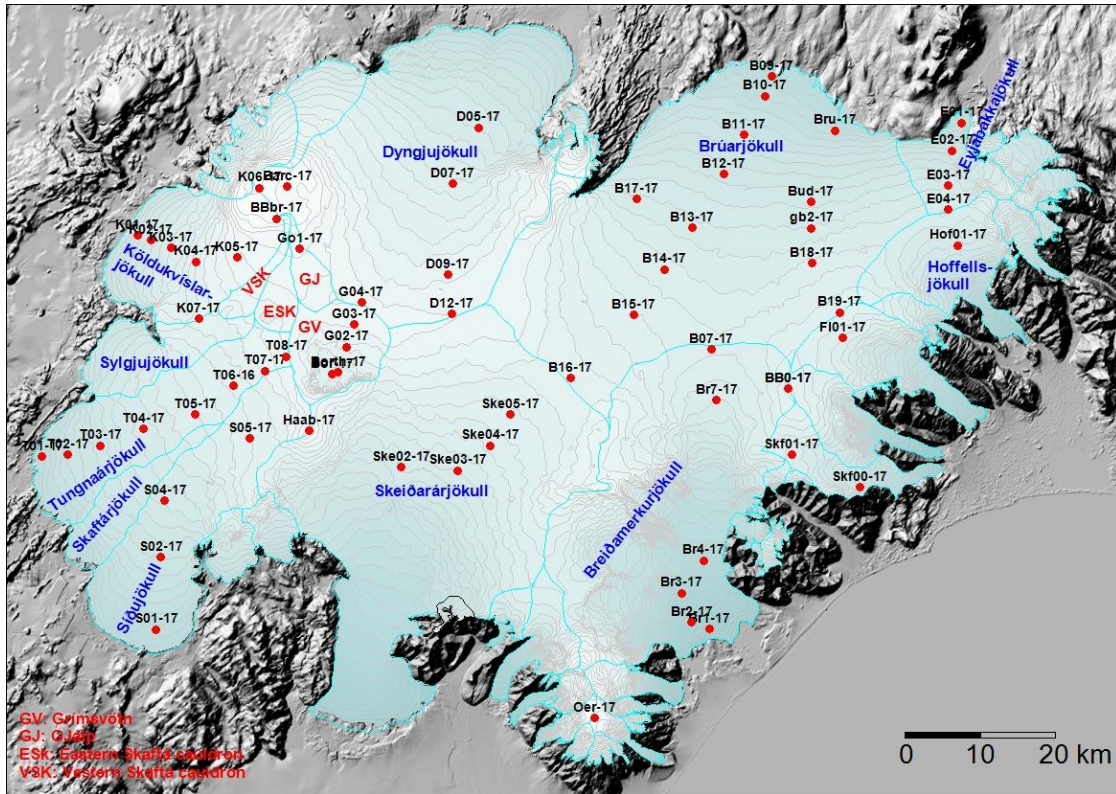


Figure 1. Outlets of Vatnajökull and location of mass balance survey sites 2016_17.

Digital maps are created for winter, summer and net balance for the whole ice cap based on site measurements. The mass balance is calculated over both the ice and water drainage basins. The summer balance over the water basin is an estimate of meltwater contribution to rivers and groundwater storage. This estimate, however, does not include precipitation that falls as rain on the glacier or snow, which falls and melts during the summer. The meltwater contribution is compared with river runoff at stream flow gauges closest to the glacier. For this comparison, we define the glaciological year from the start of October to the end of September and the period draining meltwater from the glacier during the summer from June through September. It would be misleading to include May in the summer period because runoff from the glacier melt in May is delayed due to refreezing during elimination of the cold wave.

3. 2 Results of mass balance measurements.

Mass balance measurements were done at 67 sites in spring 2017 (Fig. 1). The specific mass balance at individual sites is shown in Fig. 2. Most sites are on central flow lines at individual outlets. The specific mass balance along approximate flow lines is given in Fig 3. for the glacier outlets: Sýðujökull, Tungnaárjökull, Köldukvíslarjökull, Dyngjujökull, Brúarjökull (west and east), Eyjabakkajökull, Hoffellsjökull and Breiðamerkurjökull.

Digital maps for winter, summer and net balance are shown in Figure 4. Although no balance measurements are available for Skeiðarárjökull, the balance has been estimated by interpolating the balance values from the neighboring outlets, based on our experience from previous years. The mass balance of individual outlet is discussed in the following subsections.

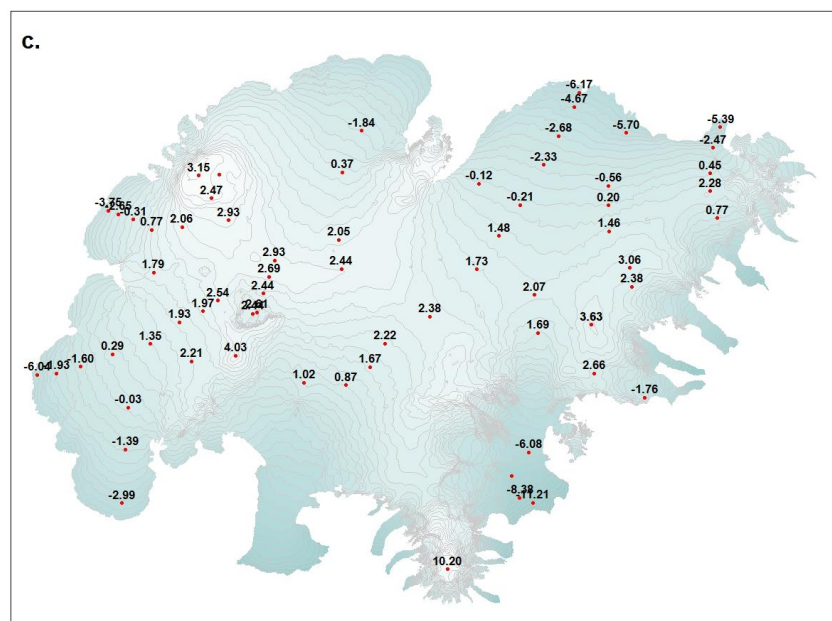
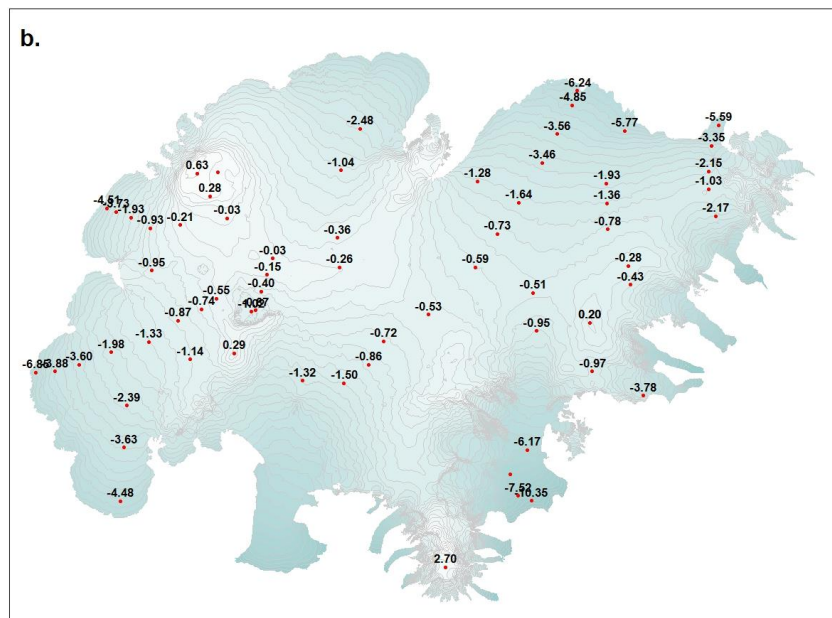
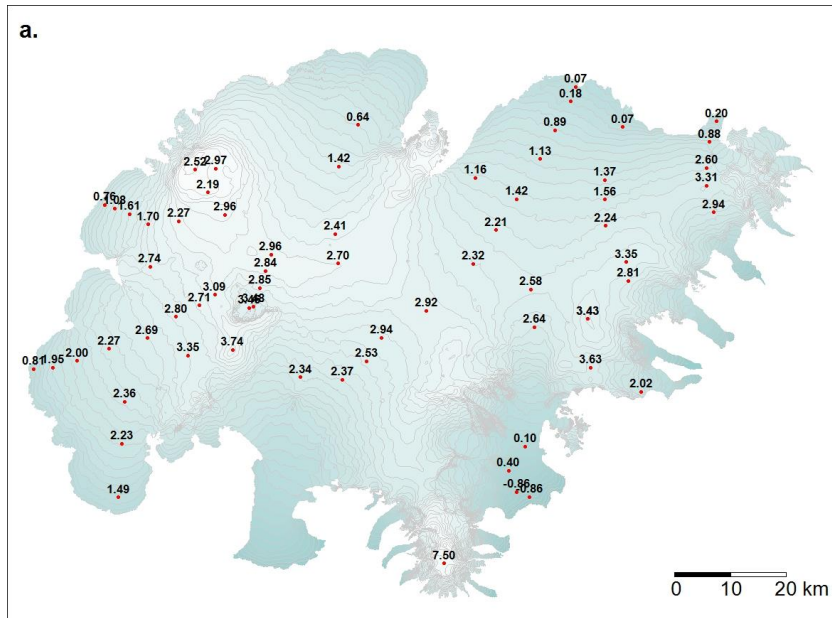


Figure 2. Maps showing point values of specific mass balance in m water equivalent (m_{we}), 2016_17. a. winter, b. summer, c. net balance.

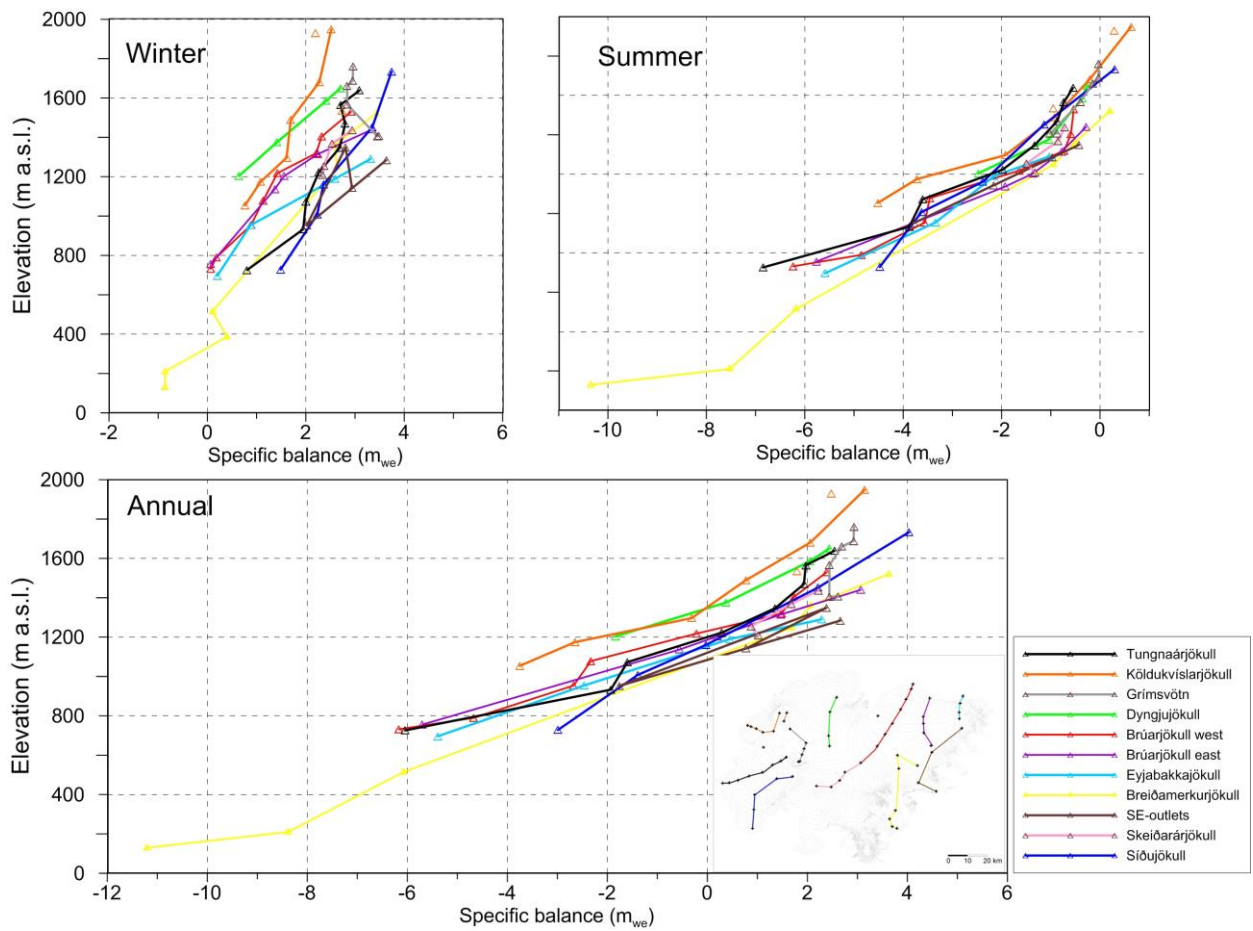


Figure 3. a. Specific mass balance (m_{we}), along all mass balance profiles 2016_17.

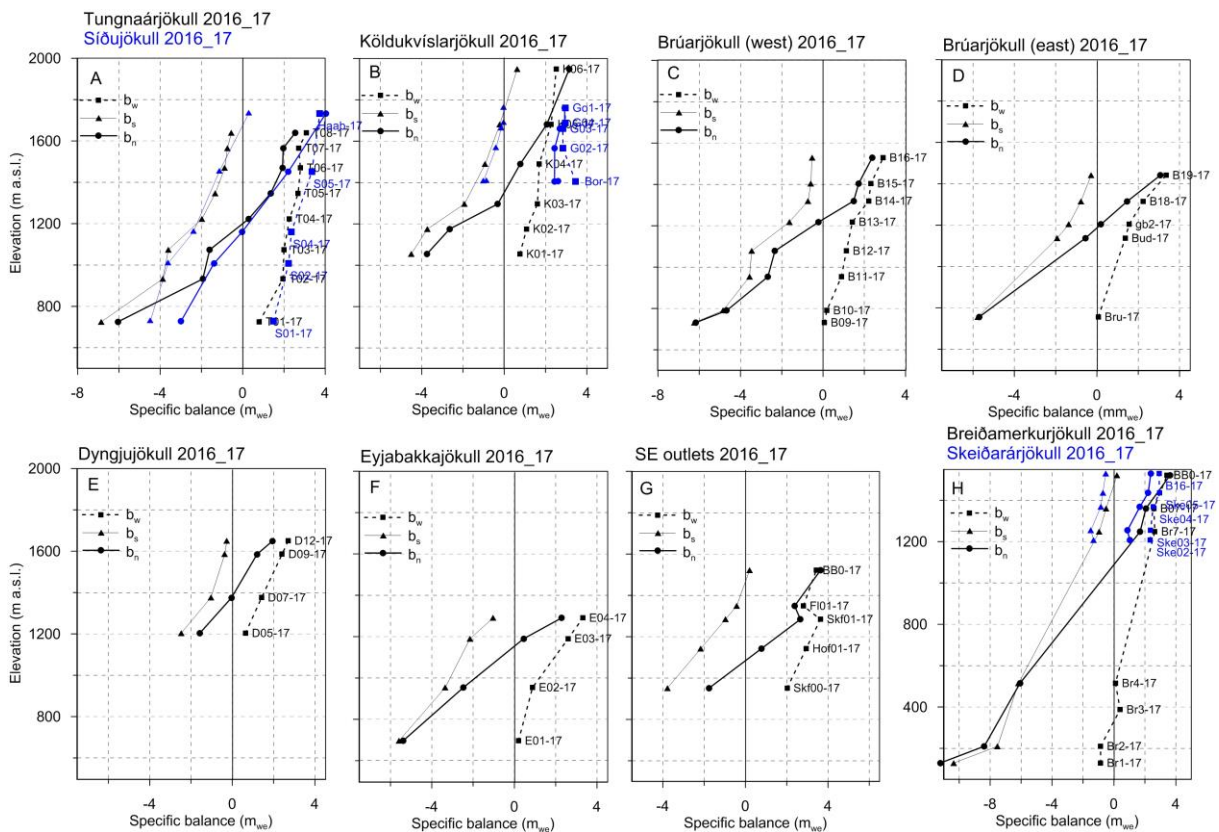


Figure 3b. Specific mass balance (m_{we}) 2016_17 as a function of elevation on central flow lines on Vatnajökull outlets.

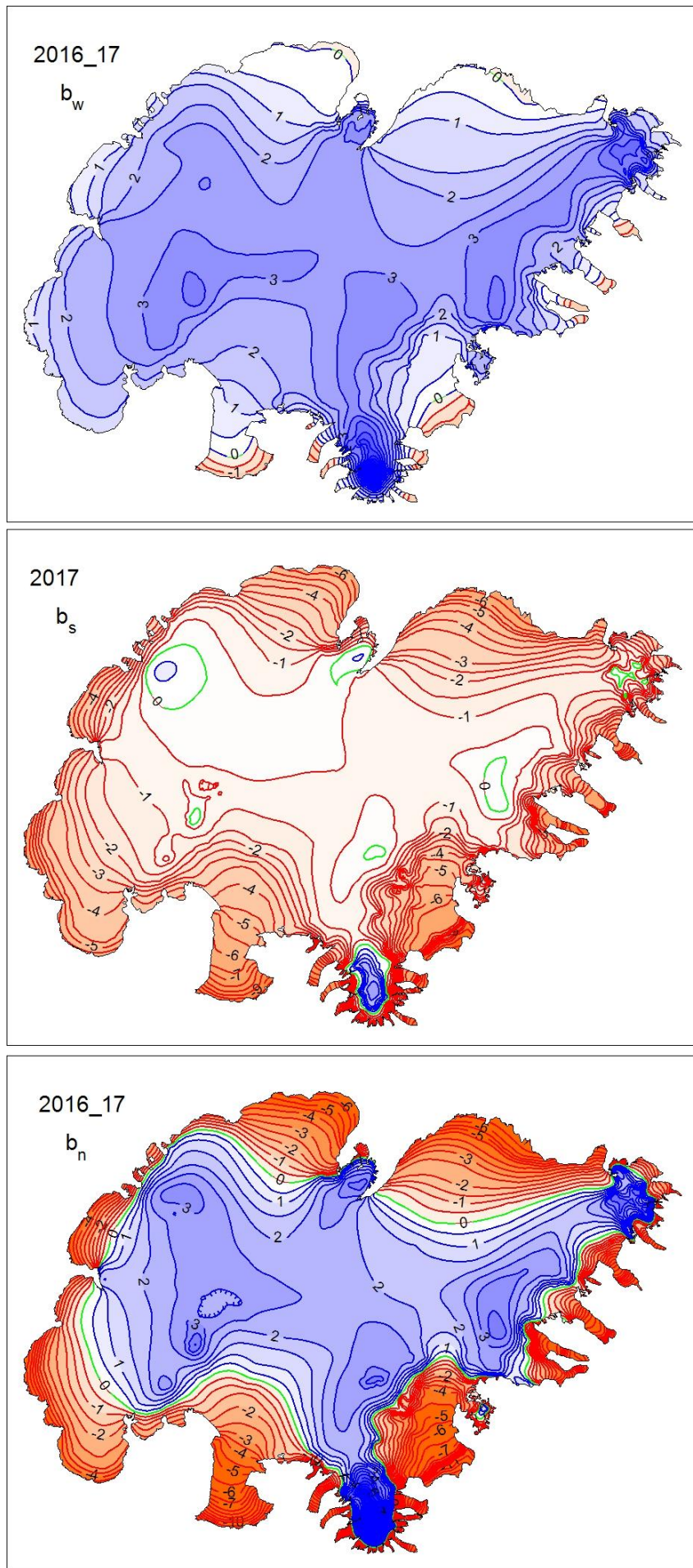


Figure 4. Specific mass balance (m_{we}) maps of Vatnajökull 2016_17. Top: winter, Centre: summer, Bottom: net balance.

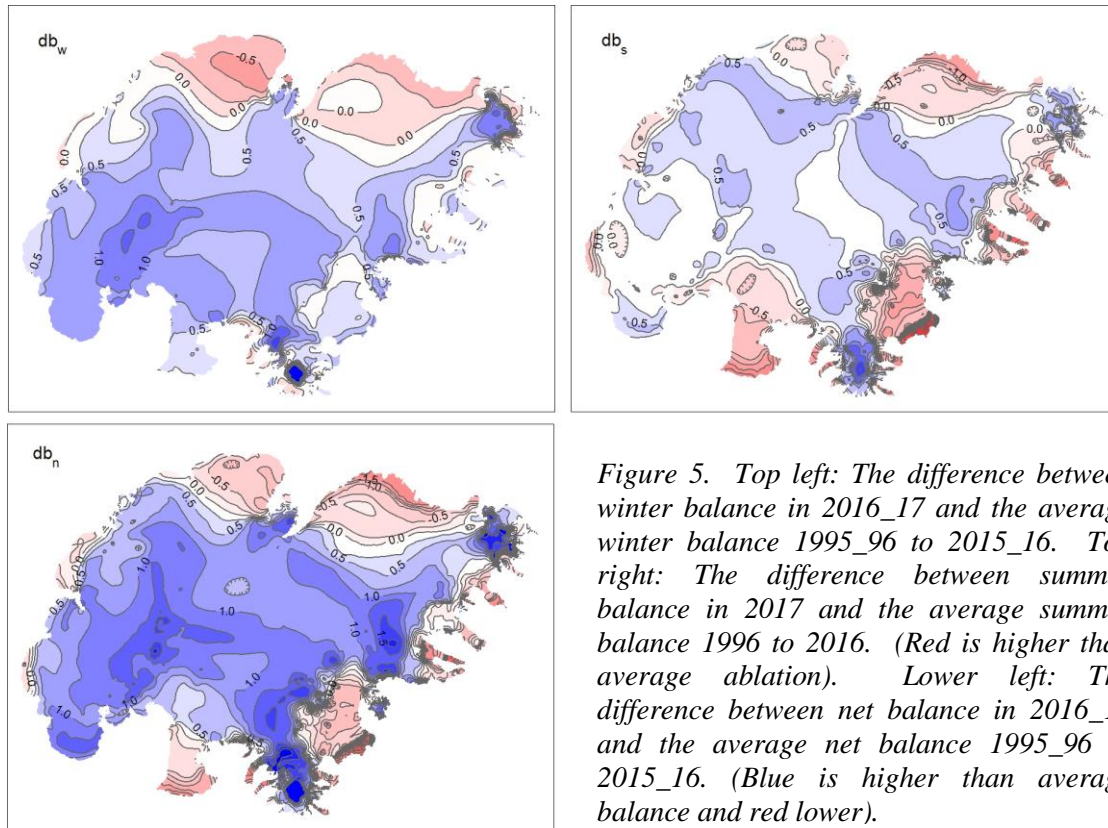


Figure 5. Top left: The difference between winter balance in 2016_17 and the average winter balance 1995_96 to 2015_16. Top right: The difference between summer balance in 2017 and the average summer balance 1996 to 2016. (Red is higher than average ablation). Lower left: The difference between net balance in 2016_17 and the average net balance 1995_96 to 2015_16. (Blue is higher than average balance and red lower).

A surface DEM is needed for surface area distribution and delineation of ice divides for individual outlets and catchments. A new surface DEM was created of Vatnajökull for this work. The DEM is mostly based on SPOT5 satellite images in 2010, and partly from LiDAR survey 2010, -11 and -12 (Jóhannesson et al. 2013), but the large GPS profile set measured in spring 2015 was used to locally shift the older DEMs. This new DEM representing the surface of 2015 was used in all area distributions, but ice and water divides were not reworked.

The weather in the autumn and first winter months, 2016-17, was extremely wet but warm, not much snow below ~1000 m. The latter half winter into, especially February and May were also warm with more than average precipitation. The spring was relatively cold but dry.

Figure 5 (top left) shows that the winter accumulation is by far over average at all the accumulation zone, higher than average in the SW but less than average in the north. Winter

melting at the low lying S outlets was more than average.

First summer months were calm and mostly dry, but cloudy in the SE over Vatnajökull. The last week of July and well into August were extremely as was the autumn. Melting at lower ablation zone extended well into October and even November. This resulted in total melt more than average melt in the ablation zone but less than average in the accumulation zone, where cold and cloudy first summer and occasional snow fall reduced the melt.

SPOT 5 HRG images were made available by the French Space Agency (CNES) through the ISIS (Incentive for the Scientific use of Images from the SPOT system) program and SPOT 5 HRS digital elevation models by the Spot Image project Planet Action (www.planet-action.org) and the SPIRIT SPOT 5 stereoscopic survey of Polar Ice.

Jóhannesson, T., Björnsson, H., Magnússon, E., Guðmundsson, S., Pálsson, F., Sigurðsson, O., Thorsteinsson, T., and Berthier, E.:

Ice-volume changes, bias estimation of mass-balance measurements and changes in subglacial lakes derived by lidar mapping of the surface Icelandic glaciers, *Ann. Glaciol.*, 54, 63–74, doi:10.3189/2013AoG63A422, 2013.

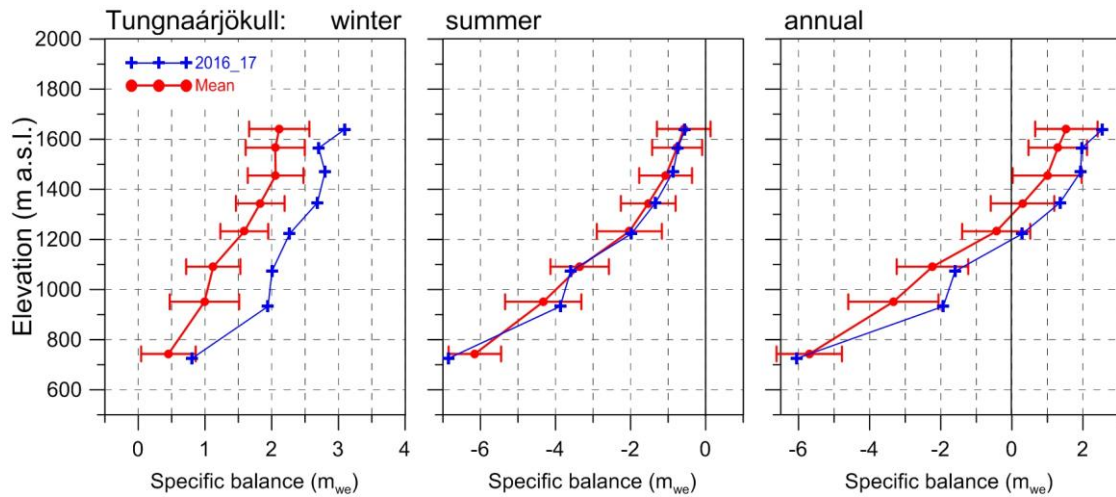


Figure 6. Mass balance at a central flow line of Tungnaárjökull 2016_17 and average mass balance 1991_92 to 2014_15.

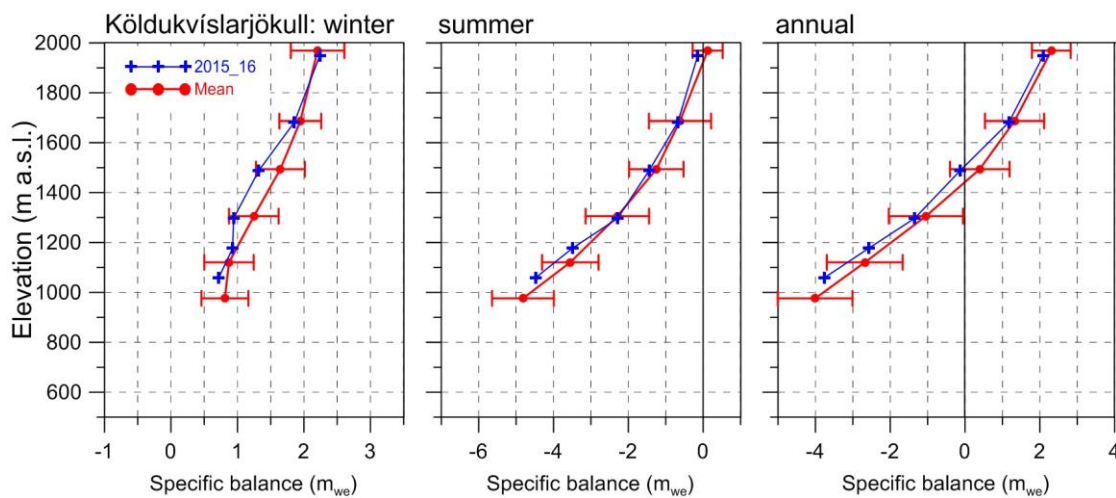


Figure 7. Mass balance at a central flow line of Köldukvíslarjökull 2016_17 and average mass balance 1991_92 to 2014_15.

3.2.1 Tungnaárjökull.

Area = 340 km²

$B_w = 0,74 \text{ km}^3_{we}$; $b_w = 2,17 \text{ m}_{we}$

$B_s = -0,89 \text{ km}^3_{we}$; $b_s = -2,62 \text{ m}_{we}$

$B_n = -0,15 \text{ km}^3_{we}$; $b_n = -1,45 \text{ m}_{we}$

ELA = 1200 m a.s.l. (at profile)

AAR = 53 %

(The terms are defined at the foot of this page)

Variation of mass balance along a central flow line on Tungnaárjökull is shown in Fig. 6. The winter accumulation far over average at all survey sites, by ~1 to 2 std. The total winter balance was 44% over average. Summer melting was also close to average at all survey sites. The summer balance was 1% less negative than the average during the survey period. The

net balance was more negative, but only 40% of the average of the survey period. This is the 23 year out of the 26 surveyed with negative net balance.

3.2.2 Köldukvíslarjökull

Area = 298 km²

$B_w = 0,52 \text{ km}^3_{we}$; $b_w = 1,73 \text{ m}_{we}$

$B_s = -0,53 \text{ km}^3_{we}$; $b_s = -1,77 \text{ m}_{we}$

$B_n = -0,01 \text{ km}^3_{we}$; $b_n = -0,04 \text{ m}_{we}$

ELA = 1355 m a.s.l. (at profile)

AAR = 46 %

Variation of mass balance along a central flow line on Köldukvíslarjökull is shown in Fig. 7. Accumulation was close to average except at the mid elevation sites (K03 and K04) where it was ~1 std. more than average. The

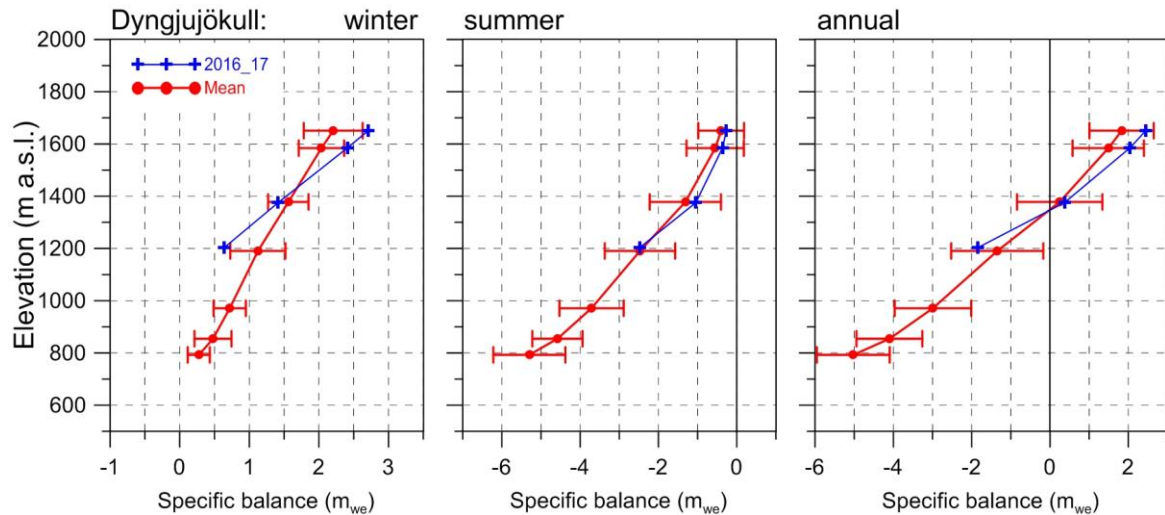


Figure 8. Mass balance at a central flow line on Dyngjufjökull 2016_17, and average mass balance 1991_92 to 2014_15 (except 1998_99 – 2003_04 at all but the top elevation).

total winter balance was about 17% over the average since 1991_92. Summer balance was almost average at all survey sites. In all, the summer balance was negative, by 91% of the average summer of the survey period. The net balance was almost zero, the mass loss only 1/10 of the average.

3.2.3 Dyngjufjökull

Area = 1059 km²

$B_w = 1,81 \text{ km}^3_{we}$; $b_w = 1,71 \text{ m}_{we}$

$B_s = -1,57 \text{ km}^3_{we}$; $b_s = -1,48 \text{ m}_{we}$

$B_n = 0,24 \text{ km}^3_{we}$; $b_n = 0,23 \text{ m}_{we}$

ELA = 1350 m a.s.l. (at profile)

AAR = 64 %

Variation of mass balance along a flow line on Dyngjufjökull is shown on Fig. 8. Mass balance is not measured at the lowest elevations, but assumed to be correlated (as a function of elevation) to that of Brúarjökull and Köldukvíslarjökull. Inspection of the winter Modis images shown in appendix F suggest that at the glacier snout snow cover was very thin, less than average below 1400 m but ~1 std. above average in the high accumulation zone. The total winter balance was 8% over the average.

Summer balance was very close to average at all survey sites. The summer balance was negative, at 92% of an average summer. The net balance was positive, now 0,23 m_{we} while the average is slightly negative (-0,03 m_{we}).

Dyngjufjökull has often has had mass balance close to zero, and the net balance has been slightly positive in some years of the two decade period of continuous mass loss for Vatnajökull as a whole.

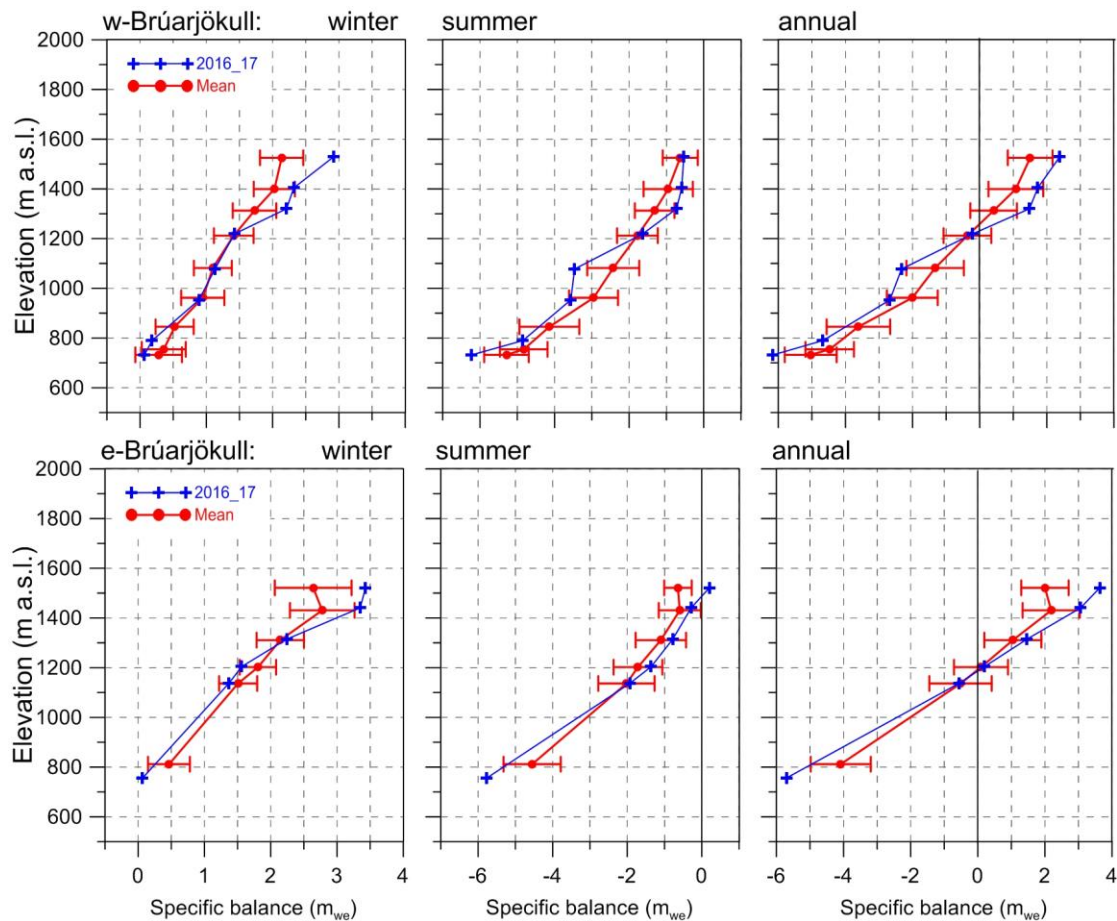


Figure 9. Mass balance at two flow lines on Brúarjökull 2016_17, and average mass balance 1992_93 to 2014_15.

3.2.4 Brúarjökull

Area = 1524 km²
 $B_w = 2,74 \text{ km}^3_{we}$; $b_w = 1,80 \text{ m}_{we}$
 $B_s = -2,70 \text{ km}^3_{we}$; $b_s = -1,77 \text{ m}_{we}$
 $B_n = 0,39 \text{ km}^3_{we}$; $b_n = 0,03 \text{ m}_{we}$
 ELA = 1230 m a.s.l. (western flow line)
 ELA = 1200 m a.s.l. (eastern flow line)
 AAR = 61 %

Variation of mass balance along two flow lines on Brúarjökull is shown on Fig. 9. Accumulation was close to average at mid elevations survey sties, over 1 std. over average at the highest sites (on Breiðabunga) and less than 1 std. at the lowest sites. The winter balance was about 13% higher than average since 1992_93. Summer balance (melt) was less than average in the mid accumulation zone and the upper eastern sites, but more than

average melt occurred at the lowest sites. On Breiðabunga (Sites B19 and BB0) more snow collected than melted during the summer. The summer balance was negative by 94% of an average summer of the survey period. The net balance was by far more positive than average at the highest sites, but by far more negative than average in the ablation zone. In total the net balance was positive, 0.33 m we higher than the average.

During the survey period, there have been 7 years of positive balance but 18 years with negative balance.

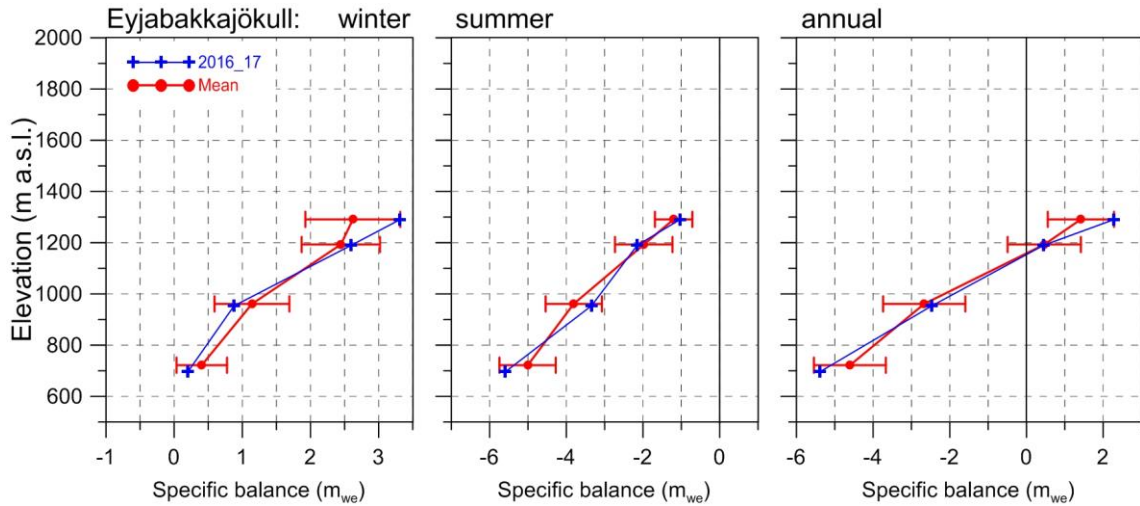


Figure 10. Mass balance at a central flow line of Eyjabakkajökull 2016_17 and average mass balance 1995_96 to 2014_15.

3.2.5 Eyjabakkajökull

Area = 112 km²
 $B_w = 0,22 \text{ km}^3_{we}$; $b_w = 2,00 \text{ m}_{we}$
 $B_s = -0,27 \text{ km}^3_{we}$; $b_s = -2,50 \text{ m}_{we}$
 $B_n = -0,05 \text{ km}^3_{we}$; $b_n = -0,50 \text{ m}_{we}$
 ELA = 1155 m a.s.l. (at profile)
 AAR = 44 %

Variation of mass balance along a central flow line on Eyjabakkajökull is shown on Fig. 10. Accumulation was close average at the lower sites, but 1 std. more than average at the top site, reflecting cold latter half of winter. The total winter balance 2016_17 was ~10% over the average 1995_96 to 2014_15. Summer melting was not far from average at all survey sites. There was slight mass loss at the upper sites

but as expect the unusually thick snow on the snout resulted in net balance less negative than average (91%). In total the net balance was at average.

3.2.6 Breiðamerkurjökull

Area = 936 km²
 $B_w = 1,94 \text{ km}^3_{we}$; $b_w = 2,07 \text{ m}_{we}$
 $B_s = -2,45 \text{ km}^3_{we}$; $b_s = -2,61 \text{ m}_{we}$
 $B_n = -0,51 \text{ km}^3_{we}$; $b_n = -0,54 \text{ m}_{we}$
 ELA = 1095 m a.s.l. (at profile)
 AAR = 58 %

Variation of mass balance along a central flow line on Breiðamerkurjökull is shown on Fig. 11. Winter accumulation was well over average at the survey sites in the accumulation zone.

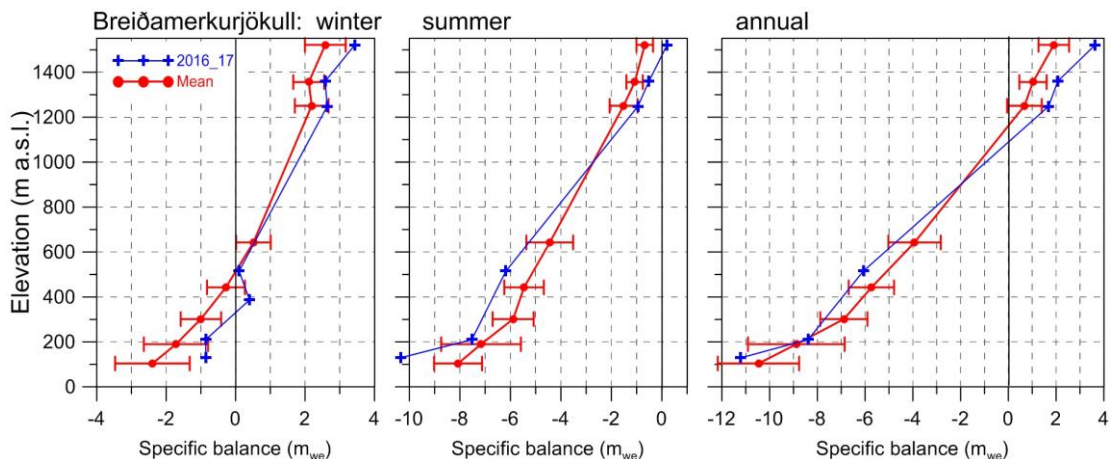


Figure 11. Mass balance at a central flow line of Breiðamerkurjökull 2016_17, and average mass balance 1995_96 to 2014_15.

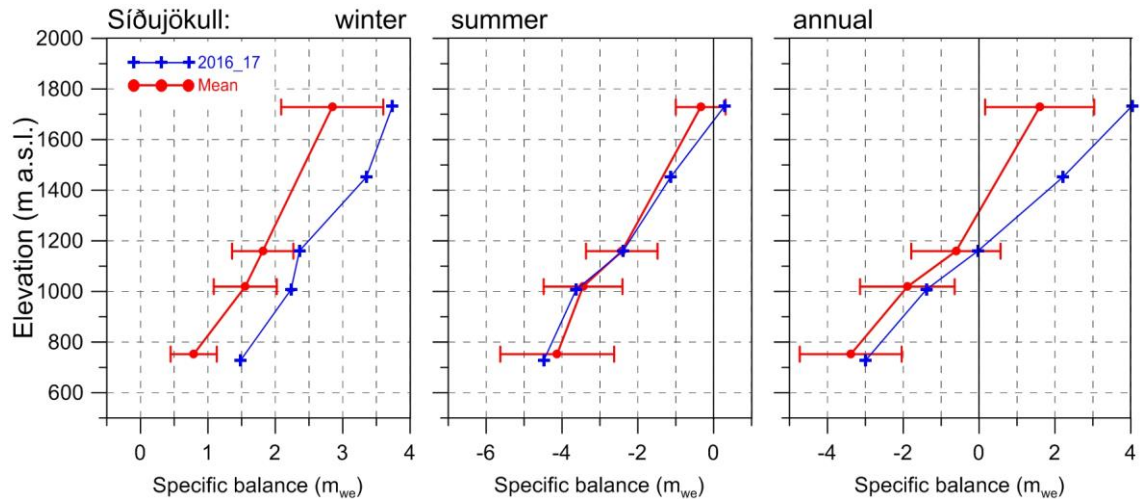


Figure 12. Mass balance at a central flow line of Síðujökull 2016_17 and average mass balance 2004_05 to 2014_15.

At the lowest sites about 1 std. less mass loss in winter. The total winter balance was ~41% over average. Summer mass loss was by far less than average at the tope sites, but by far more at the lowest sites. The total negative summer balance was only almost at average during the survey period. The net balance was about half that of an average year.

3.2.7 Síðujökull

Area = 423 km²
 $B_w = 1,03 \text{ km}^3_{we}; b_w = 2,43 \text{ m}_{we}$
 $B_s = -1,14 \text{ km}^3_{we}; b_s = -2,69 \text{ m}_{we}$
 $B_n = -0,11 \text{ km}^3_{we}; b_n = -0,27 \text{ m}_{we}$
 ELA = 1160 m a.s.l. (at profile)
 AAR = 49 %

Variation of mass balance along a central flow line on Síðujökull is shown on Fig. 12. Snow accumulation more than 1 std. over average at all sites, up to about 1.5 std. at the lowest site.

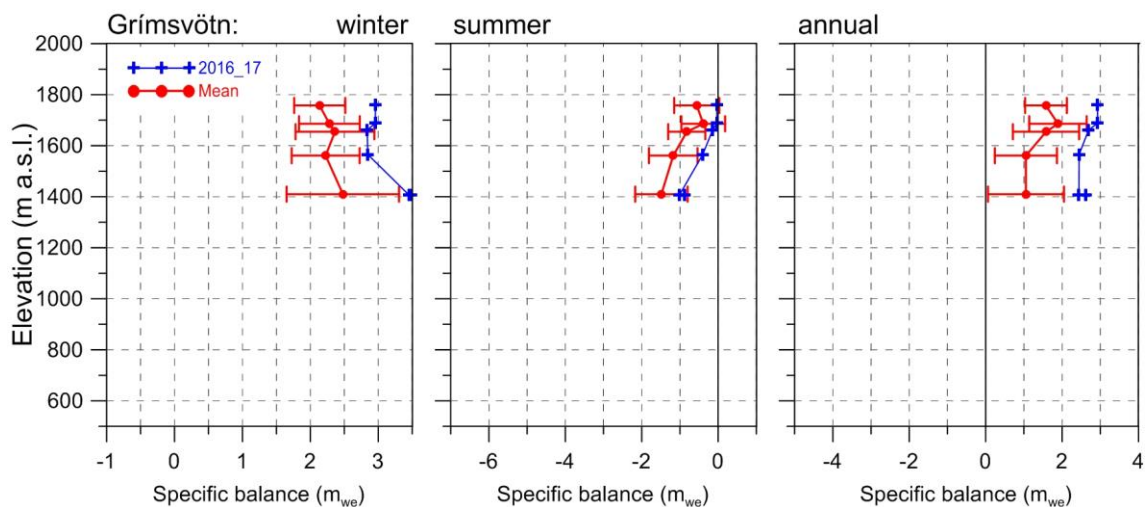


Figure 13. Mass balance at a central flow line towards Grímsvötn 2016_17 and average mass balance 1991_92 to 2014_15.

The total winter balance was 51% over the average (past decade). Summer balance was about average, except at the highest, where summer balance was positive. The total summer balance was negative by ~91% of the average during the survey period. The net balance negative but 1 m less so than in an average year of the survey period.

3.2.6 Grímsvötn-Gjálp

Area = 174 km²
 $B_w = 0,53 \text{ km}^3_{we}; b_w = 3,05 \text{ m}_{we}$
 $B_s = -0,07 \text{ km}^3_{we}; b_s = -0,39 \text{ m}_{we}$
 $B_n = 0,46 \text{ km}^3_{we}; b_n = 2,66 \text{ m}_{we}$

Variation of mass balance close to a central flow line from Bárðarbunga towards Grímsvötn center is shown in Fig. 13. Snow accumulation was ~1 std. over average at all survey sites. The total winter balance was ~30% over average. Summer balance negative at all sites, but ~1 Std. less than average. The net balance was highly positive, ~70% over the average of the survey period.

3.3 The mass balance record for Vatnajökull.

From the digital maps the total volumes of winter, summer and net balance for Vatnajökull (and selected outlets) have been calculated by integration (appendix D, gives balance values as a function of elevation) and are as follows:

$B_w = 16,45 \text{ km}^3_{we}; b_w = 2,07 \text{ m}_{we}$
 $B_s = -16,49 \text{ km}^3_{we}; b_s = -2,08 \text{ m}_{we}$
 $B_n = -0,04 \text{ km}^3_{we}; b_n = -0,01 \text{ m}_{we}$
AAR = 61%

The autumn of 2016 was wet and windy, followed by a winter colder than average this century. In winter the precipitation in NE and E Iceland was over average reflecting snowfall in

E, and NE wind directions. The spring weather was calm, and unusually dry. The total winter balance was 33% higher than average (over the observation period from 1991_92, Fig. 14). The zero mass balance turnover for Vatnajökull (current topography) is close to 13,5 km³_{we} (1,7 m_{we}) and the winter balance 2016_17 is ~22% higher.

In spite of a calm and dry summer in Iceland, on Vatnajökull most of the summer was cloudy, about 1/3 of the summer-days were close to cloud free (see Modis images in Appendix F). Latter half of September and first weeks of October were unusually

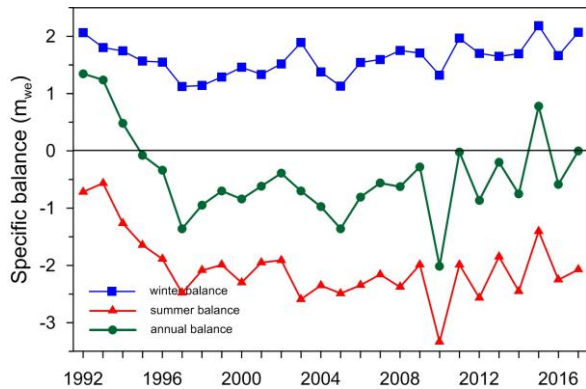


Figure 14. Specific mass balance record for Vatnajökull 1991_92 – 2016_17.

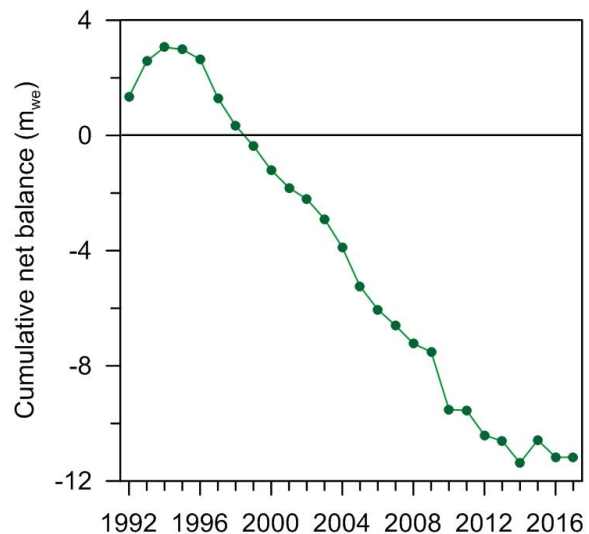


Figure 15. Cumulative specific mass balance of Vatnajökull 1991_92 – 2016_17.

favorable for ablation both warm and windy. The total summer balance was negative but only ~94% of the average since 1995. As mentioned above, zero mass balance turnover for Vatnajökull (current topography) is close to $13,5 \text{ km}^3_{\text{we}}$ ($1,7 \text{ m}_{\text{we}}$), the summer balance 2017 was $-16.49 \text{ km}^3_{\text{we}}$ or ~22 % more loss than the zero balance turnover. The net balance was only marginally negative this year. It has been negative since 1994_95 (except 2014_15).

However the ~20 year period of high mass seems to have halted, and currently Vatnajökull is close balance. For each of the 4 consecutive years of close to zero balance, the reasons vary. For this year the explanation is the extremely high winter balance, summer balance is not that far from average of the survey period.

The temporal variability of mass balance for different outlets is shown in Fig. 16. The greatest variability of

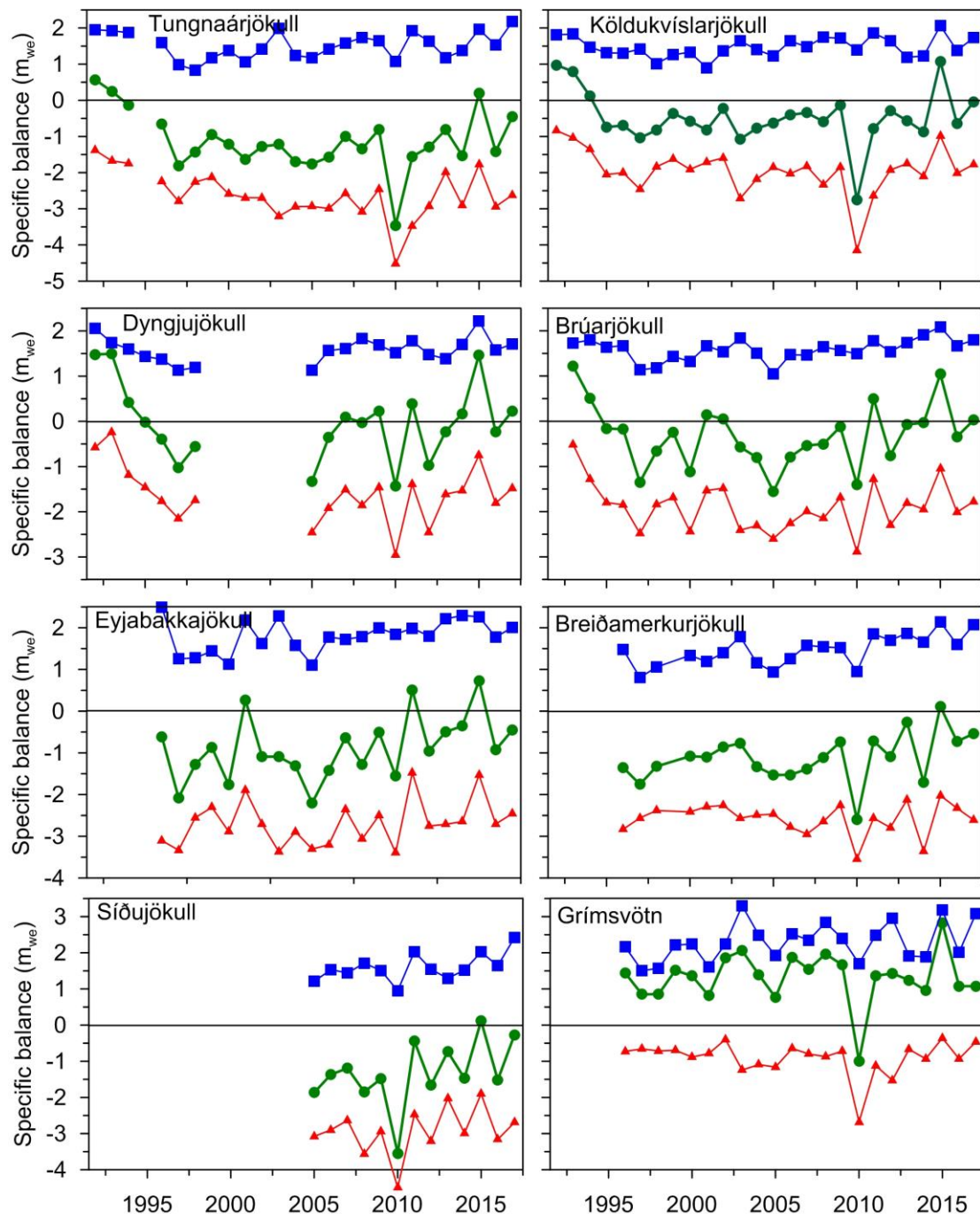


Figure 16. Specific mass balance record for Vatnajökull outlets 1991_92-2016_17.

the winter balance is for Eyjabakkajökull the eastern most of the studied outlets. This part of the glacier is receives precipitation from all south- and east- and north-easterly wind directions, and thus has high snow accumulation in winters when the paths of the North Atlantic lows are just east of Iceland. This is also the case for the eastern part of Brúarjökull. During the period of net mass loss since 1994_95, the northern outlets have had several years of close to zero and positive mass balance.

The cumulative net balance curves for the outlets of Vatnajökull in Fig. 17 show that all outlets have been losing mass since 1994_95. The slope for mass loss is about $0,7 \text{ m}_{\text{we}}\text{a}^{-1}$ for the northern outlets but $1,5 \text{ m}_{\text{we}}\text{a}^{-1}$ for the south and western outlets.

In Fig. 18 the relation of the annual net balance to the accumulation area ratio (AAR) and equilibrium line altitude (ELA) is shown for different outlets over the survey period. The b_n -AAR gradient is similar for all outlets, about $0,5 \text{ m}_{\text{we}}$ for 10% change in AAR. The zero-balance AAR varies for different outlets from about 60-65%, similar for all outlets except for the southern outlet Breiðamerkurjökull.

Breiðamerkurjökull is far from equi-

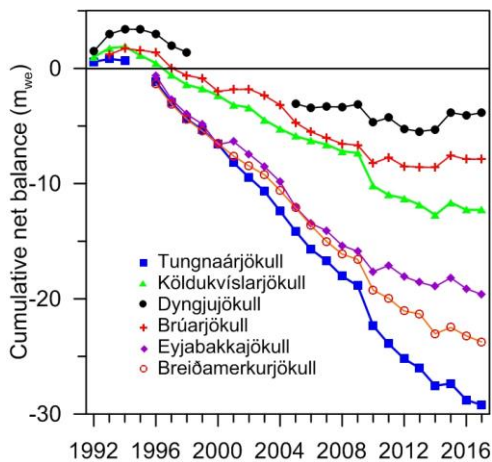


Figure 17. Cumulative specific mass balance for several of Vatnajökull outlets 1991_92 – 2015_17.

librium, the ablation area is too large. A large part of the glacier has carved 200-300 m through the former sediment bed, and the surface elevation has lowered accordingly. Breiðamerkurjökull is now retreating at a high rate.

Similarly the zero-balance ELA varies from about 1000-1100 m a.s.l. for the southern outlets to 1400 m a.s.l. for the NW outlets. The b_n -ELA slope is similar for all outlets $-0,7 \text{ m}_{\text{we}}$ per 100 m, except Eyjabakkajökull with a slope of -1 m_{we} per 100.

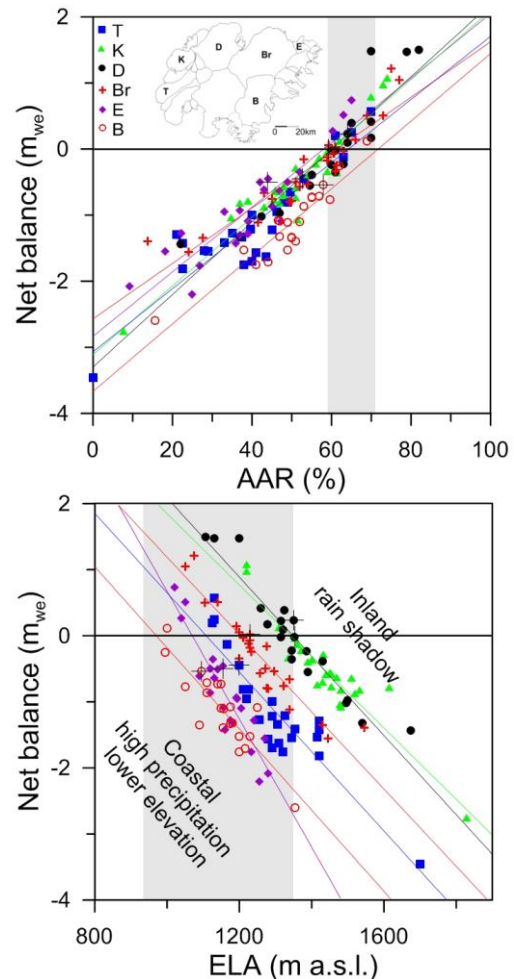


Figure 18. The relation between net annual balance (b_n) and accumulation area ratio (AAR)(upper) and b_n and equilibrium line altitude (ELA), for Vatnajökull outlets during the survey period. (This years points are marked with a black +).

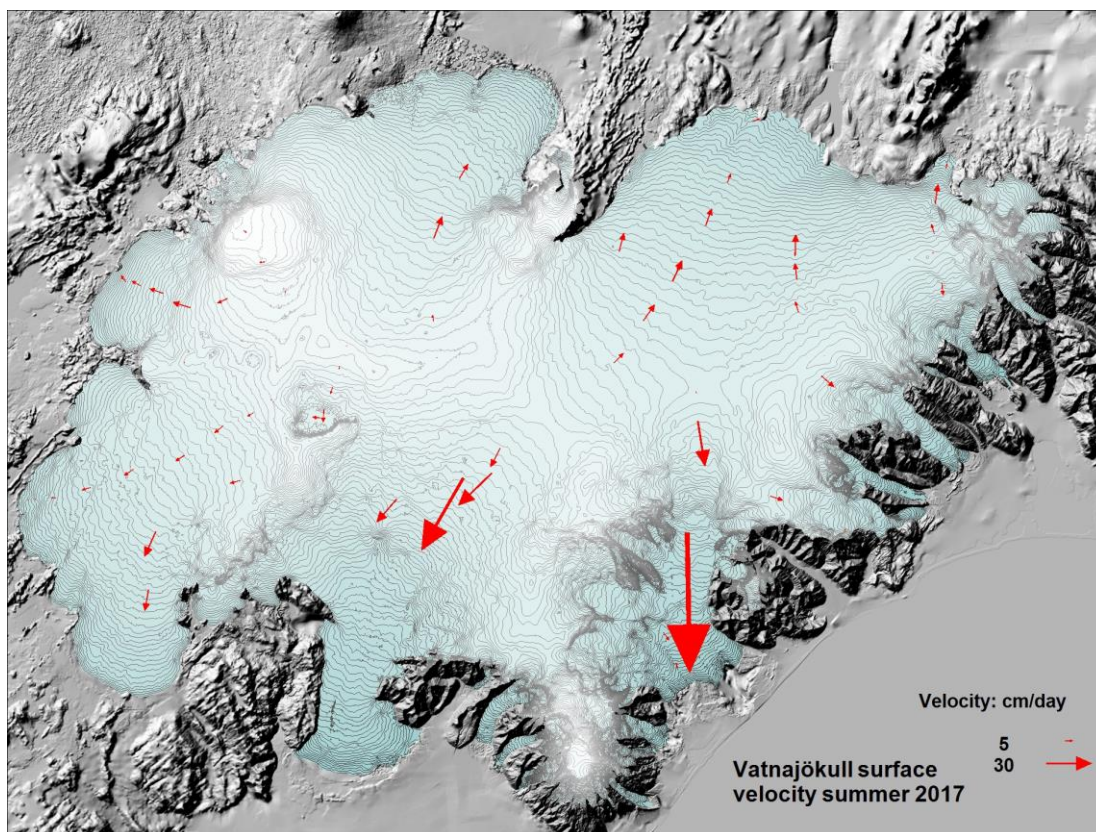


Figure 19. Average surface velocity at survey sites in 2016_17.

4. SURFACE VELOCITY MEASUREMENTS

The surface velocity of the glacier was calculated from DGPS (accuracy within 1 m), fast static (accuracy about 1 cm) and kinematic GPS (accuracy about 3 cm) positioning of the ablation stakes. All sites were surveyed in spring and autumn (most kinematic, some DGPS), and many also in June (kinematic), August (fast static) and October (kinematic). At a few sites stakes from previous years were found and resurveyed, making it possible to calculate surface velocity over a year or longer time span. The average summer surface velocity is shown on Figure 19.

At sites close to the glacier edge very small horizontal movement is measured. This indicates that the glacier snouts are almost stagnant. In the centre areas of some of the outlets

especially close to the equilibrium line, there is an increase in velocity during summer compared to winter. The summer velocity is of the order of two-fold the winter velocity. This suggests that basal sliding is increased in the melting season, and is of the same magnitude as the deformation velocity. To better understand this continuous GPS has been run during summer at several sites.

From previous velocity measurements, surging of outlets has been predicted. No signs of a starting surge are seen from this year's survey.

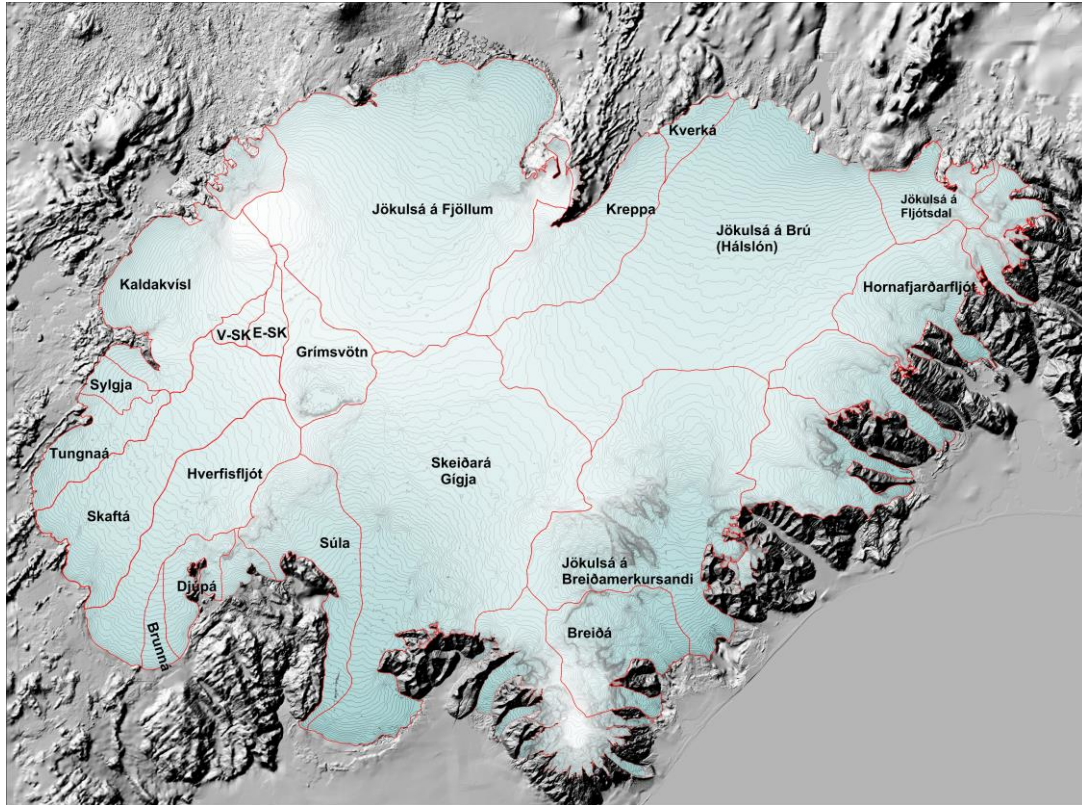


Figure 20. Water divides and drainage basins of selected rivers draining water from Vatnajökull.

5. Melt water runoff.

Water divides and drainage basins for rivers draining water from Vatnajökull have been defined from water pressure potential maps. The potential maps were produced from existing surface (year 2010) and bedrock digital elevation models.

Figure 20 shows the water divides and drainage areas for selected rivers draining melt water from Vatnajökull. The summer balance over the water basin is an estimate of meltwater contribution to rivers and groundwater storage. This estimate, however, does not include precipitation that falls as rain on the glacier, nor snow that falls and melts during the summer. The meltwater contribution can be compared with river runoff at stream flow gauges closest to the glacier. For this comparison, we define the glaciological year from the start of October to the end of September and the period draining meltwater from the

glacier during the summer from June through September. It would be misleading to include May in the summer period because runoff from

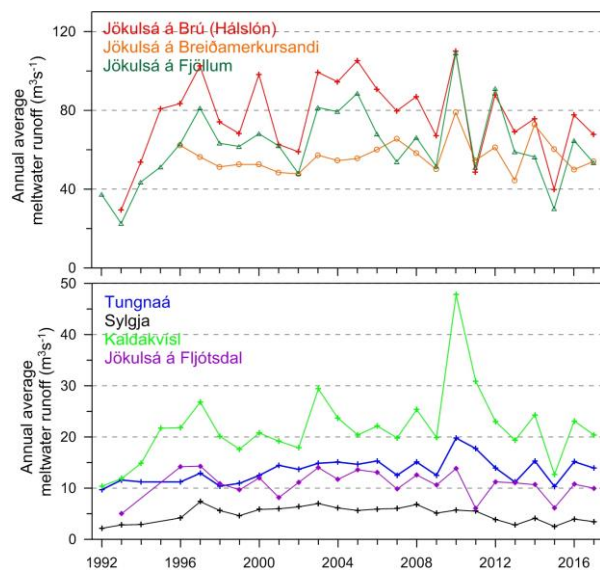


Figure 21. The temporal variation of average annual meltwater runoff to selected river catchments.

Table I. Melt water drainage to selected rivers.

Water Catchment:	Area (km ²)	ΣQ_s (10 ⁶ m ³)	Q_s (m ³ s ⁻¹)	Q_a (m ³ s ⁻¹)	q_s (ls ⁻¹ km ⁻²)
Vatnajökull	7890,0	16639,3	1578,6	527,6	66,9
Tungnaá	121,8	439,3	41,7	13,9	114,4
Sylgja	39,7	108,6	10,3	3,4	86,7
Kaldakvísl	367,9	643,5	61,0	20,4	55,5
Jokulsa a Fjöllum	1188,3	1685,0	159,9	53,4	45,0
Kreppa	291,2	365,4	34,7	11,6	39,8
Kverka	47,0	220,9	21,0	7,0	149,0
Jokulsa a Brú	1214,8	2136,6	202,7	67,8	55,8
Jökulsá á Fljótssdal	130,6	314,8	29,9	10,0	76,4
Jökulsá í Lóni	101,3	220,5	20,9	7,0	69,0
Hornafjarðarfjót	239,1	589,1	55,9	18,7	78,1
Jökulsá á Breiðamerkursandi	739,5	1703,6	161,6	54,0	73,1
Breiðá-Fjallsá	234,6	934,7	88,7	29,6	126,3
Skeiðará-Gígja	1165,2	2296,2	217,8	72,8	62,5
Súla	255,8	814,2	77,2	25,8	100,9
Brunná	35,8	155,8	14,8	4,9	138,0
Djúpá	83,7	276,6	26,2	8,8	104,8
Hverfisfjót	317,7	675,0	64,0	21,4	67,4
Skaftá	394,9	974,3	92,4	30,9	78,2
Grímsvötn	173,3	67,7	6,4	2,1	12,4
Eystri Skaftárketill	39,4	11,8	1,1	0,4	9,5
Vestari Skaftárketill	25,1	11,8	1,1	0,4	14,9
Hólmsá	164,9	403,4	38,3	12,8	77,6
Heinabergsvötn	229,6	623,0	59,1	19,8	86,1
Skjálfafljót	97,2	105,2	10,0	3,3	34,3

ΣQ_s : total summer melt water; Q_s : average runoff (averaged over summer, 4 months, June – September)
 Q_a : average runoff (averaged over a whole year); q_s : average runoff per km² (averaged over a whole year)

the glacier melt in May is delayed due to refreezing during elimination of the cold wave and because of the contribution of the spring melt from the highlands to the runoff. Some melting also occurs during winter, especially in the low snouts of the southern outlets.

Average melt water runoff to different rivers is given in Table I, and temporal variation of the average meltwater runoff in Fig. 21. The average specific runoff (q_s) differs from basin to basin from ~10 to 150 ls⁻¹km⁻². This is mainly due to different elevation distributions, for example, the water drainage basins for Tungnaá and Kverká are within the ablation area, while that of Grímsvötn and

Skaftárkatlar are high in the accumulation zone.

6. Conclusions

The weather in the autumn and first winter months, 2016-17, was extremely wet but warm, not much snow below ~1000 m. The latter half winter into, especially February and May were also warm with more than average precipitation. The spring was relatively cold but dry. Winter accumulation is by far over average at all the accumulation zone, higher than average in the SW but less than average in the north. Winter melting at the low lying S outlets was more than average.

First summer months were calm and mostly dry, but cloudy in the SE over Vatnajökull. The last week of July and well into August were extremely as was the autumn. Melting at lower ablation zone extended well into October and even November. This resulted in total melt more than average melt in the ablation zone but less than average in the accumulation zone, where cold and cloudy first summer and occasional snow fall reduced the melt.

The total winter balance was 33% higher than average (over the observation period from 1991_92.

The total summer balance was about 94% of the average since 1995. The net balance was negative as it has been since 1994_95 (except 2014_15), but now only marginally so.

The about 20 year period of high mass loss seems to have halted; the past few years have all had net balance close to zero, and there has been a positive trend in the net balance since about

2009, although with high variability.

This years close to zero balance is primarily explained by the extremely high winter balance, summer balance is not that far from the average of the survey period.

The total mass loss over the 26 year survey period is 11,2 m_{we} (ice volume of ~99 km³) since 1991_92 (or since 1994_95, 14,2 m_{we} (ice volume of 126 km³)). The volume loss since 1991_92 amounts to ~3% of total ice volume (~4% since 1994_95).

Glacier meltwater runoff in summer 2017 (estimated from summer balance only, summer rain and snow that falls and melts during summer is not included; averages refer to the survey period of each outlet): to Tungnaá 95% of the average, 92 % of the average to Kaldakvísl, 86% of the average to Jökulsá á Fjöllum, 95% of the average to Hálslón, 92% of average to Jökulsá í Fljótsdal and 97% of the average to Jökulsá á Breiðamerkursandi.

Mass balance summary 2016_17:

$$B_w = 16,45 \text{ km}^3_{we}$$

$$B_s = -16,49 \text{ km}^3_{we}$$

$$B_n = -0,04 \text{ km}^3_{we}$$

$$AAR = 61\%$$

Specific Values:

$$b_w = 2,07 \text{ m}_{we}$$

$$b_s = -2,08 \text{ m}_{we}$$

$$b_n = -0,01 \text{ m}_{we}$$

Appendix A: Mass balance at measurement sites 2016_17.

b_w : specific winter balance, b_s : specific summer balance, b_n : specific net balance,
 l_a : new snow in autumn (all in water equivalent).

Site	Position			Elevation (m a.s.l.)	Date in spring	Date in autumn	b_w (m)	b_s (m)	b_n (m)	l_a (m)	
	Latitude	Longitude									
B09-17	64	45,05	16	5,45	731,7	20170505	20171215	0,07	-6,235	-6,169	0,09
B10-17	64	43,69	16	6,70	789,8	20170505	20171215	0,18	-4,851	-4,671	0,07
B11-17	64	40,97	16	10,46	953,8	20170504	20171215	0,89	-3,563	-2,675	0,27
B12-17	64	38,27	16	14,13	1077,9	20170504	20171025	1,13	-3,461	-2,331	0,1
B13-17	64	34,53	16	19,70	1218,4	20170504	20171024	1,42	-1,637	-0,214	0,12
B14-17	64	31,64	16	24,70	1320,0	20170504	20171024	2,21	-0,728	1,482	0,12
B15-17	64	28,49	16	30,02	1404,1	20170504	20171024	2,32	-0,591	1,729	0,16
B16-17	64	24,13	16	40,85	1529,3	20170507	20171025	2,92	-0,534	2,384	0,28
B17-17	64	36,74	16	28,79	1214,5	20170504	20171024	1,16	-1,277	-0,115	0,12
Br1-17	64	5,84	16	19,72	129,2	20170424	20171029	-0,86	-10,350	-11,210	0
Br2-17	64	6,37	16	22,54	210,0	20170424	20171029	-0,86	-7,524	-8,384	0
Br3-17	64	8,48	16	24,06	387,1	20170501		0,40			
Br4-17	64	10,72	16	20,19	514,8	20170501	20171029	0,10	-6,175	-6,075	0
Br7-17	64	22,14	16	16,95	1248,1	20170503	20171024	2,64	-0,950	1,690	0,12
B07-17	64	25,80	16	17,45	1359,9	20170504	20171024	2,58	-0,513	2,067	0,19
BB0-17	64	22,71	16	5,05	1521,2	20170503	20171024	3,43	0,200	3,630	0,41
Bru-17	64	40,98	15	55,31	755,8	20170504	20171024	0,07	-5,767	-5,701	0
Bud-17	64	35,99	15	59,89	1137,2	20170505	20171024	1,37	-1,928	-0,558	0,13
gb2-17	64	34,10	16	0,01	1204,0	20170505	20171024	1,56	-1,360	0,200	0,14
B18-17	64	31,58	16	0,13	1314,8	20170505	20171024	2,24	-0,778	1,464	0,22
B19-17	64	27,99	15	55,98	1440,5	20170503	20171024	3,35	-0,284	3,064	0,39
BB0-17	64	22,71	16	5,05	1521,2	20170503	20171024	3,43	0,200	3,630	0,41
D05-17	64	42,23	16	54,67	1203,5	20170505	20171025	0,64	-2,476	-1,836	0,02
D07-17	64	38,28	16	59,26	1375,5	20170505	20171025	1,42	-1,043	0,372	0,28
D09-17	64	31,80	17	0,55	1585,4	20170505	20171025	2,41	-0,364	2,046	0,2
D12-17	64	28,98	17	0,15	1650,0	20170505	20171025	2,70	-0,264	2,440	0,29
E01-17	64	41,07	15	34,10	696,2	20170504	20171024	0,20	-5,591	-5,391	0
E02-17	64	39,13	15	35,98	953,9	20170504	20171024	0,88	-3,346	-2,468	0,04
E03-17	64	36,66	15	36,92	1189,8	20170504	20171024	2,60	-2,152	0,446	0,15
E04-17	64	34,95	15	37,11	1290,3	20170504	20171024	3,32	-1,032	2,283	0,16
K01-17	64	35,17	17	51,81	1054,1	20170506	20171026	0,76	-4,513	-3,751	0
K02-17	64	34,81	17	49,68	1174,9	20170506	20171026	1,08	-3,726	-2,646	0,04
K03-17	64	34,25	17	46,38	1296,6	20170506	20171026	1,61	-1,925	-0,315	0,01
K04-17	64	33,21	17	42,25	1488,8	20170506	20171026	1,70	-0,927	0,769	0,15
K05-17	64	33,45	17	35,44	1681,5	20170506	20171026	2,28	-0,213	2,062	0,18
K06-17	64	38,36	17	31,41	1948,8	20170608	20171025	2,52	0,630	3,147	0,51
K07-17	64	29,1124	17	42,013	1535	20170506	20171026	2,74	-0,948	1,790	0,2
S01-17	64	6,99966	17	49,965	728,4	20170506	20171026	1,49	-4,478	-2,990	0
S02-17	64	12,1628	17	48,959	1008	20170506	20171026	2,23	-3,625	-1,393	0,02
S04-17	64	16,1825	17	48,202	1161	20170506	20171026	2,36	-2,387	-0,027	0,05
S05-17	64	20,4949	17	34,002	1452	20170506	20171026	3,35	-1,137	2,213	0,3
Haab-17	64	20,96	17	24,12	1733,3	20170606	20171026	3,74	0,294	4,034	0,47

T01-17	64	19,4861	18	8,2297	725,8	20170506	20171026	0,81	-6,849	-6,043	0
T02-17	64	19,59	18	3,97	932,9	20170506	20171026	1,95	-3,876	-1,931	0
T03-17	64	20,21	17	58,60	1073,2	20170506	20171026	2,00	-3,602	-1,599	0,01
T04-17	64	21,33	17	51,50	1222,9	20170506	20171026	2,27	-1,978	0,290	0,13
T05-17	64	22,27	17	42,98	1346,6	20170506	20171026	2,69	-1,332	1,355	0,12
T06-17	64	24,27	17	36,52	1469,2	20170506	20171026	2,80	-0,870	1,930	0,21
T07-17	64	25,29	17	31,20	1565,1	20170505	20171025	2,71	-0,738	1,967	0,27
T08-17	64	26,29	17	27,76	1638,6	20170505	20171025	3,09	-0,548	2,542	0,33
Borth-17	64	25,06	17	19,17	1407,2	20170505	20171027	3,48	-0,870	2,610	
Bor-17	64	24,94	17	20,16	1405,3	20170605	20171025	3,46	-1,017	2,439	0,15
G02-17	64	26,85	17	17,73	1565,9	20170605	20171025	2,85	-0,403	2,443	0,19
G03-17	64	28,45	17	16,35	1660,2	20170605	20171025	2,84	-0,149	2,689	0,25
G04-17	64	30,01	17	15,00	1688,8	20170605	20171025	2,96	-0,030	2,925	0,18
Go1-17	64	33,97	17	24,96	1760,6	20170608	20171025	2,96	-0,030	2,930	0,3
Hof01-17	64	32,33	15	35,84	1142,8	20170504	20171025	2,94	-2,165	0,775	0,11
FI01-17	64	26,16	15	55,62	1348,9	20170503	20171024	2,81	-0,429	2,380	0,26
Skf00-17	64	15,46	15	54,06	951,8	20170503	20171024	2,02	-3,784	-1,764	0,1
Skf01-17	64	18,00	16	5,00	1284,5	20170503	20171024	3,63	-0,973	2,661	0,23
Barc-17	64	38,41	17	26,78	1887,5	20170608		2,97			
BBbr-17	64	36,14	17	28,69	1928,6	20170608	20171025	2,19	0,282	2,472	0,35
Ske02-17	64	18,16	17	9,18	1207,7	20170606	20171025	2,34	-1,317	1,023	0,08
Ske03-17	64	17,80	17	0,00	1254,2	20170507	20171025	2,37	-1,496	0,874	0,06
Ske04-17	64	19,50	16	54,50	1367,9	20170507	20171025	2,53	-0,856	1,674	0,11
Ske05-17	64	21,70	16	51,01	1436,4	20170507	20171025	2,94	-0,720	2,216	0,15

Appendix B: Balance distribution by elevation in 2016_17.

ΔS : area in elevation range, $\Sigma\Delta S$: cumulative area above given elevation, b_w : specific winter balance, b_s : specific summer balance. b_n : specific winter balance, ΔB_w : winter balance at a given elevation range, $\Sigma\Delta B_w$: cumulative winter balance above given elevation, ΔB_s summer balance at a given elevation range, $\Sigma\Delta B_s$: cumulative summer balance above given elevation, ΔB_n : net annual balance in a given elevation range, ΣB_n : cumulative net annual balance above given elevation.

Vatnajökull

Elevation (m a.s.l.)			ΔS (km^2)	$\Sigma\Delta S$ (km^2)	b_w (mm)	b_s (mm)	b_n (mm)	ΔB_w ($10^6 m^3$)	$\Sigma\Delta B_w$ ($10^6 m^3$)	ΔB_s ($10^6 m^3$)	$\Sigma\Delta B_s$ ($10^6 m^3$)	ΔB_n ($10^6 m^3$)	ΣB_n ($10^6 m^3$)
2000	2050	2025	0,4	0,4	5847	2321	8169	2,6	2,6	1,0	1,0	3,7	3,7
1950	2000	1975	8,8	9,2	3042	830	3873	26,7	29,3	7,3	8,3	33,9	37,6
1900	1950	1925	36,6	45,8	2681	579	3261	98,0	127,3	21,2	29,5	119,2	156,8
1850	1900	1875	47,4	93,2	3182	572	3754	150,9	278,3	27,1	56,7	178,1	334,9
1800	1850	1825	47,0	140,2	3669	694	4364	172,3	450,6	32,6	89,3	205,0	539,9
1750	1800	1775	54,5	194,7	3175	298	3473	173,2	623,8	16,3	105,6	189,5	729,4
1700	1750	1725	104,3	299,0	2946	9	2955	307,4	931,2	1,0	106,6	308,4	1037,7
1650	1700	1675	222,4	521,4	2937	-178	2758	653,3	1584,5	-39,7	66,8	613,5	1651,3
1600	1650	1625	373,0	894,4	2881	-322	2559	1074,7	2659,2	-120,2	-53,4	954,5	2605,8
1550	1600	1575	353,6	1248,0	2855	-431	2424	1009,8	3668,9	-152,4	-205,8	857,4	3463,1
1500	1550	1525	420,6	1668,6	2830	-548	2281	1190,3	4859,2	-230,7	-436,5	959,6	4422,8
1450	1500	1475	453,2	2121,8	2786	-622	2163	1262,8	6122,0	-282,1	-718,6	980,6	5403,4
1400	1450	1425	503,8	2625,6	2732	-639	2092	1376,5	7498,5	-322,2	-1040,8	1054,2	6457,6
1350	1400	1375	548,7	3174,3	2625	-737	1887	1440,7	8939,1	-404,8	-1445,6	1035,9	7493,6
1300	1350	1325	540,9	3715,2	2510	-946	1563	1357,7	10296,8	-511,8	-1957,4	845,9	8339,4
1250	1300	1275	512,0	4227,2	2337	-1239	1097	1197,1	11493,9	-634,9	-2592,3	562,2	8901,6
1200	1250	1225	453,3	4680,5	2088	-1632	456	946,7	12440,6	-739,8	-3332,1	206,9	9108,5
1150	1200	1175	403,5	5084,0	1868	-2058	-189	753,9	13194,5	-830,6	-4162,7	-76,6	9031,8
1100	1150	1125	362,5	5446,5	1752	-2481	-728	635,3	13829,9	-899,5	-5062,2	-264,2	8767,7
1050	1100	1075	323,6	5770,1	1648	-2890	-1242	533,5	14363,4	-935,4	-5997,6	-401,9	8365,7
1000	1050	1025	301,1	6071,2	1524	-3236	-1712	459,0	14822,3	-974,5	-6972,1	-515,5	7850,2
950	1000	975	270,8	6342,0	1401	-3552	-2150	379,6	15201,9	-962,0	-7934,1	-582,4	7267,8
900	950	925	238,3	6580,3	1323	-3862	-2538	315,5	15517,4	-920,4	-8854,5	-605,0	6662,9
850	900	875	210,2	6790,5	1230	-4158	-2928	258,7	15776,1	-874,3	-9728,9	-615,6	6047,2
800	850	825	192,1	6982,6	1129	-4456	-3326	217,0	15993,1	-856,2	-10585,1	-639,2	5408,1
750	800	775	174,8	7157,4	985	-4868	-3882	172,2	16165,4	-850,9	-11436,0	-678,7	4729,4
700	750	725	141,2	7298,6	977	-5116	-4138	138,1	16303,4	-722,5	-12158,5	-584,4	4145,0
650	700	675	121,3	7419,9	889	-5313	-4423	107,9	16411,4	-644,4	-12802,9	-536,5	3608,5
600	650	625	74,6	7494,5	888	-5407	-4518	66,3	16477,7	-403,4	-13206,3	-337,1	3271,3
550	600	575	65,8	7560,3	783	-5592	-4808	51,6	16529,2	-368,1	-13574,4	-316,5	2954,8
500	550	525	48,0	7608,3	663	-5832	-5168	31,8	16561,1	-279,7	-13854,2	-247,9	2706,9
450	500	475	40,4	7648,7	513	-6197	-5683	20,8	16581,8	-250,4	-14104,5	-229,6	2477,3
400	450	425	44,5	7693,2	353	-6496	-6142	15,8	16597,6	-289,4	-14393,9	-273,6	2203,7
350	400	375	40,0	7733,2	123	-6744	-6620	4,9	16602,5	-269,8	-14663,7	-264,9	1938,8
300	350	325	38,1	7771,3	-149	-7014	-7163	-5,7	16596,8	-267,1	-14930,8	-272,8	1666,0
250	300	275	36,6	7807,9	-390	-7295	-7685	-14,3	16582,5	-267,2	-15198,0	-281,5	1384,5
200	250	225	37,5	7845,4	-614	-7869	-8483	-23,0	16559,5	-294,9	-15492,9	-317,9	1066,6
150	200	175	32,5	7877,9	-853	-8796	-9649	-27,7	16531,8	-285,4	-15778,3	-313,1	753,5
100	150	125	28,3	7906,2	-1027	-9449	-10477	-29,1	16502,7	-267,5	-16045,9	-296,6	456,9
50	100	75	25,9	7932,1	-1196	-9862	-11058	-31,0	16471,8	-255,3	-16301,2	-286,3	170,6
0	50	25	18,3	7950,4	-1154	-10289	-11444	-21,1	16450,6	-188,4	-16489,6	-209,5	-39,0

Tungnaárjökull

Elevation (m a.s.l.)			ΔS (km^2)	$\Sigma \Delta S$ (km^2)	b_w (mm)	b_s (mm)	b_n (mm)	ΔB_w (10^6m^3)	$\Sigma \Delta B_w$ (10^6m^3)	ΔB_s (10^6m^3)	$\Sigma \Delta B_s$ (10^6m^3)	ΔB_n (10^6m^3)	ΣB_n (10^6m^3)
1650	1700	1675	1,8	1,8	3033	-486	2546	5,6	5,6	-0,9	-0,9	4,7	4,7
1600	1650	1625	12,7	14,5	3030	-557	2472	38,6	44,2	-7,1	-8,0	31,5	36,2
1550	1600	1575	15,7	30,2	2956	-669	2287	46,4	90,6	-10,5	-18,5	35,9	72,1
1500	1550	1525	15,5	45,7	2889	-793	2095	44,8	135,5	-12,3	-30,8	32,5	104,6
1450	1500	1475	18,4	64,1	2804	-899	1905	51,5	186,9	-16,5	-47,3	35,0	139,6
1400	1450	1425	23,0	87,1	2767	-1053	1713	63,5	250,5	-24,2	-71,5	39,3	179,0
1350	1400	1375	21,4	108,5	2681	-1235	1446	57,2	307,7	-26,4	-97,9	30,9	209,8
1300	1350	1325	27,5	136,0	2519	-1435	1084	69,3	377,0	-39,5	-137,4	29,8	239,7
1250	1300	1275	21,1	157,1	2399	-1661	738	50,7	427,7	-35,1	-172,5	15,6	255,3
1200	1250	1225	23,1	180,2	2297	-2003	293	53,0	480,8	-46,3	-218,7	6,8	262,0
1150	1200	1175	21,0	201,2	2219	-2526	-307	46,6	527,4	-53,1	-271,8	-6,5	255,6
1100	1150	1125	18,4	219,6	2121	-3065	-944	39,0	566,4	-56,3	-328,1	-17,4	238,2
1050	1100	1075	19,1	238,7	1980	-3506	-1526	37,9	604,3	-67,1	-395,2	-29,2	209,0
1000	1050	1025	17,5	256,2	1787	-3754	-1966	31,2	635,5	-65,5	-460,8	-34,3	174,7
950	1000	975	17,3	273,5	1576	-3993	-2417	27,3	662,7	-69,1	-529,8	-41,8	132,9
900	950	925	16,4	289,9	1393	-4354	-2960	22,9	685,6	-71,5	-601,3	-48,6	84,3
850	900	875	13,5	303,4	1239	-4888	-3648	16,7	702,3	-66,0	-667,3	-49,3	35,0
800	850	825	14,1	317,5	1112	-5483	-4371	15,6	718,0	-77,1	-744,4	-61,5	-26,5
750	800	775	11,4	328,9	966	-6162	-5196	11,0	729,0	-70,1	-814,6	-59,1	-85,6
700	750	725	7,8	336,7	879	-6634	-5755	6,8	735,8	-51,7	-866,3	-44,8	-130,4
650	700	675	3,7	340,4	839	-6852	-6013	3,1	738,9	-25,4	-891,6	-22,2	-152,7

Sylgjujökull

Elevation (m a.s.l.)			ΔS (km^2)	$\Sigma \Delta S$ (km^2)	b_w (mm)	b_s (mm)	b_n (mm)	ΔB_w (10^6m^3)	$\Sigma \Delta B_w$ (10^6m^3)	ΔB_s (10^6m^3)	$\Sigma \Delta B_s$ (10^6m^3)	ΔB_n (10^6m^3)	ΣB_n (10^6m^3)
1600	1650	1625	1,7	1,7	2774	-574	2199	4,7	4,7	-1,0	-1,0	3,7	3,7
1550	1600	1575	5,5	7,2	2760	-662	2098	15,1	19,8	-3,6	-4,6	11,5	15,2
1500	1550	1525	18,6	25,8	2753	-819	1934	51,2	71,0	-15,2	-19,8	35,9	51,2
1450	1500	1475	13,2	39,0	2735	-950	1784	36,1	107,1	-12,5	-32,4	23,5	74,7
1400	1450	1425	8,3	47,3	2648	-1099	1548	21,9	129,0	-9,1	-41,5	12,8	87,5
1350	1400	1375	5,6	52,9	2530	-1268	1261	14,1	143,1	-7,1	-48,5	7,0	94,6
1300	1350	1325	5,2	58,1	2353	-1522	830	12,1	155,2	-7,8	-56,4	4,3	98,8
1250	1300	1275	10,1	68,2	2240	-1765	474	22,5	177,7	-17,7	-74,1	4,8	103,6
1200	1250	1225	12,0	80,2	2185	-2043	141	26,3	204,0	-24,6	-98,7	1,7	105,3
1150	1200	1175	13,6	93,8	2101	-2371	-269	28,6	232,6	-32,3	-131,0	-3,7	101,6
1100	1150	1125	12,8	106,6	1926	-2783	-857	24,6	257,2	-35,5	-166,5	-10,9	90,7
1050	1100	1075	12,3	118,9	1640	-3184	-1544	20,1	277,3	-39,0	-205,6	-18,9	71,8
1000	1050	1025	10,9	129,8	1385	-3672	-2287	15,0	292,4	-39,8	-245,4	-24,8	46,9
950	1000	975	3,8	133,6	1342	-4063	-2721	5,1	297,4	-15,4	-260,8	-10,3	36,6
900	950	925	1,7	135,3	1342	-4367	-3024	2,3	299,7	-7,4	-268,2	-5,1	31,5
850	900	875	0,3	135,6	1272	-4602	-3330	0,4	300,1	-1,5	-269,7	-1,1	30,5

Köldukvísarljökul

Elevation (m a.s.l.)			ΔS (km ²)	$\Sigma \Delta S$ (km ²)	b_w (mm)	b_s (mm)	b_n (mm)	ΔB_w (10 ⁶ m ³)	$\Sigma \Delta B_w$ (10 ⁶ m ³)	ΔB_s (10 ⁶ m ³)	$\Sigma \Delta B_s$ (10 ⁶ m ³)	ΔB_n (10 ⁶ m ³)	ΣB_n (10 ⁶ m ³)
1950	2000	1975	0,8	0,8	2385	589	2974	2,0	2,0	0,5	0,5	2,5	2,5
1900	1950	1925	13,9	14,7	2291	474	2766	31,9	33,9	6,6	7,1	38,5	41,0
1850	1900	1875	6,4	21,1	2217	307	2525	14,2	48,1	2,0	9,1	16,1	57,1
1800	1850	1825	6,0	27,1	2224	199	2423	13,4	61,5	1,2	10,3	14,6	71,8
1750	1800	1775	10,3	37,4	2328	120	2448	24,0	85,5	1,2	11,5	25,2	97,0
1700	1750	1725	17,0	54,4	2348	-51	2297	39,9	125,4	-0,9	10,6	39,0	136,0
1650	1700	1675	15,9	70,3	2287	-293	1994	36,4	161,7	-4,7	6,0	31,7	167,7
1600	1650	1625	14,1	84,4	2235	-506	1729	31,6	193,3	-7,2	-1,2	24,4	192,2
1550	1600	1575	18,7	103,1	2210	-677	1533	41,3	234,6	-12,6	-13,8	28,6	220,8
1500	1550	1525	20,3	123,4	2298	-842	1455	46,7	281,3	-17,1	-30,9	29,6	250,3
1450	1500	1475	19,4	142,8	2179	-955	1223	42,3	323,6	-18,5	-49,5	23,8	274,1
1400	1450	1425	15,3	158,1	1986	-1130	855	30,3	353,9	-17,3	-66,7	13,1	287,2
1350	1400	1375	15,1	173,2	1783	-1442	340	27,0	380,8	-21,8	-88,5	5,1	292,3
1300	1350	1325	17,3	190,5	1653	-1878	-224	28,6	409,4	-32,5	-121,0	-3,9	288,4
1250	1300	1275	18,0	208,5	1484	-2377	-893	26,7	436,1	-42,8	-163,8	-16,1	272,3
1200	1250	1225	17,4	225,9	1258	-2998	-1740	21,8	458,0	-52,1	-215,8	-30,2	242,1
1150	1200	1175	16,3	242,2	1061	-3567	-2505	17,3	475,3	-58,2	-274,0	-40,9	201,2
1100	1150	1125	14,8	257,0	907	-3998	-3091	13,4	488,7	-59,1	-333,1	-45,7	155,6
1050	1100	1075	13,4	270,4	780	-4360	-3580	10,5	499,1	-58,4	-391,5	-48,0	107,6
1000	1050	1025	10,5	280,9	676	-4702	-4026	7,1	506,3	-49,5	-441,1	-42,4	65,2
950	1000	975	9,7	290,6	593	-5027	-4434	5,7	512,0	-48,6	-489,6	-42,8	22,4
900	950	925	6,3	296,9	523	-5281	-4757	3,3	515,3	-33,5	-523,1	-30,2	-7,8
850	900	875	0,9	297,8	461	-5516	-5054	0,4	515,7	-4,8	-527,9	-4,4	-12,2

Dyngjujökull

Elevation (m a.s.l.)			ΔS (km ²)	$\Sigma \Delta S$ (km ²)	b_w (mm)	b_s (mm)	b_n (mm)	ΔB_w (10 ⁶ m ³)	$\Sigma \Delta B_w$ (10 ⁶ m ³)	ΔB_s (10 ⁶ m ³)	$\Sigma \Delta B_s$ (10 ⁶ m ³)	ΔB_n (10 ⁶ m ³)	ΣB_n (10 ⁶ m ³)
1950	2000	1975	3,3	3,3	2373	452	2826	7,8	7,8	1,5	1,5	9,3	9,3
1900	1950	1925	12,7	16,0	2548	455	3004	32,4	40,2	5,8	7,3	38,2	47,5
1850	1900	1875	25,1	41,1	2805	291	3096	70,5	110,7	7,3	14,6	77,9	125,3
1800	1850	1825	14,8	55,9	2888	143	3032	42,7	153,4	2,1	16,7	44,8	170,1
1750	1800	1775	15,7	71,6	2876	12	2888	45,1	198,5	0,2	16,9	45,3	215,4
1700	1750	1725	28,1	99,7	2904	-89	2815	81,6	280,1	-2,5	14,4	79,1	294,5
1650	1700	1675	73,5	173,2	2870	-172	2698	210,9	491,0	-12,7	1,7	198,2	492,7
1600	1650	1625	118,8	292,0	2714	-275	2439	322,5	813,5	-32,7	-31,0	289,8	782,5
1550	1600	1575	95,5	387,5	2585	-338	2247	247,0	1060,5	-32,3	-63,3	214,7	997,2
1500	1550	1525	87,8	475,3	2401	-428	1973	210,8	1271,3	-37,6	-100,9	173,2	1170,4
1450	1500	1475	73,7	549,0	2104	-557	1546	155,2	1426,5	-41,1	-142,1	114,0	1284,4
1400	1450	1425	61,2	610,2	1786	-719	1067	109,4	1535,8	-44,0	-186,1	65,3	1349,7
1350	1400	1375	49,5	659,7	1490	-955	535	73,7	1609,6	-47,2	-233,4	26,5	1376,2
1300	1350	1325	36,5	696,2	1243	-1261	-17	45,4	1655,0	-46,1	-279,4	-0,7	1375,5
1250	1300	1275	39,9	736,1	1022	-1643	-621	40,8	1695,8	-65,6	-345,0	-24,8	1350,8
1200	1250	1225	45,4	781,5	804	-2157	-1352	36,5	1732,3	-98,0	-443,0	-61,4	1289,3
1150	1200	1175	45,7	827,2	602	-2750	-2147	27,5	1759,8	-125,6	-568,6	-98,1	1191,3
1100	1150	1125	43,0	870,2	450	-3223	-2773	19,4	1779,2	-138,8	-707,3	-119,4	1071,9
1050	1100	1075	31,5	901,7	345	-3543	-3198	10,9	1790,1	-111,8	-819,1	-100,9	971,0
1000	1050	1025	33,0	934,7	288	-3844	-3556	9,5	1799,6	-126,8	-945,9	-117,3	853,7
950	1000	975	30,6	965,3	217	-4240	-4022	6,6	1806,3	-129,5	-1075,5	-122,9	730,8
900	950	925	25,7	991,0	137	-4667	-4529	3,5	1809,8	-120,0	-1195,5	-116,5	614,3
850	900	875	23,6	1014,6	70	-5048	-4977	1,7	1811,5	-119,3	-1314,8	-117,6	496,7
800	850	825	21,6	1036,2	20	-5390	-5369	0,4	1811,9	-116,3	-1431,1	-115,8	380,9
750	800	775	17,8	1054,0	-21	-5819	-5840	-0,4	1811,6	-103,3	-1534,4	-103,7	277,2
700	750	725	5,4	1059,4	-50	-6180	-6230	-0,3	1811,3	-33,1	-1567,5	-33,4	243,8

Brúarjökull

Elevation (m a.s.l.)			ΔS (km ²)	$\Sigma \Delta S$ (km ²)	b_w (mm)	b_s (mm)	b_n (mm)	ΔB_w (10 ⁶ m ³)	$\Sigma \Delta B_w$ (10 ⁶ m ³)	ΔB_s (10 ⁶ m ³)	$\Sigma \Delta B_s$ (10 ⁶ m ³)	ΔB_n (10 ⁶ m ³)	ΣB_n (10 ⁶ m ³)
1850	1900	1875	1,2	1,2	3083	288	3372	3,7	3,8	0,3	0,3	4,0	4,1
1800	1850	1825	4,4	5,6	3042	390	3432	13,4	17,2	1,7	2,1	15,2	19,3
1750	1800	1775	2,9	8,5	2926	161	3087	8,4	25,6	0,5	2,5	8,8	28,1
1700	1750	1725	3,9	12,4	2832	-43	2789	11,1	36,7	-0,2	2,4	10,9	39,0
1650	1700	1675	5,5	17,9	2790	-176	2613	15,3	52,0	-1,0	1,4	14,4	53,4
1600	1650	1625	50,9	68,8	2774	-356	2418	141,3	193,3	-18,2	-16,8	123,2	176,6
1550	1600	1575	46,0	114,8	2805	-451	2354	129,0	322,4	-20,7	-37,5	108,3	284,8
1500	1550	1525	72,6	187,4	2806	-525	2280	203,6	526,0	-38,1	-75,6	165,5	450,3
1450	1500	1475	78,3	265,7	2652	-553	2098	207,7	733,7	-43,4	-119,0	164,3	614,6
1400	1450	1425	111,2	376,9	2684	-473	2211	298,6	1032,2	-52,6	-171,6	245,9	860,6
1350	1400	1375	155,9	532,8	2550	-549	2001	397,7	1429,9	-85,7	-257,3	312,0	1172,6
1300	1350	1325	147,2	680,0	2290	-697	1592	337,0	1766,9	-102,6	-359,9	234,4	1407,0
1250	1300	1275	141,8	821,8	2018	-990	1027	286,2	2053,1	-140,5	-500,4	145,7	1552,6
1200	1250	1225	117,9	939,7	1660	-1352	308	195,8	2248,9	-159,5	-659,9	36,3	1589,0
1150	1200	1175	102,7	1042,4	1387	-1753	-366	142,5	2391,3	-180,1	-840,0	-37,6	1551,3
1100	1150	1125	83,4	1125,8	1225	-2356	-1131	102,3	2493,6	-196,6	-1036,6	-94,4	1457,0
1050	1100	1075	69,8	1195,6	1107	-2964	-1857	77,3	2570,9	-206,9	-1243,5	-129,6	1327,3
1000	1050	1025	62,5	1258,1	969	-3311	-2342	60,6	2631,4	-206,9	-1450,4	-146,3	1181,0
950	1000	975	56,4	1314,5	817	-3614	-2797	46,1	2677,5	-203,9	-1654,3	-157,8	1023,2
900	950	925	46,3	1360,8	640	-4021	-3380	29,6	2707,2	-186,2	-1840,5	-156,6	866,6
850	900	875	42,6	1403,4	456	-4432	-3976	19,4	2726,6	-188,7	-2029,2	-169,2	697,4
800	850	825	38,1	1441,5	298	-4775	-4477	11,4	2738,0	-182,0	-2211,2	-170,7	526,7
750	800	775	37,0	1478,5	156	-5476	-5320	5,8	2743,8	-202,8	-2414,0	-197,0	329,7
700	750	725	25,6	1504,1	57	-6127	-6070	1,5	2745,2	-156,9	-2571,0	-155,5	174,2
650	700	675	17,5	1521,6	-21	-6510	-6531	-0,4	2744,9	-113,6	-2684,6	-114,0	60,3
600	650	625	3,0	1524,6	-82	-6727	-6810	-0,2	2744,6	-20,2	-2704,8	-20,4	39,8

Eyjabakkajökull

Elevation (m a.s.l.)			ΔS (km ²)	$\Sigma \Delta S$ (km ²)	b_w (mm)	b_s (mm)	b_n (mm)	ΔB_w (10 ⁶ m ³)	$\Sigma \Delta B_w$ (10 ⁶ m ³)	ΔB_s (10 ⁶ m ³)	$\Sigma \Delta B_s$ (10 ⁶ m ³)	ΔB_n (10 ⁶ m ³)	ΣB_n (10 ⁶ m ³)
1550	1600	1575	0,0	0,0	4140	70	4211	0,4	0,4	0,0	0,0	0,4	0,4
1500	1550	1525	1,0	1,0	4032	32	4064	3,9	4,3	0,0	0,0	3,9	4,4
1450	1500	1475	1,8	2,8	3997	-59	3938	7,4	11,7	-0,1	0,0	7,3	11,6
1400	1450	1425	2,5	5,3	3926	-317	3608	9,9	21,7	-0,8	-0,9	9,1	20,8
1350	1400	1375	4,1	9,4	3833	-653	3179	15,8	37,4	-2,7	-3,6	13,1	33,9
1300	1350	1325	13,7	23,1	3355	-1141	2214	46,0	83,5	-15,6	-19,2	30,4	64,2
1250	1300	1275	13,4	36,5	2979	-1553	1425	39,9	123,4	-20,8	-40,0	19,1	83,3
1200	1250	1225	14,4	50,9	2459	-1939	520	35,4	158,8	-27,9	-67,9	7,5	90,8
1150	1200	1175	12,1	63,0	1851	-2283	-431	22,4	181,2	-27,7	-95,6	-5,2	85,6
1100	1150	1125	10,4	73,4	1430	-2660	-1229	14,8	196,1	-27,6	-123,2	-12,8	72,8
1050	1100	1075	10,1	83,5	1150	-3005	-1854	11,6	207,7	-30,3	-153,6	-18,7	54,1
1000	1050	1025	7,6	91,1	917	-3416	-2499	6,9	214,6	-25,8	-179,4	-18,9	35,2
950	1000	975	4,9	96,0	732	-3810	-3077	3,6	218,2	-18,8	-198,2	-15,2	20,0
900	950	925	4,0	100,0	629	-4088	-3458	2,5	220,7	-16,2	-214,4	-13,7	6,3
850	900	875	3,1	103,1	548	-4334	-3785	1,7	222,4	-13,3	-227,7	-11,6	-5,3
800	850	825	3,0	106,1	417	-4756	-4338	1,3	223,7	-14,5	-242,1	-13,2	-18,5
750	800	775	2,6	108,7	221	-5328	-5106	0,6	224,3	-13,9	-256,0	-13,3	-31,8
700	750	725	3,0	111,7	-1	-5813	-5814	0,0	224,2	-17,7	-273,8	-17,7	-49,5
650	700	675	0,2	111,9	-140	-6143	-6283	0,0	224,2	-1,0	-274,8	-1,0	-50,5

Hoffellsjökull

Elevation (m a.s.l.)			ΔS (km ²)	$\Sigma \Delta S$ (km ²)	b_w (mm)	b_s (mm)	b_n (mm)	ΔB_w (10 ⁶ m ³)	$\Sigma \Delta B_w$ (10 ⁶ m ³)	ΔB_s (10 ⁶ m ³)	$\Sigma \Delta B_s$ (10 ⁶ m ³)	ΔB_n (10 ⁶ m ³)	ΣB_n (10 ⁶ m ³)
1450	1500	1475	0,9	0,9	4030	80	4110	3,7	3,7	0,0	0,0	3,8	3,8
1400	1450	1425	6,7	7,6	3502	-293	3209	25,3	29,0	-2,1	-2,0	23,2	27,0
1350	1400	1375	10,0	17,6	3407	-413	2994	34,7	63,7	-4,2	-6,3	30,5	57,5
1300	1350	1325	15,4	33,0	3298	-655	2642	53,7	117,5	-10,7	-16,9	43,1	100,5
1250	1300	1275	33,6	66,6	3206	-1163	2042	112,0	229,5	-40,7	-57,6	71,4	171,9
1200	1250	1225	26,8	93,4	3188	-1505	1683	82,4	311,9	-38,9	-96,5	43,5	215,4
1150	1200	1175	18,2	111,6	3051	-1827	1224	54,8	366,6	-32,8	-129,3	22,0	237,4
1100	1150	1125	17,5	129,1	2807	-2074	733	47,5	414,2	-35,1	-164,4	12,4	249,8
1050	1100	1075	13,6	142,7	2473	-2321	152	31,6	445,8	-29,7	-194,1	2,0	251,7
1000	1050	1025	10,0	152,7	2203	-2589	-386	21,5	467,3	-25,3	-219,3	-3,8	248,0
950	1000	975	9,0	161,7	1922	-2953	-1031	16,7	484,0	-25,6	-244,9	-8,9	239,0
900	950	925	6,4	168,1	1651	-3351	-1700	10,6	494,5	-21,5	-266,4	-10,9	228,1
850	900	875	4,3	172,4	1433	-3674	-2240	6,2	500,8	-15,9	-282,4	-9,7	218,4
800	850	825	3,6	176,0	1453	-3898	-2445	5,2	505,9	-13,8	-296,2	-8,7	209,7
750	800	775	3,9	179,9	1412	-4200	-2787	5,5	511,4	-16,3	-312,5	-10,8	198,9
700	750	725	3,8	183,7	1241	-4526	-3284	4,5	515,9	-16,3	-328,8	-11,9	187,1
650	700	675	3,4	187,1	1029	-4912	-3882	3,6	519,4	-17,0	-345,8	-13,4	173,6
600	650	625	2,5	189,6	838	-5332	-4494	2,1	521,6	-13,5	-359,3	-11,4	162,2
550	600	575	1,8	191,4	701	-5740	-5039	1,2	522,8	-9,9	-369,2	-8,7	153,6
500	550	525	1,5	192,9	589	-6150	-5560	0,9	523,7	-9,7	-378,9	-8,8	144,8
450	500	475	0,9	193,8	451	-6517	-6066	0,4	524,1	-5,7	-384,7	-5,3	139,4
400	450	425	0,9	194,7	295	-6788	-6493	0,3	524,4	-6,4	-391,1	-6,1	133,3
350	400	375	0,6	195,3	106	-6942	-6835	0,0	524,4	-4,4	-395,5	-4,4	128,9
300	350	325	0,9	196,2	-87	-7006	-7094	0,0	524,4	-5,0	-400,5	-5,1	123,8
250	300	275	2,2	198,4	-314	-7092	-7406	-0,4	524,0	-9,3	-409,8	-9,7	114,1
200	250	225	3,3	201,7	-542	-7520	-8062	-1,4	522,5	-20,1	-429,9	-21,5	92,6
150	200	175	2,6	204,3	-716	-8395	-9112	-2,1	520,4	-25,1	-455,0	-27,2	65,4
100	150	125	2,1	206,4	-909	-9149	-10058	-2,1	518,2	-21,6	-476,6	-23,7	41,6
50	100	75	2,8	209,2	-1029	-9657	-10686	-1,9	516,3	-17,9	-494,5	-19,8	21,9
0	50	25	0,6	209,8	-1199	-10193	-11392	-3,1	513,2	-26,7	-521,2	-29,8	-8,0

Breiðamerkurjökull

Elevation (m a.s.l.)			ΔS (km ²)	$\Sigma \Delta S$ (km ²)	b_w (mm)	b_s (mm)	b_n (mm)	ΔB_w (10 ⁶ m ³)	$\Sigma \Delta B_w$ (10 ⁶ m ³)	ΔB_s (10 ⁶ m ³)	$\Sigma \Delta B_s$ (10 ⁶ m ³)	ΔB_n (10 ⁶ m ³)	ΣB_n (10 ⁶ m ³)
1900	1950	1925	0,0	0,0	5037	2194	7232	0,4	0,4	0,2	0,2	0,6	0,6
1850	1900	1875	0,4	0,4	5058	2169	7228	1,9	2,3	0,8	1,0	2,7	3,3
1800	1850	1825	0,4	0,8	5009	2083	7092	2,4	4,6	1,0	2,0	3,3	6,6
1750	1800	1775	0,8	1,6	4848	1823	6671	4,8	9,5	1,8	3,8	6,7	13,3
1700	1750	1725	2,5	4,1	4077	929	5006	10,7	20,2	2,4	6,2	13,1	26,4
1650	1700	1675	5,8	9,9	3580	268	3849	21,4	41,6	1,6	7,8	23,1	49,4
1600	1650	1625	15,8	25,7	3393	-127	3266	58,2	99,8	-2,2	5,6	56,0	105,4
1550	1600	1575	25,7	51,4	3281	-345	2935	85,2	185,0	-9,0	-3,3	76,2	181,7
1500	1550	1525	32,2	83,6	3178	-440	2737	101,6	286,6	-14,1	-17,4	87,5	269,2
1450	1500	1475	44,3	127,9	3108	-389	2718	142,8	429,4	-17,9	-35,3	124,9	394,1
1400	1450	1425	58,3	186,2	3008	-440	2568	178,2	607,6	-26,1	-61,4	152,1	546,2
1350	1400	1375	88,7	274,9	2930	-555	2375	262,1	869,7	-49,7	-111,1	212,4	758,6
1300	1350	1325	96,9	371,8	2908	-786	2122	276,8	1146,5	-74,8	-185,9	202,0	960,6
1250	1300	1275	59,4	431,2	2837	-958	1878	163,4	1310,0	-55,2	-241,2	108,2	1068,8
1200	1250	1225	39,7	470,9	2743	-1204	1539	109,0	1419,0	-47,9	-289,0	61,2	1130,0
1150	1200	1175	32,6	503,5	2610	-1534	1075	82,8	1501,8	-48,7	-337,7	34,1	1164,1
1100	1150	1125	27,7	531,2	2468	-1903	564	67,3	1569,1	-51,9	-389,6	15,4	1179,5
1050	1100	1075	24,1	555,3	2308	-2226	82	55,0	1624,1	-53,0	-442,6	2,0	1181,5
1000	1050	1025	22,1	577,4	2135	-2548	-412	46,7	1670,8	-55,7	-498,3	-9,0	1172,5
950	1000	975	24,5	601,9	1934	-2935	-1000	47,1	1717,9	-71,5	-569,8	-24,4	1148,1
900	950	925	27,4	629,3	1746	-3320	-1573	47,3	1765,2	-89,9	-659,7	-42,6	1105,5
850	900	875	26,2	655,5	1566	-3672	-2106	39,9	1805,1	-93,5	-753,2	-53,6	1051,9
800	850	825	26,1	681,6	1378	-3907	-2529	35,5	1840,6	-100,7	-853,9	-65,2	986,7
750	800	775	25,3	706,9	1166	-4315	-3149	29,3	1870,0	-108,6	-962,5	-79,2	907,5
700	750	725	23,9	730,8	1007	-4662	-3654	22,4	1892,4	-103,6	-1066,1	-81,2	826,2
650	700	675	30,8	761,6	916	-4871	-3955	28,7	1921,1	-152,8	-1218,9	-124,1	702,2
600	650	625	26,2	787,8	800	-5304	-4504	20,5	1941,6	-136,1	-1355,0	-115,5	586,6
550	600	575	27,0	814,8	690	-5691	-5000	18,6	1960,2	-153,2	-1508,2	-134,6	452,0
500	550	525	15,7	830,5	608	-5983	-5374	9,5	1969,7	-93,1	-1601,3	-83,6	368,4
450	500	475	16,3	846,8	461	-6414	-5952	6,7	1976,4	-93,5	-1694,7	-86,7	281,7
400	450	425	15,9	862,7	338	-6596	-6258	5,6	1982,0	-108,6	-1803,3	-103,0	178,7
350	400	375	13,0	875,7	146	-6681	-6534	1,9	1983,9	-88,1	-1891,4	-86,1	92,5
300	350	325	13,1	888,8	-86	-6684	-6770	-1,0	1982,9	-77,5	-1968,9	-78,5	14,0
250	300	275	12,1	900,9	-338	-6903	-7241	-3,8	1979,1	-77,0	-2045,9	-80,8	-66,8
200	250	225	11,5	912,4	-587	-7820	-8407	-6,7	1972,4	-89,3	-2135,3	-96,0	-162,8
150	200	175	8,6	921,0	-804	-9443	-10247	-7,5	1964,9	-88,6	-2223,8	-96,1	-259,0
100	150	125	7,9	928,9	-944	-10427	-11372	-7,5	1957,3	-83,2	-2307,0	-90,8	-349,7
50	100	75	6,1	935,0	-1028	-10799	-11827	-7,6	1949,8	-79,5	-2386,5	-87,1	-436,8
0	50	25	3,0	938,0	-1077	-10968	-12046	-6,0	1943,7	-61,3	-2447,8	-67,3	-504,1

Síðujökull

Elevation (m a.s.l.)			ΔS (km ²)	$\Sigma \Delta S$ (km ²)	b_w (mm)	b_s (mm)	b_n (mm)	ΔB_w (10 ⁶ m ³)	$\Sigma \Delta B_w$ (10 ⁶ m ³)	ΔB_s (10 ⁶ m ³)	$\Sigma \Delta B_s$ (10 ⁶ m ³)	ΔB_n (10 ⁶ m ³)	ΣB_n (10 ⁶ m ³)
1700	1750	1725	0,8	0,8	3697	200	3897	3,1	3,1	0,2	0,2	3,3	3,3
1650	1700	1675	5,5	6,3	3578	-201	3376	19,8	22,9	-1,1	-0,9	18,7	22,0
1600	1650	1625	11,1	17,4	3421	-474	2947	37,9	60,8	-5,3	-6,2	32,7	54,6
1550	1600	1575	10,7	28,1	3379	-626	2752	36,3	97,1	-6,7	-12,9	29,6	84,2
1500	1550	1525	20,5	48,6	3359	-769	2590	68,7	165,8	-15,7	-28,7	53,0	137,2
1450	1500	1475	39,0	87,6	3280	-960	2320	128,1	293,9	-37,5	-66,2	90,6	227,8
1400	1450	1425	25,9	113,5	3168	-1103	2065	82,1	376,0	-28,6	-94,8	53,5	281,3
1350	1400	1375	21,2	134,7	2995	-1236	1758	63,4	439,4	-26,2	-121,0	37,2	318,5
1300	1350	1325	17,3	152,0	2860	-1441	1418	49,5	489,0	-25,0	-145,9	24,6	343,1
1250	1300	1275	15,9	167,9	2754	-1627	1127	43,9	532,9	-25,9	-171,8	18,0	361,0
1200	1250	1225	21,1	189,0	2654	-1908	746	56,1	588,9	-40,3	-212,2	15,8	376,8
1150	1200	1175	18,3	207,3	2500	-2291	209	45,6	634,6	-41,8	-254,0	3,8	380,6
1100	1150	1125	17,2	224,5	2429	-2685	-256	41,9	676,4	-46,3	-300,2	-4,4	376,2
1050	1100	1075	16,2	240,7	2353	-3097	-743	38,2	714,6	-50,2	-350,5	-12,1	364,1
1000	1050	1025	20,5	261,2	2238	-3477	-1238	45,9	760,5	-71,3	-421,8	-25,4	338,7
950	1000	975	20,2	281,4	2069	-3775	-1705	41,8	802,3	-76,2	-498,0	-34,4	304,3
900	950	925	21,6	303,0	1905	-3969	-2063	41,2	843,5	-85,9	-583,9	-44,6	259,6
850	900	875	19,8	322,8	1786	-4108	-2321	35,3	878,8	-81,3	-665,1	-45,9	213,7
800	850	825	21,3	344,1	1679	-4257	-2577	35,7	914,5	-90,5	-755,6	-54,8	158,9
750	800	775	23,3	367,4	1566	-4415	-2848	36,6	951,1	-103,1	-858,7	-66,5	92,4
700	750	725	23,6	391,0	1435	-4699	-3263	33,9	985,0	-110,9	-969,5	-77,0	15,4
650	700	675	19,9	410,9	1298	-5133	-3835	25,8	1010,8	-101,9	-1071,4	-76,1	-60,7
600	650	625	10,9	421,8	1200	-5466	-4265	13,1	1023,9	-59,6	-1131,1	-46,5	-107,2
550	600	575	1,5	423,3	1142	-5641	-4498	1,8	1025,6	-8,7	-1139,8	-6,9	-114,2

Skaftárjökull

Elevation (m a.s.l.)			ΔS (km ²)	$\Sigma \Delta S$ (km ²)	b_w (mm)	b_s (mm)	b_n (mm)	ΔB_w (10 ⁶ m ³)	$\Sigma \Delta B_w$ (10 ⁶ m ³)	ΔB_s (10 ⁶ m ³)	$\Sigma \Delta B_s$ (10 ⁶ m ³)	ΔB_n (10 ⁶ m ³)	ΣB_n (10 ⁶ m ³)
1350	1400	1375	2,3	2,3	2858	-1259	1599	6,7	6,7	-2,9	-2,9	3,7	3,7
1300	1350	1325	5,4	7,7	2754	-1407	1347	14,7	21,4	-7,5	-10,5	7,2	11,0
1250	1300	1275	4,2	11,9	2606	-1658	947	11,1	32,5	-7,0	-17,5	4,0	15,0
1200	1250	1225	6,5	18,4	2450	-2036	414	15,9	48,3	-13,2	-30,7	2,7	17,6
1150	1200	1175	7,9	26,3	2338	-2459	-121	18,4	66,8	-19,4	-50,1	-1,0	16,7
1100	1150	1125	11,2	37,5	2257	-2864	-607	25,2	91,9	-31,9	-82,0	-6,8	9,9
1050	1100	1075	12,9	50,4	2164	-3253	-1088	28,0	119,9	-42,0	-124,1	-14,1	-4,2
1000	1050	1025	12,9	63,3	2042	-3586	-1543	26,4	146,3	-46,4	-170,5	-20,0	-24,1
950	1000	975	8,5	71,8	1884	-3932	-2048	16,1	162,4	-33,5	-204,0	-17,5	-41,6
900	950	925	5,5	77,3	1774	-4211	-2436	9,7	172,1	-23,0	-227,0	-13,3	-54,9
850	900	875	5,3	82,6	1663	-4516	-2853	8,9	181,0	-24,1	-251,1	-15,2	-70,2
800	850	825	5,0	87,6	1548	-4840	-3292	7,7	188,7	-24,2	-275,3	-16,4	-86,6
750	800	775	4,8	92,4	1437	-5149	-3711	6,9	195,6	-24,8	-300,1	-17,9	-104,5
700	750	725	4,4	96,8	1307	-5531	-4223	5,8	201,4	-24,4	-324,6	-18,7	-123,1
650	700	675	2,6	99,4	1213	-5863	-4650	3,1	204,6	-15,1	-339,7	-12,0	-135,1
600	650	625	0,7	100,1	1097	-6128	-5030	0,7	205,3	-4,0	-343,7	-3,3	-138,5

Vestari Skaftárketill

Elevation (m a.s.l.)			ΔS (km ²)	$\Sigma \Delta S$ (km ²)	b_w (mm)	b_s (mm)	b_n (mm)	ΔB_w (10 ⁶ m ³)	$\Sigma \Delta B_w$ (10 ⁶ m ³)	ΔB_s (10 ⁶ m ³)	$\Sigma \Delta B_s$ (10 ⁶ m ³)	ΔB_n (10 ⁶ m ³)	ΣB_n (10 ⁶ m ³)
1900	1950	1925	0,6	0,6	2439	276	2715	1,4	1,4	0,2	0,2	1,5	1,5
1850	1900	1875	0,6	1,2	2524	225	2749	1,6	2,9	0,1	0,3	1,7	3,2
1800	1850	1825	0,8	2,0	2532	179	2711	2,0	4,9	0,1	0,4	2,1	5,3
1750	1800	1775	2,6	4,6	2624	69	2694	6,8	11,7	0,2	0,6	7,0	12,3
1700	1750	1725	5,5	10,1	2630	-99	2531	14,5	26,2	-0,6	0,0	14,0	26,3
1650	1700	1675	6,6	16,7	2617	-358	2259	17,4	43,6	-2,4	-2,3	15,0	41,2
1600	1650	1625	7,6	24,3	2640	-525	2114	20,0	63,6	-4,0	-6,3	16,1	57,3
1550	1600	1575	5,5	29,8	2644	-629	2014	14,5	78,1	-3,4	-9,8	11,0	68,3
1500	1550	1525	1,5	31,3	2657	-667	1989	4,0	82,1	-1,0	-10,8	3,0	71,3

Eystri Skaftárketill

Elevation (m a.s.l.)			ΔS (km ²)	$\Sigma \Delta S$ (km ²)	b_w (mm)	b_s (mm)	b_n (mm)	ΔB_w (10 ⁶ m ³)	$\Sigma \Delta B_w$ (10 ⁶ m ³)	ΔB_s (10 ⁶ m ³)	$\Sigma \Delta B_s$ (10 ⁶ m ³)	ΔB_n (10 ⁶ m ³)	ΣB_n (10 ⁶ m ³)
1750	1800	1775	1,1	1,1	2744	14	2758	2,9	2,9	0,0	0,0	3,0	3,0
1700	1750	1725	10,2	11,3	2787	-151	2635	28,4	31,4	-1,5	-1,5	26,9	29,8
1650	1700	1675	16,5	27,8	2867	-324	2542	47,4	78,8	-5,4	-6,9	42,0	71,9
1600	1650	1625	9,7	37,5	2860	-452	2407	27,6	106,4	-4,4	-11,3	23,2	95,1
1550	1600	1575	2,4	39,9	2858	-476	2381	6,9	113,3	-1,2	-12,4	5,8	100,9

Gjálp

Elevation (m a.s.l.)			ΔS (km ²)	$\Sigma \Delta S$ (km ²)	b_w (mm)	b_s (mm)	b_n (mm)	ΔB_w (10 ⁶ m ³)	$\Sigma \Delta B_w$ (10 ⁶ m ³)	ΔB_s (10 ⁶ m ³)	$\Sigma \Delta B_s$ (10 ⁶ m ³)	ΔB_n (10 ⁶ m ³)	ΣB_n (10 ⁶ m ³)
1900	1950	1925	0,4	0,4	2518	290	2808	1,0	1,0	0,1	0,1	1,1	1,1
1850	1900	1875	0,7	1,1	2644	206	2850	1,9	2,9	0,2	0,3	2,1	3,1
1800	1850	1825	1,1	2,2	2694	128	2822	3,1	6,0	0,1	0,4	3,2	6,4
1750	1800	1775	4,9	7,1	2838	8	2847	13,8	19,8	0,0	0,5	13,8	20,2
1700	1750	1725	18,8	25,9	2941	-143	2797	55,2	74,9	-2,7	-2,2	52,5	72,7
1650	1700	1675	13,5	39,4	2961	-190	2770	40,0	114,9	-2,6	-4,8	37,4	110,1

Grímsvötn

Elevation (m a.s.l.)			ΔS (km ²)	$\Sigma \Delta S$ (km ²)	b_w (mm)	b_s (mm)	b_n (mm)	ΔB_w (10 ⁶ m ³)	$\Sigma \Delta B_w$ (10 ⁶ m ³)	ΔB_s (10 ⁶ m ³)	$\Sigma \Delta B_s$ (10 ⁶ m ³)	ΔB_n (10 ⁶ m ³)	ΣB_n (10 ⁶ m ³)
1700	1750	1725	0,7	0,7	2968	-175	2793	2,2	2,2	-0,1	-0,1	2,1	2,1
1650	1700	1675	40,6	41,3	2956	-234	2721	120,0	122,2	-9,5	-9,7	110,5	112,6
1600	1650	1625	30,8	72,1	3038	-384	2654	93,6	215,8	-11,8	-21,5	81,8	194,3
1550	1600	1575	19,2	91,3	3027	-460	2567	58,2	274,0	-8,8	-30,3	49,3	243,6
1500	1550	1525	16,9	108,2	3110	-579	2530	52,6	326,6	-9,8	-40,1	42,8	286,5
1450	1500	1475	10,0	118,2	3245	-723	2522	32,6	359,2	-7,3	-47,4	25,3	311,8
1400	1450	1425	11,7	129,9	3337	-921	2415	39,0	398,2	-10,8	-58,2	28,2	340,0
1350	1400	1375	4,3	134,2	3362	-925	2436	14,6	412,8	-4,0	-62,2	10,6	350,6
1300	1350	1325	0,7	134,9	3429	-784	2644	2,6	415,3	-0,6	-62,8	2,0	352,6

Appendix C: Coordinates at velocity measurement stakes in 2017.

Position of velocity measurement stakes determined by GPS sub-metre differential (I), fast static (FS) and kinematic (K). (Accuracy of horizontal position 0.5 – 1.0 m, and vertical accuracy 1-2 m for DGPS, about 1cm for fast static, and 3 cm for kinematic).

The station Hofn in Höfn í Hornafirði is used as a stationary reference for all measurements, ÍSN93 datum, h_1 is elevation above ellipsoid, dL antenna height, N estimated difference between ellipsoid and sea-level, H elevation in metres above sea level ($H = h_1 + N + dL$). X and Y are ÍSN93 Lambert conformal conic projected coordinates. M is a quality marker.

Site	time	Calender				Latitude	Longitude	h_1 (m a. e.)	dL (m)	N (m)	H (m a. s. l.)	X	Y	M
		Date	#	Year	Day									
B07-17	9,883	4	5	124	2017	64 25,79760	16 17,44950	1426,89	0,00	-67,05	1359,85	630479,26	439247,87	K
B07-17	14,673	24	10	297	2017	64 25,79667	16 17,44870	1423,17	0,00	-67,05	1356,12	630479,97	439246,18	K
B09-16	10,932	5	5	125	2017	64 45,05081	16 5,44809	798,37	0,00	-66,66	731,71	638460,58	475410,50	K
B09-17	10,932	5	5	125	2017	64 45,05081	16 5,44809	798,37	0,00	-66,66	731,71	638460,58	475410,50	K
B09-17	11,955	15	12	249	2017	64 45,05052	16 5,44798	791,26	0,00	-66,66	724,60	638460,70	475409,97	K
B10-17	10,694	5	5	125	2017	64 43,68813	16 6,70247	856,54	0,00	-66,71	789,84	637581,90	472835,65	K
B10-17	11,314	15	12	249	2017	64 43,68791	16 6,70191	851,35	0,00	-66,71	784,64	637582,36	472835,27	K
B11-17	16,957	4	5	124	2017	64 40,96943	16 10,45583	1020,65	0,00	-66,81	953,84	634829,81	467654,67	K
B11-17	11,023	15	12	249	2017	64 40,97355	16 10,45208	1017,01	0,00	-66,81	950,20	634832,45	467662,46	K
B12-17	16,125	4	5	124	2017	64 38,26554	16 14,12954	1144,79	0,00	-66,90	1077,89	632129,80	462506,48	K
B12-17	9,802	25	10	298	2017	64 38,27645	16 14,11959	1141,52	0,00	-66,90	1074,62	632136,83	462527,09	K
B13-17	14,862	4	5	124	2017	64 34,52623	16 19,70040	1285,45	0,00	-67,01	1218,44	627988,36	455374,26	K
B13-17	16,965	24	10	297	2017	64 34,53874	16 19,68559	1282,67	0,00	-67,01	1215,66	627999,19	455397,98	K
B13ror15	15,282	4	5	124	2017	64 34,55771	16 19,69296	1284,37	0,00	-67,01	1217,36	627991,82	455432,94	K
B13ror15	17,790	24	10	297	2017	64 34,57024	16 19,67813	1281,24	3,62	-67,01	1217,85	628002,68	455456,71	K
B14-17	11,689	4	5	124	2017	64 31,63534	16 24,70212	1387,12	0,00	-67,11	1320,01	624216,94	449841,36	K
B14-17	16,232	24	10	297	2017	64 31,64513	16 24,68496	1384,41	0,00	-67,11	1317,30	624229,92	449860,09	K
B15-17	11,157	4	5	124	2017	64 28,48799	16 30,01568	1471,29	0,00	-67,21	1404,07	620200,26	443827,13	K
B15-17	15,473	24	10	297	2017	64 28,49377	16 30,00178	1467,70	0,00	-67,21	1400,49	620210,97	443838,29	K
B16-17	17,557	7	5	127	2017	64 24,12603	16 40,84597	1596,64	0,00	-67,33	1529,31	611821,97	435397,23	K
B16-17	11,383	25	10	298	2017	64 24,12642	16 40,84499	1593,87	0,00	-67,33	1526,54	611822,73	435397,99	K
B17-17	12,859	4	5	124	2017	64 36,74030	16 28,79477	1281,65	0,00	-67,12	1214,53	620567,14	459186,54	K
B17-17	17,568	24	10	297	2017	64 36,75145	16 28,78669	1279,69	0,00	-67,12	1212,58	620572,75	459207,51	K
B18-17	12,871	5	5	125	2017	64 31,58423	16 0,12900	1381,74	0,00	-66,92	1314,81	643862,84	450614,87	K
B18-17	13,171	24	10	297	2017	64 31,59073	16 0,13247	1378,46	0,00	-66,92	1311,53	643859,49	450626,80	K
B19-17	20,931	3	5	123	2017	64 27,99425	15 55,98018	1507,38	0,00	-66,89	1440,50	647502,01	444111,72	K
B19-17	12,562	24	10	297	2017	64 27,99458	15 55,98042	1503,04	0,00	-66,89	1436,15	647501,79	444112,32	K
BB0-17	19,042	3	5	123	2017	64 22,71282	16 5,05255	1588,06	0,00	-66,85	1521,20	640687,74	433965,14	K
BB0-17	12,025	24	10	297	2017	64 22,71271	16 5,05393	1584,36	0,00	-66,85	1517,51	640686,64	433964,90	K
BBbr-17	17,125	8	6	159	2017	64 36,14450	17 28,68782	1997,93	-1,45	-67,87	1928,62	572848,87	456553,01	K
BBbr-17	16,161	25	10	298	2017	64 36,14438	17 28,69377	1995,56	0,00	-67,87	1927,69	572844,13	456552,66	K
Barc-17	16,075	8	6	159	2017	64 38,40960	17 26,78203	1956,83	-1,45	-67,87	1887,51	574265,58	460797,26	K
Bor-17	13,396	5	6	156	2017	64 24,94232	17 20,15835	1472,99	0,00	-67,70	1405,29	580199,98	435918,07	K
Bor-17	17,439	25	10	298	2017	64 24,94293	17 20,16999	1490,02	0,00	-67,70	1422,32	580190,60	435918,96	K
Bor-17a	17,371	25	10	298	2017	64 24,93648	17 20,16201	1490,10	0,00	-67,70	1422,40	580197,32	435907,15	K
Borth-17	11,734	5	6	156	2017	64 25,06229	17 19,16914	1474,86	0,00	-67,70	1407,16	580988,47	436161,92	K
Borth-17	19,470	27	10	300	2017	64 25,05578	17 19,17041	1500,52	-2,80	-67,70	1430,02	580987,75	436149,77	K
Br1-16	17,847	28	3	87	2017	64 5,83905	16 19,72054	196,64	-1,60	-65,88	129,16	630223,93	402120,00	F
Br1-16	10,635	29	10	302	2017	64 5,83849	16 19,71997	183,30	-0,60	-65,88	116,82	630224,44	402118,97	K
Br2k	17,573	28	3	87	2017	64 6,37303	16 22,54033	277,68	-1,60	-66,04	210,04	627893,06	403015,35	F
Br2k	11,649	29	10	302	2017	64 6,36914	16 22,53828	267,53	-0,60	-66,04	200,90	627895,03	403008,20	K
Br3-16	17,259	28	3	87	2017	64 8,47618	16 24,05672	454,97	-1,60	-66,27	387,10	626501,49	406868,91	F
Br4-16	16,369	28	3	87	2017	64 10,72134	16 20,19379	582,77	-1,60	-66,36	514,81	629457,57	411167,23	F
Br7-17	22,245	3	5	123	2017	64 22,14173	16 16,94599	1315,13	0,00	-67,01	1248,12	631175,09	432478,87	K
Br7-17	13,984	24	10	297	2017	64 22,11353	16 16,93908	1310,64	0,00	-67,01	1243,63	631182,90	432426,78	K
Bru-17	21,925	4	5	124	2017	64 40,98432	15 55,30956	822,58	0,00	-66,74	755,84	646864,38	468244,75	K
Bru-17	17,644	24	10	297	2017	64 40,98477	15 55,30967	815,91	0,00	-66,74	749,17	646864,25	468245,58	K
Bud-17	10,861	5	5	125	2017	64 35,99071	15 59,89448	1204,06	0,00	-66,88	1137,18	643661,66	458801,76	K
Bud-17	13,569	24	10	297	2017	64 36,00382	15 59,89215	1200,38	0,00	-66,88	1133,50	643662,36	458826,18	K

D05-17	16,337	5	5	125	2017	64	42,23132	16	54,66872	1270,88	0,00	-67,35	1203,53	599607,16	468631,17	K
D05-17	13,009	25	10	298	2017	64	42,23988	16	54,65570	1268,48	0,00	-67,35	1201,13	599616,97	468647,42	K
D07-17	15,632	5	5	125	2017	64	38,28332	16	59,25634	1442,95	0,00	-67,50	1375,45	596195,87	461181,25	K
D07-17	12,490	25	10	298	2017	64	38,29658	16	59,24346	1440,17	0,00	-67,50	1372,67	596205,34	461206,21	K
D09-17	15,194	5	5	125	2017	64	31,79856	17	0,55322	1652,97	0,00	-67,56	1585,41	595542,35	449105,84	K
D09-17	11,964	25	10	298	2017	64	31,80254	17	0,55484	1650,75	0,00	-67,56	1583,19	595540,82	449113,21	K
D12-17	14,569	5	5	125	2017	64	28,97779	17	0,14955	1717,55	0,00	-67,55	1650,00	596030,70	443877,67	K
D12-17	11,765	25	10	298	2017	64	28,97817	17	0,14934	1715,20	0,00	-67,55	1647,65	596030,85	443878,38	K
E01-16	20,680	4	5	124	2017	64	41,06507	15	34,09521	762,88	0,00	-66,69	696,19	663710,01	469263,10	K
E01-17	20,680	4	5	124	2017	64	41,06507	15	34,09521	762,88	0,00	-66,69	696,19	663710,01	469263,10	K
E01-17	16,000	24	10	297	2017	64	41,06600	15	34,09387	758,89	0,00	-66,69	692,20	663710,97	469264,88	P
E02-17	20,158	4	5	124	2017	64	39,12731	15	35,98136	1020,67	0,00	-66,79	953,88	662405,39	465586,92	K
E02-17	14,911	24	10	297	2017	64	39,13944	15	35,97601	1016,31	0,00	-66,78	949,52	662408,44	465609,65	K
E03-17	19,515	4	5	124	2017	64	36,66252	15	36,91865	1256,68	0,00	-66,85	1189,83	661905,07	460973,86	K
E03-17	14,491	24	10	297	2017	64	36,66845	15	36,92219	1251,38	0,00	-66,85	1184,53	661901,66	460984,72	K
E04-17	18,555	4	5	124	2017	64	34,95110	15	37,10682	1357,13	0,00	-66,83	1290,30	661925,20	457790,57	K
E04-17	14,314	24	10	297	2017	64	34,95206	15	37,10623	1352,42	0,00	-66,83	1285,59	661925,58	457792,39	K
FI01-17	20,121	3	5	123	2017	64	26,15533	15	55,62448	1415,72	0,00	-66,82	1348,90	647952,92	440712,89	K
FI01-17	12,844	24	10	297	2017	64	26,14817	15	55,60745	1410,87	0,00	-66,82	1344,04	647967,22	440700,26	K
G02-17	16,537	5	6	156	2017	64	26,84943	17	17,72578	1633,65	0,00	-67,73	1565,92	582058,00	439512,26	K
G02-17	17,082	25	10	298	2017	64	26,84599	17	17,72883	1631,25	0,00	-67,73	1563,52	582055,72	439505,79	K
G03-17	17,516	5	6	156	2017	64	28,45061	17	16,34886	1727,96	0,00	-67,74	1660,22	583081,18	442516,12	K
G03-17	16,914	25	10	298	2017	64	28,44913	17	16,34976	1725,57	0,00	-67,74	1657,84	583080,54	442513,35	K
G04-17	18,887	5	6	156	2017	64	30,00662	17	15,00253	1756,56	0,00	-67,73	1688,83	584080,03	445435,76	K
G04-17	16,732	25	10	298	2017	64	30,00685	17	15,00218	1754,64	0,00	-67,73	1686,91	584080,30	445436,18	K
gb2-17	11,903	5	5	125	2017	64	34,10497	16	0,00980	1270,87	0,00	-66,90	1203,97	643735,94	455297,64	K
gb2-17	13,400	24	10	297	2017	64	34,11500	16	0,01153	1267,34	0,00	-66,90	1200,44	643733,68	455316,19	K
Go1-17	12,258	8	6	159	2017	64	33,97211	17	24,95704	1829,89	-1,45	-67,84	1760,60	575925,81	452591,10	K
Go1-17	13,836	25	10	298	2017	64	33,97087	17	24,95601	1826,75	0,00	-67,84	1758,91	575926,69	452588,81	K
Haab-17	16,450	6	6	157	2017	64	20,96170	17	24,11860	1800,82	0,00	-67,54	1733,28	577206,45	428442,36	K
Haab-17	9,604	26	10	299	2017	64	20,96200	17	24,11848	1797,93	0,00	-67,54	1730,39	577206,53	428442,91	K
Hof01-17	17,278	4	5	124	2017	64	32,33351	15	35,84431	1209,46	0,00	-66,67	1142,78	663193,46	452988,20	K
Hof01-17	14,140	24	10	297	2017	64	32,32625	15	35,84350	1204,66	0,00	-66,67	1137,99	663194,84	452974,77	K
K01-16	17,907	6	5	126	2017	64	35,16888	17	51,81304	1121,71	0,00	-67,58	1054,13	554434,47	454352,69	K
K01-17	17,907	6	5	126	2017	64	35,16888	17	51,81304	1121,71	0,00	-67,58	1054,13	554434,47	454352,69	K
K01-17	11,384	26	10	299	2017	64	35,17022	17	51,81976	1117,40	0,00	-67,58	1049,82	554429,06	454355,08	K
K02-17	17,729	6	5	126	2017	64	34,81107	17	49,67879	1242,50	0,00	-67,61	1174,89	556150,40	453719,11	K
K02-17	11,051	26	10	299	2017	64	34,81411	17	49,69232	1237,86	0,00	-67,61	1170,25	556139,50	453724,55	K
K03-17	17,104	6	5	126	2017	64	34,24732	17	46,38108	1364,25	0,00	-67,67	1296,59	558803,59	452721,81	K
K03-17	10,550	26	10	299	2017	64	34,25034	17	46,40010	1360,90	0,00	-67,67	1293,23	558788,28	452727,14	K
K04-17	18,943	6	5	126	2017	64	33,21043	17	42,25223	1556,52	0,00	-67,73	1488,79	562140,56	450861,48	K
K04-17	10,058	26	10	299	2017	64	33,21401	17	42,27723	1552,56	0,00	-67,73	1484,82	562120,45	450867,72	K
K05-17	19,594	6	5	126	2017	64	33,44996	17	35,43641	1749,29	0,00	-67,82	1681,47	567577,38	451422,98	K
K05-17	9,759	26	10	299	2017	64	33,44722	17	35,45104	1746,81	0,00	-67,82	1679,00	567565,81	451417,63	K
K06-17	13,067	8	6	159	2017	64	38,36479	17	31,40962	2018,17	-1,45	-67,88	1948,84	570581,47	460625,68	K
K06-17	15,633	25	10	298	2017	64	38,36394	17	31,40620	2014,82	0,00	-67,88	1946,94	570584,24	460624,15	K
K07-17	16,716	6	5	126	2017	64	29,11237	17	42,01332	1602,84	0,00	-67,69	1535,15	562488,03	443252,84	K
K07-17	12,043	26	10	299	2017	64	29,11236	17	42,01504	1599,97	0,00	-67,69	1532,28	562486,65	443252,79	K
Li50-17	23,104	4	6	155	2017	64	24,22127	17	23,24420	1504,32	-2,00	-67,69	1436,63	577755,92	434514,56	F
Li51-17	23,846	4	6	155	2017	64	24,07574	17	22,63306	1477,68	-2,00	-67,68	1410,00	578253,89	434256,81	F
Li61-17	14,454	5	6	156	2017	64	24,21037	17	23,47716	1535,80	-2,00	-67,69	1468,11	577569,26	434489,54	F
Li62-17	15,812	5	6	156	2017	64	24,46484	17	23,69253	1525,45	-2,00	-67,69	1457,76	577384,22	434957,80	F
Li63-17	16,941	5	6	156	2017	64	24,47127	17	23,76697	1518,54	-2,00	-67,69	1450,85	577324,11	434968,21	F
Li65-17	17,925	5	6	156	2017	64	24,41691	17	23,64995	1529,10	-2,00	-67,69	1461,40	577420,68	434869,63	F
Li69-17	19,091	5	6	156	2017	64	24,58145	17	23,48568	1511,94	-2,00	-67,70	1444,24	577544,87	435178,60	F
Li80-17	10,904	7	6	158	2017	64	24,12797	17	20,69614	1460,76	-2,00	-67,67	1393,09	579807,69	434394,17	F
Li81-17	11,679	7	6	158	2017	64	23,99970	17	21,54551	1449,51	-2,00	-67,67	1381,83	579131,42	434138,14	F
Li82-17	13,546	7	6	158	2017	64	24,10461	17	22,07242	1481,89	-2,00	-67,68	1414,21	578702,99	434322,04	F
Li83-17	14,533	7	6	158	2017	64	24,10767	17	22,45957	1487,46	-2,00	-67,68	1419,78	578391,76	434319,70	F
Li84-17	15,358	7	6	158	2017	64	24,06451	17	22,65967	1476,25	-2,00	-67,68	1408,58	578233,04	434235,41	F
Li85-17	16,346	7	6	158	2017	64	24,35582	17	23,33096	1521,86	-2,00	-67,69	1454,17	577679,84	434762,69	F
Li86-17	17,475	7	6	158	2017	64	24,45811	17	23,39051	1530,56	-2,00	-67,69	1462,87	577627,16	434951,47	F
Li90-17	11,596	8	6	159	2017	64	23,63895	17	22,81798	1672,89	-2,00	-67,66	1605,23	578126,09	433441,72	F
Li91-17	13,221	8	6	159	2017	64	23,94041	17	23,43085	1547,02	-2,00	-67,68	1479,35	577619,24	433989,07	F
Li93-17	15,350	8	6	159	2017	64	28,83938	17	31,61100	1657,14	-2,00	-67,79	1589,35	570833,44	442928,57	F
Li94-17	16,391	8	6	159	2017	64	29,71642	17	30,31931	1671,59	-2,00	-67,82	1603,77	571829,87	444581,95	F
Li95-17	17,187	8	6	159	2017	64	29,27005	17	30,41268	1646,07	-2,00	-67,81	1578,26	571774,69	443751,05	F
Li96-17	17,654	8	6	159	2017	64	29,30046	17	30,26848	1644,64	-2,00	-67,82	1576,82	571888,86	443810,27	F
Li97-17	17,966	8	6	159	2017	64	29,22443	17	30,36032	1645,28	-2,00	-67,81	1577,47	571818,63	443667,30	F
Li98-17	18,483	8	6	159	2017	64	28,20217	17	30,57414	1680,19	-2,00	-67,79	1612,40	571692,12	441764,43	F

S01-17	12,358	6	5	126	2017	64	6,99966	17	49,96536	795,26	0,00	-66,84	728,42	556875,67	402049,76	K
S01-17	11,701	26	10	299	2017	64	6,99959	17	49,96559	789,35	0,00	-66,84	722,51	556875,48	402049,62	K
S02-17	11,391	6	5	126	2017	64	12,16279	17	48,95941	1074,60	0,00	-67,05	1007,56	557512,84	411656,56	K
S02-17	10,850	26	10	299	2017	64	12,14982	17	48,96533	1069,16	0,00	-67,04	1002,12	557508,50	411632,38	K
S04-17	10,557	6	5	126	2017	64	16,18246	17	48,20223	1227,75	0,00	-67,21	1160,54	557984,40	419135,39	K
S04-17	10,344	26	10	299	2017	64	16,16711	17	48,21855	1223,05	0,00	-67,21	1155,84	557971,76	419106,64	K
S05-17	9,197	6	5	126	2017	64	20,49492	17	34,00209	1519,48	0,00	-67,51	1451,97	569269,09	427384,48	K
S05-17	9,916	26	10	299	2017	64	20,49333	17	34,01680	1515,48	0,00	-67,51	1447,97	569257,31	427381,26	K
Ske02-17	14,116	6	6	157	2017	64	18,15880	17	9,18472	1274,93	0,00	-67,19	1207,74	589380,57	423564,40	K
Ske02-17	15,866	25	10	298	2017	64	18,14758	17	9,20881	1270,36	0,00	-67,19	1203,17	589361,76	423543,00	K
Ske03-17	19,421	7	5	127	2017	64	17,79964	17	0,00193	1321,33	0,00	-67,17	1254,16	596805,90	423122,77	K
Ske03-17	14,446	25	10	298	2017	64	17,75646	17	0,06450	1316,27	0,00	-67,17	1249,10	596757,98	423040,97	K
Ske04-17	18,816	7	5	127	2017	64	19,49558	16	54,50168	1435,15	0,00	-67,27	1367,88	601137,29	426415,72	K
Ske04-17	13,964	25	10	298	2017	64	19,47657	16	54,54995	1431,80	0,00	-67,27	1364,53	601099,57	426379,12	K
Ske05-17	18,182	7	5	127	2017	64	21,69652	16	51,00916	1503,70	0,00	-67,34	1436,36	603811,75	430597,12	K
Ske05-17	13,347	25	10	298	2017	64	21,68542	16	51,02327	1500,26	0,00	-67,34	1432,91	603801,09	430576,13	K
Skf00-17	16,371	3	5	123	2017	64	15,46114	15	54,06429	1017,83	0,00	-66,03	951,79	650177,54	420927,99	K
Skf00-17	10,929	24	10	297	2017	64	15,46266	15	54,06099	1012,07	0,00	-66,03	946,04	650180,07	420930,95	K
Skf01-17	18,989	3	5	123	2017	64	18,00314	16	5,00055	1351,11	0,00	-66,64	1284,47	641133,12	425225,76	K
Skf01-17	11,255	24	10	297	2017	64	18,00022	16	4,98321	1346,69	0,00	-66,64	1280,05	641147,35	425220,98	K
Skja1-17	12,142	8	6	159	2017	64	33,97383	17	24,94075	1829,94	-1,45	-67,84	1760,65	575938,74	452594,62	K
Skja2-17	11,776	8	6	159	2017	64	35,24045	17	10,46558	1603,97	-1,45	-67,64	1534,88	587431,37	455258,88	K
T01-17	14,748	6	5	126	2017	64	19,48610	18	8,22965	793,01	0,00	-67,25	725,76	541727,53	425009,56	K
T01-17	15,908	26	10	299	2017	64	19,48629	18	8,22927	785,43	0,00	-67,25	718,18	541727,84	425009,92	K
T01ve-17	16,851	6	5	126	2017	64	19,54222	18	7,06548	853,24	0,00	-67,26	785,98	542664,36	425126,78	K
T01ve-17	15,504	26	10	299	2017	64	19,54095	18	7,06455	844,53	0,00	-67,26	777,27	542665,14	425124,42	K
T02-17	13,994	6	5	126	2017	64	19,59279	18	3,97378	1000,17	0,00	-67,27	932,90	545154,65	425256,51	K
T02-17	14,193	26	10	299	2017	64	19,59296	18	3,98038	994,11	0,00	-67,27	926,84	545149,33	425256,76	K
T03-17	13,076	6	5	126	2017	64	20,20525	17	58,59886	1140,54	0,00	-67,30	1073,24	549467,82	426461,38	K
T03-17	13,886	26	10	299	2017	64	20,20372	17	58,61106	1135,90	0,00	-67,30	1068,60	549458,03	426458,38	K
T04-17	11,721	6	5	126	2017	64	21,32627	17	51,50247	1290,24	0,00	-67,36	1222,88	555146,82	428641,80	K
T04-17	13,098	26	10	299	2017	64	21,32243	17	51,51563	1285,95	0,00	-67,36	1218,59	555136,36	428634,49	K
T05-17	10,700	6	5	126	2017	64	22,27201	17	42,98482	1414,10	0,00	-67,47	1346,63	561967,74	430530,17	K
T05-17	12,621	26	10	299	2017	64	22,26846	17	42,99792	1410,59	0,00	-67,47	1343,12	561957,34	430523,37	K
T05rorg	12,769	26	10	299	2017	64	22,26613	17	43,09119	1409,32	1,67	-67,47	1343,52	561882,39	430517,51	K
T06-17	9,700	6	5	126	2017	64	24,26898	17	36,51640	1536,76	0,00	-67,61	1469,15	567089,88	434349,76	K
T06-17	11,918	26	10	299	2017	64	24,26479	17	36,52882	1533,35	0,00	-67,61	1465,74	567080,07	434341,75	K
T07-17	18,901	5	5	125	2017	64	25,28838	17	31,20189	1632,76	0,00	-67,70	1565,06	571315,68	436340,27	K
T07-17	17,864	25	10	298	2017	64	25,28620	17	31,21090	1629,28	0,00	-67,70	1561,58	571308,55	436336,05	K
T08-17	18,282	5	5	125	2017	64	26,29185	17	27,76164	1706,38	0,00	-67,75	1638,63	574032,75	438270,11	K
T08-17	17,716	25	10	298	2017	64	26,29138	17	27,76347	1703,27	0,00	-67,75	1635,52	574031,31	438269,19	K

Appendix D: Measured surface velocity on Vatnajökull in 2017.

Site	Calendar		Calendar		# of days	translation		velocity	
	day date	#	day date	#		(m)	(°)	(cm/day)	(m/annum)
B07-17	170504	124	171024	297	173	1,8	160	1,1	3,9
B09-16	161011	285	170505	125	205	10,1	69	4,9	17,9
B09-17	170505	125	171215	249	124	0,5	171	0,4	1,6
B10-17	170505	125	171215	249	124	0,6	133	0,5	1,8
B11-17	170504	124	171215	249	125	8,2	21	6,6	23,9
B12-17	170504	124	171025	298	174	21,7	21	12,5	45,5
B13-17	170504	124	171024	297	173	26,0	27	15,0	54,9
B13ror15	160508	129	170504	124	360	28,4	28	7,9	28,8
B13ror15	170504	124	171024	297	173	26,1	27	15,1	55,0
B14-17	170504	124	171024	297	173	22,7	37	13,1	48,0
B15-17	170504	124	171024	297	173	15,5	46	8,9	32,6
B16-17	170507	127	171025	298	171	1,1	47	0,6	2,3
B17-17	170504	124	171024	297	173	21,6	17	12,5	45,6
B18-17	170505	125	171024	297	172	12,4	347	7,2	26,2
B19-17	170503	123	171024	297	174	0,6	343	0,4	1,3
BB0-17	170503	123	171024	297	174	1,1	260	0,7	2,4
BBbr-17	170608	159	171025	298	139	4,8	267	3,4	12,5
Bor-17	170605	156	171025	298	142	9,4	277	6,6	24,2
Borth-17	170605	156	171027	300	144	12,1	185	8,4	30,7
Br1-16	160118	18	170328	87	434	1,7	180	0,4	1,4
Br1-16	170328	87	171029	302	215	1,1	156	0,5	1,9
Br2k	160119	19	170328	87	433	12,4	180	2,9	10,5
Br2k	170328	87	171029	302	215	7,4	167	3,4	12,6
Br3-16	160119	19	170328	87	433	28,4	147	6,6	23,9
Br4-16	160508	129	170328	87	323	300,2	181	92,9	339,2
Br7-17	170503	123	171024	297	174	52,5	174	30,2	110,2
Bru-17	170504	124	171024	297	173	0,8	354	0,5	1,8
Bud-17	170505	125	171024	297	172	24,4	4	14,2	51,7
D05-17	170505	125	171025	298	173	18,9	33	10,9	39,9
D07-17	170505	125	171025	298	173	26,6	23	15,4	56,2
D09-17	170505	125	171025	298	173	7,5	350	4,3	15,8
D12-17	170505	125	171025	298	173	0,7	13	0,4	1,5
E01-16	161010	284	170504	124	205	6,7	16	3,3	12,0
E01-17	170504	124	171024	297	173	2,0	32	1,2	4,3
E02-17	170504	124	171024	297	173	22,9	11	13,2	48,2
E03-17	170504	124	171024	297	173	11,3	346	6,6	23,9
E04-17	170504	124	171024	297	173	1,8	15	1,1	3,9
FI01-17	170503	123	171024	297	174	19,0	134	10,9	39,9
G02-17	170605	156	171025	298	142	6,8	201	4,8	17,5
G03-17	170605	156	171025	298	142	2,8	195	2,0	7,3
G04-17	170605	156	171025	298	142	0,5	33	0,4	1,3
gb2-17	170505	125	171024	297	172	18,6	356	10,8	39,5
Go1-17	170608	159	171025	298	139	2,4	160	1,8	6,4
Haab-17	170606	157	171026	299	142	0,6	10	0,4	1,5
Hof01-17	170504	124	171024	297	173	13,5	177	7,8	28,4

K01-16	161015	289	170506	126	202	10,8	326	5,4	19,6
K01-17	170506	126	171026	299	173	5,9	295	3,4	12,5
K02-17	170506	126	171026	299	173	12,2	298	7,0	25,7
K03-17	170506	126	171026	299	173	16,2	290	9,4	34,1
K04-17	170506	126	171026	299	173	21,1	288	12,2	44,4
K05-17	170506	126	171026	299	173	12,7	247	7,4	26,9
K06-17	170608	159	171025	298	139	3,2	120	2,3	8,3
K07-17	170506	126	171026	299	173	1,4	269	0,8	2,9
S01-17	170506	126	171026	299	173	0,2	235	0,1	0,5
S02-17	170506	126	171026	299	173	24,5	191	14,2	51,7
S04-17	170506	126	171026	299	173	31,3	205	18,1	66,1
S05-17	170506	126	171026	299	173	12,2	256	7,1	25,8
Ske02-17	170606	157	171025	298	141	28,5	223	20,2	73,6
Ske03-17	170507	127	171025	298	171	94,6	212	55,3	201,8
Ske04-17	170507	127	171025	298	171	52,5	228	30,7	112,0
Ske05-17	170507	127	171025	298	171	23,5	209	13,7	50,1
Skf00-17	170503	123	171024	297	174	3,9	43	2,2	8,1
Skf01-17	170503	123	171024	297	174	15,0	111	8,6	31,5
T01-17	170506	126	171026	299	173	0,5	41	0,3	1,0
T01ve-17	170506	126	171026	299	173	2,5	162	1,4	5,2
T02-17	170506	126	171026	299	173	5,3	273	3,1	11,2
T03-17	170506	126	171026	299	173	10,2	254	5,9	21,6
T04-17	170506	126	171026	299	173	12,8	236	7,4	26,9
T05-17	170506	126	171026	299	173	12,4	238	7,2	26,2
T05rorg	161015	289	171026	299	375	23,3	238	6,2	22,7
T06-17	170506	126	171026	299	173	12,6	232	7,3	26,7
T07-17	170505	125	171025	298	173	8,3	241	4,8	17,5
T08-17	170505	125	171025	298	173	1,7	239	1,0	3,6

Appendix E: Melt water runoff to selected rivers in summer 2017, derived from summer balance.

ΔS : area in a given elevation range where summer balance is negative, $\Sigma\Delta S$: cumulative area above a given elevation, ΔQ_s : melt water runoff from a given elevation range, $\Sigma\Delta Q_s$: cumulative melt water runoff from an area above given elevation.

Tungnaá water drainage basin

Elevation (m a. s. l.)		ΔS km^2	$\Sigma\Delta S$ km^2	ΔQ_s (10^6m^3)	$\Sigma\Delta Q_s$ (10^6m^3)
1350	1400	0,4	0,4	0,5	0,5
1300	1350	6,1	6,4	9,0	9,5
1250	1300	10,2	16,7	17,7	27,2
1200	1250	10,9	27,6	22,4	49,7
1150	1200	9,9	37,5	25,6	75,3
1100	1150	11,9	49,4	36,4	111,7
1050	1100	11,9	61,4	42,0	153,7
1000	1050	9,6	71,0	36,3	189,9
950	1000	9,6	80,6	38,4	228,4
900	950	9,2	89,8	40,1	268,5
850	900	7,8	97,5	38,4	306,9
800	850	7,7	105,2	42,7	349,5
750	800	7,0	112,1	43,4	392,9
700	750	4,7	116,9	31,8	424,6
650	700	2,1	119,0	14,7	439,3

Sylgja water drainage basin

Elevation (m a. s. l.)		ΔS km^2	$\Sigma\Delta S$ km^2	ΔQ_s (10^6m^3)	$\Sigma\Delta Q_s$ (10^6m^3)
1300	1350	1,1	1,1	1,8	1,8
1250	1300	3,6	4,7	6,3	8,1
1200	1250	5,9	10,5	12,0	20,1
1150	1200	8,3	18,8	19,6	39,7
1100	1150	6,1	24,9	16,9	56,7
1050	1100	6,9	31,8	22,3	79,0
1000	1050	5,1	36,9	19,1	98,1
950	1000	1,8	38,7	7,3	105,4
900	950	0,7	39,3	3,0	108,3
850	900	0,0	39,4	0,3	108,6

Western Skaftá cauldron water drainage basin

Elevation (m a. s. l.)		ΔS km^2	$\Sigma\Delta S$ km^2	ΔQ_s (10^6m^3)	$\Sigma\Delta Q_s$ (10^6m^3)
1700	1750	2,5	2,5	0,5	0,5
1650	1700	7,2	9,7	2,5	2,9
1600	1650	8,5	18,2	4,5	7,5
1550	1600	5,4	23,6	3,4	10,8
1500	1550	1,5	25,1	1,0	11,8

Eastern Skaftár cauldron water drainage basin

Elevation (m a. s. l.)		ΔS km ²	$\Sigma \Delta S$ km ²	ΔQ_s (10 ⁶ m ³)	$\Sigma \Delta Q_s$ (10 ⁶ m ³)
1750	1800	0,5	0,5	0,0	0,0
1700	1750	9,9	10,4	1,4	1,4
1650	1700	14,9	25,2	4,9	6,2
1600	1650	9,7	34,9	4,4	10,6
1550	1600	2,4	37,4	1,2	11,8

Grímsvötn water drainage basin

Elevation (m a. s. l.)		ΔS km ²	$\Sigma \Delta S$ km ²	ΔQ_s (10 ⁶ m ³)	$\Sigma \Delta Q_s$ (10 ⁶ m ³)
1750	1800	2,3	2,3	0,0	0,0
1700	1750	18,6	20,9	2,7	2,8
1650	1700	53,3	74,2	11,8	14,6
1600	1650	30,9	105,0	11,9	26,5
1550	1600	19,3	124,3	8,8	35,3
1500	1550	16,8	141,0	9,7	45,1
1450	1500	10,0	151,1	7,3	52,3
1400	1450	11,7	162,7	10,8	63,1
1350	1400	4,3	167,1	4,0	67,1
1300	1350	0,7	167,8	0,6	67,7

Kaldakvísl water drainage basin

Elevation (m a. s. l.)		ΔS km ²	$\Sigma \Delta S$ km ²	ΔQ_s (10 ⁶ m ³)	$\Sigma \Delta Q_s$ (10 ⁶ m ³)
1750	1800	0,4	0,4	0,0	0,0
1700	1750	14,9	15,3	1,3	1,3
1650	1700	17,1	32,4	5,0	6,3
1600	1650	14,5	46,9	7,3	13,6
1550	1600	19,1	66,0	12,8	26,4
1500	1550	25,3	91,2	21,4	47,8
1450	1500	28,8	120,0	27,6	75,4
1400	1450	24,0	144,0	27,3	102,7
1350	1400	22,1	166,1	31,4	134,1
1300	1350	21,2	187,3	39,2	173,3
1250	1300	22,4	209,8	51,7	225,0
1200	1250	21,7	231,4	61,5	286,5
1150	1200	20,0	251,4	67,0	353,5
1100	1150	18,0	269,4	67,3	420,8
1050	1100	16,9	286,2	68,7	489,5
1000	1050	14,6	300,8	64,0	553,5
950	1000	10,4	311,3	51,7	605,2
900	950	6,3	317,6	33,5	638,7
850	900	0,9	318,5	4,8	643,5

Jökulsá á Fjöllum water drainage basin

Elevation (m a. s. l.)		ΔS km ²	$\Sigma \Delta S$ km ²	ΔQ_s (10 ⁶ m ³)	$\Sigma \Delta Q_s$ (10 ⁶ m ³)
1900	1950	0,0	0,0	0,0	0,0
1850	1900	0,0	0,0	0,0	0,0
1800	1850	0,5	0,5	0,1	0,1
1750	1800	9,1	9,6	1,8	1,9
1700	1750	30,2	39,9	4,7	6,6
1650	1700	74,2	114,1	16,0	22,6
1600	1650	118,5	232,6	34,1	56,7
1550	1600	100,3	332,9	34,7	91,4
1500	1550	93,6	426,5	40,7	132,1
1450	1500	80,6	507,1	45,5	177,6
1400	1450	69,8	576,9	51,0	228,6
1350	1400	56,3	633,2	55,0	283,5
1300	1350	43,3	676,6	56,2	339,8
1250	1300	47,2	723,7	79,4	419,2
1200	1250	51,6	775,3	112,0	531,2
1150	1200	51,4	826,7	141,5	672,7
1100	1150	44,8	871,5	144,1	816,8
1050	1100	32,3	903,8	114,4	931,3
1000	1050	33,5	937,3	128,7	1060,0
950	1000	31,0	968,3	131,2	1191,2
900	950	26,0	994,3	121,3	1312,5
850	900	23,7	1018,0	119,8	1432,3
800	850	21,6	1039,6	116,3	1548,5
750	800	17,8	1057,4	103,3	1651,9
700	750	5,4	1062,7	33,1	1685,0

Kreppa and Kverká water drainage basin

Elevation (m a. s. l.)		ΔS km ²	$\Sigma \Delta S$ km ²	ΔQ_s (10 ⁶ m ³)	$\Sigma \Delta Q_s$ (10 ⁶ m ³)
1900	1950	0,0	0,0	0,0	0,0
1750	1800	0,6	0,6	0,0	0,0
1700	1750	2,3	2,9	0,4	0,4
1650	1700	4,9	7,8	0,9	1,4
1600	1650	41,4	49,2	13,8	15,2
1550	1600	20,5	69,7	8,9	24,1
1500	1550	13,4	83,0	7,0	31,1
1450	1500	16,3	99,3	9,3	40,4
1400	1450	19,8	119,1	11,7	52,1
1350	1400	25,5	144,6	15,8	67,9
1300	1350	20,0	164,6	14,4	82,3
1250	1300	15,5	180,1	14,8	97,1
1200	1250	17,7	197,9	22,7	119,8
1150	1200	17,7	215,5	29,5	149,2
1100	1150	16,9	232,4	40,4	189,6
1050	1100	11,1	243,5	34,1	223,7
1000	1050	13,4	256,9	44,1	267,8
950	1000	15,1	272,0	53,1	320,9
900	950	13,5	285,5	53,6	374,5
850	900	14,2	299,7	62,4	436,9
800	850	11,0	310,7	51,8	488,7
750	800	10,5	321,2	56,5	545,2
700	750	4,8	326,0	29,5	574,7
650	700	1,8	327,8	11,6	586,3

Hálslón water drainage basin

Elevation (m a. s. l.)		ΔS km ²	$\Sigma \Delta S$ km ²	ΔQ_s (10 ⁶ m ³)	$\Sigma \Delta Q_s$ (10 ⁶ m ³)
1600	1650	11,2	11,2	4,6	4,6
1550	1600	31,8	43,0	14,9	19,5
1500	1550	63,6	106,7	33,6	53,0
1450	1500	67,2	173,9	37,9	91,0
1400	1450	91,5	265,4	44,6	135,6
1350	1400	131,7	397,2	70,6	206,2
1300	1350	129,4	526,5	89,8	296,0
1250	1300	126,1	652,6	125,4	421,4
1200	1250	99,2	751,9	135,4	556,8
1150	1200	84,7	836,5	150,0	706,8
1100	1150	66,5	903,1	156,1	862,9
1050	1100	58,7	961,8	173,0	1036,0
1000	1050	49,4	1011,1	163,7	1199,7
950	1000	41,4	1052,6	151,2	1350,9
900	950	32,9	1085,5	133,0	1483,9
850	900	28,5	1113,9	126,5	1610,4
800	850	27,2	1141,1	130,3	1740,7
750	800	26,6	1167,7	146,2	1886,9
700	750	20,8	1188,5	127,5	2014,4
650	700	15,7	1204,1	102,0	2116,4
600	650	3,0	1207,1	20,2	2136,6

Jökulsá á Fljótsdal water drainage basin

Elevation (m a. s. l.)		ΔS km^2	$\Sigma \Delta S$ km^2	ΔQ_s (10^6m^3)	$\Sigma \Delta Q_s$ (10^6m^3)
1450	1500	0,2	0,2	0,0	0,0
1400	1450	1,2	1,4	0,2	0,2
1350	1400	2,8	4,2	1,1	1,3
1300	1350	5,4	9,6	3,9	5,2
1250	1300	16,2	25,8	18,3	23,5
1200	1250	16,0	41,8	24,1	47,6
1150	1200	17,3	59,1	32,0	79,6
1100	1150	15,0	74,1	33,1	112,7
1050	1100	12,4	86,5	32,8	145,5
1000	1050	11,9	98,4	36,1	181,6
950	1000	8,8	107,2	30,7	212,3
900	950	5,5	112,7	21,7	234,0
850	900	4,4	117,1	18,6	252,6
800	850	3,2	120,3	14,6	267,2
750	800	3,0	123,4	15,0	282,3
700	750	2,6	126,0	14,0	296,3
650	700	3,0	129,0	17,5	313,9
600	650	0,2	129,2	1,0	314,8

Hornafjarðarfljót water drainage basin

Elevation (m a. s. l.)		ΔS km ²	$\Sigma \Delta S$ km ²	ΔQ_s (10 ⁶ m ³)	$\Sigma \Delta Q_s$ (10 ⁶ m ³)
1450	1500	0,0	0,0	0,0	0,0
1400	1450	6,2	6,3	2,8	2,8
1350	1400	12,0	18,3	5,6	8,3
1300	1350	19,1	37,5	12,9	21,2
1250	1300	37,9	75,4	43,7	64,9
1200	1250	29,1	104,5	43,5	108,3
1150	1200	20,5	125,0	37,7	146,1
1100	1150	19,1	144,1	39,9	186,0
1050	1100	14,5	158,5	33,8	219,8
1000	1050	11,4	170,0	29,7	249,5
950	1000	10,7	180,7	31,7	281,3
900	950	8,2	188,8	27,2	308,5
850	900	5,5	194,3	20,4	328,8
800	850	4,4	198,7	17,2	346,0
750	800	4,2	202,9	17,5	363,5
700	750	3,7	206,6	16,9	380,4
650	700	3,6	210,2	17,5	397,9
600	650	2,6	212,8	14,1	412,0
550	600	1,9	214,7	10,9	422,9
500	550	1,9	216,6	11,6	434,6
450	500	1,3	217,9	8,3	442,9
400	450	1,3	219,2	8,9	451,7
350	400	0,8	220,1	5,8	457,6
300	350	0,9	221,0	6,3	463,9
250	300	1,5	222,5	10,4	474,3
200	250	2,9	225,3	21,6	495,9
150	200	3,1	228,5	26,4	522,3
100	150	2,4	230,9	22,2	544,6
50	100	1,8	232,8	17,9	562,4
0	50	2,6	235,4	26,7	589,1

Jökulsá á Breiðamerkursandi water drainage basin

Elevation (m a. s. l.)		ΔS km ²	$\Sigma \Delta S$ km ²	ΔQ_s (10 ⁶ m ³)	$\Sigma \Delta Q_s$ (10 ⁶ m ³)
1650	1700	2,2	2,2	0,4	0,4
1600	1650	13,2	15,4	3,9	4,3
1550	1600	18,9	34,4	7,8	12,2
1500	1550	22,1	56,5	11,8	24,0
1450	1500	26,1	82,6	14,8	38,8
1400	1450	46,9	129,5	22,1	60,9
1350	1400	84,2	213,7	46,1	107,0
1300	1350	83,4	297,1	63,3	170,3
1250	1300	51,6	348,8	48,7	218,9
1200	1250	35,1	383,9	42,1	261,0
1150	1200	28,2	412,0	43,9	304,9
1100	1150	24,1	436,2	46,3	351,2
1050	1100	20,5	456,6	46,3	397,5
1000	1050	17,6	474,2	45,7	443,2
950	1000	18,9	493,1	55,8	498,9
900	950	20,0	513,2	67,1	566,1
850	900	19,9	533,1	73,5	639,5
800	850	20,1	553,2	78,0	717,5
750	800	19,5	572,8	83,4	800,9
700	750	19,2	592,0	88,1	889,0
650	700	27,6	619,6	131,7	1020,7
600	650	18,4	638,0	97,1	1117,8
550	600	18,7	656,7	105,3	1223,1
500	550	7,6	664,2	43,8	1266,9
450	500	6,5	670,7	41,8	1308,7
400	450	6,4	677,1	42,2	1350,9
350	400	5,3	682,3	34,9	1385,8
300	350	5,7	688,0	37,8	1423,6
250	300	5,5	693,5	37,5	1461,1
200	250	5,9	699,4	46,2	1507,4
150	200	5,3	704,7	50,9	1558,3
100	150	4,9	709,6	51,4	1609,7
50	100	4,8	714,4	51,8	1661,5
0	50	3,9	718,3	42,1	1703,6

Breiðárlón/Fjallsárlón water drainage basin

Elevation (m a. s. l.)		ΔS km ²	$\Sigma \Delta S$ km ²	ΔQ_s (10 ⁶ m ³)	$\Sigma \Delta Q_s$ (10 ⁶ m ³)
1550	1600	0,0	0,0	0,0	0,0
1500	1550	0,7	0,8	0,0	0,0
1450	1500	1,9	2,7	0,3	0,4
1400	1450	4,3	7,0	1,5	1,9
1350	1400	6,3	13,3	4,1	6,0
1300	1350	12,6	25,9	12,3	18,4
1250	1300	6,5	32,4	7,4	25,7
1200	1250	5,6	38,0	7,5	33,3
1150	1200	4,9	42,9	7,6	40,9
1100	1150	4,5	47,3	8,6	49,5
1050	1100	5,0	52,3	10,9	60,4
1000	1050	6,0	58,3	14,6	75,0
950	1000	6,9	65,2	20,1	95,1
900	950	8,3	73,4	26,7	121,8
850	900	6,6	80,1	23,8	145,5
800	850	8,1	88,2	31,8	177,4
750	800	8,7	96,9	38,0	215,3
700	750	6,2	103,1	29,5	244,9
650	700	7,1	110,1	35,9	280,8
600	650	7,9	118,0	42,5	323,2
550	600	8,6	126,6	50,1	373,4
500	550	8,7	135,3	53,3	426,6
450	500	9,1	144,4	58,0	484,6
400	450	11,0	155,4	72,1	556,8
350	400	8,9	164,3	59,6	616,3
300	350	6,9	171,1	46,2	662,5
250	300	6,9	178,0	48,0	710,5
200	250	7,1	185,1	54,6	765,2
150	200	5,3	190,4	48,5	813,7
100	150	4,3	194,7	43,6	857,3
50	100	4,1	198,8	42,4	899,7
0	50	3,3	202,1	35,0	934,7

Skeiðarársandur (Gígja) water drainage basin (Gígja)

Elevation (m a. s. l.)		ΔS km ²	$\Sigma \Delta S$ km ²	ΔQ_s (10 ⁶ m ³)	$\Sigma \Delta Q_s$ (10 ⁶ m ³)
1700	1750	0,0	0,0	0,0	0,0
1650	1700	15,3	15,4	4,4	4,4
1600	1650	79,0	94,3	27,8	32,1
1550	1600	82,0	176,3	37,5	69,6
1500	1550	105,5	281,8	59,5	129,1
1450	1500	96,3	378,1	63,6	192,7
1400	1450	92,7	470,8	66,7	259,4
1350	1400	81,5	552,2	66,1	325,5
1300	1350	69,9	622,2	66,8	392,3
1250	1300	62,9	685,1	72,9	465,2
1200	1250	52,5	737,6	73,6	538,8
1150	1200	44,8	782,4	79,1	617,9
1100	1150	37,2	819,7	79,4	697,2
1050	1100	30,5	850,2	77,8	775,0
1000	1050	24,6	874,7	71,4	846,4
950	1000	23,1	897,8	73,3	919,7
900	950	23,4	921,2	81,2	1000,9
850	900	28,4	949,6	107,4	1108,3
800	850	21,2	970,9	85,5	1193,8
750	800	18,6	989,5	78,5	1272,3
700	750	20,1	1009,5	89,0	1361,4
650	700	14,2	1023,7	69,2	1430,6
600	650	11,6	1035,3	60,9	1491,5
550	600	13,9	1049,1	76,2	1567,7
500	550	9,4	1058,5	53,0	1620,7
450	500	6,3	1064,8	37,9	1658,6
400	450	6,6	1071,4	41,8	1700,4
350	400	9,2	1080,6	61,9	1762,4
300	350	12,3	1092,8	88,5	1850,9
250	300	12,7	1105,6	97,3	1948,2
200	250	12,6	1118,2	102,0	2050,2
150	200	10,5	1128,7	90,4	2140,6
100	150	8,9	1137,6	80,1	2220,7
50	100	7,9	1145,5	74,0	2294,6
0	50	0,2	1145,7	1,6	2296,2

Súla water drainage basin

Elevation (m a. s. l.)		ΔS km ²	$\Sigma \Delta S$ km ²	ΔQ_s (10 ⁶ m ³)	$\Sigma \Delta Q_s$ (10 ⁶ m ³)
1650	1700	0,9	0,9	0,0	0,0
1600	1650	2,5	3,4	1,0	1,1
1550	1600	4,0	7,5	2,5	3,6
1500	1550	5,9	13,3	4,4	8,0
1450	1500	11,1	24,4	10,2	18,2
1400	1450	11,0	35,4	11,2	29,4
1350	1400	9,3	44,7	10,6	40,0
1300	1350	8,2	52,9	9,9	49,9
1250	1300	6,6	59,5	8,7	58,6
1200	1250	7,9	67,4	11,8	70,4
1150	1200	8,8	76,2	15,4	85,7
1100	1150	15,2	91,4	30,7	116,5
1050	1100	16,0	107,3	39,2	155,7
1000	1050	16,7	124,0	47,9	203,6
950	1000	18,0	142,0	58,0	261,6
900	950	15,4	157,4	54,1	315,7
850	900	11,4	168,7	42,5	358,2
800	850	11,9	180,6	47,5	405,7
750	800	7,4	188,0	31,2	436,9
700	750	5,9	193,9	26,7	463,6
650	700	5,1	199,0	24,8	488,3
600	650	5,6	204,6	29,5	517,8
550	600	11,1	215,7	62,1	579,9
500	550	10,5	226,2	61,1	640,9
450	500	7,3	233,5	44,1	685,1
400	450	6,5	240,0	41,1	726,2
350	400	5,1	245,0	34,0	760,2
300	350	2,7	247,7	19,6	779,8
250	300	1,0	248,7	8,2	787,9
200	250	0,8	249,6	6,8	794,7
150	200	0,7	250,3	5,9	800,5
100	150	0,7	251,0	6,5	807,0
50	100	0,7	251,7	7,2	814,2

Djúpá water drainage basin

Elevation (m a. s. l.)		ΔS km^2	$\Sigma \Delta S$ km^2	ΔQ_s (10^6m^3)	$\Sigma \Delta Q_s$ (10^6m^3)
1450	1500	0,0	0,0	0,1	0,1
1400	1450	0,3	0,4	0,4	0,5
1350	1400	0,7	1,1	1,0	1,6
1300	1350	3,5	4,6	5,7	7,3
1250	1300	3,4	8,0	5,9	13,2
1200	1250	3,0	11,0	5,9	19,1
1150	1200	3,5	14,5	7,9	27,1
1100	1150	5,3	19,9	13,5	40,6
1050	1100	6,1	26,0	18,4	59,0
1000	1050	9,2	35,2	31,4	90,3
950	1000	7,3	42,4	27,4	117,7
900	950	7,8	50,2	31,3	149,0
850	900	6,7	56,9	27,8	176,8
800	850	8,0	64,8	34,1	211,0
750	800	6,6	71,4	28,9	239,9
700	750	3,7	75,1	17,0	256,9
650	700	2,9	78,0	14,4	271,3
600	650	1,0	79,0	5,3	276,6

Brunná water drainage basin

Elevation (m a. s. l.)		ΔS km^2	$\Sigma \Delta S$ km^2	ΔQ_s (10^6m^3)	$\Sigma \Delta Q_s$ (10^6m^3)
1050	1100	0,0	0,0	0,0	0,0
1000	1050	0,9	1,0	3,4	3,4
950	1000	2,5	3,5	9,5	12,9
900	950	4,3	7,8	17,2	30,1
850	900	4,2	12,0	17,2	47,3
800	850	4,2	16,2	17,4	64,6
750	800	4,6	20,7	19,6	84,2
700	750	5,6	26,4	26,0	110,2
650	700	4,8	31,2	24,8	135,0
600	650	3,2	34,4	17,9	152,9
550	600	0,5	34,9	3,0	155,8

Hverfisfljót water drainage basin

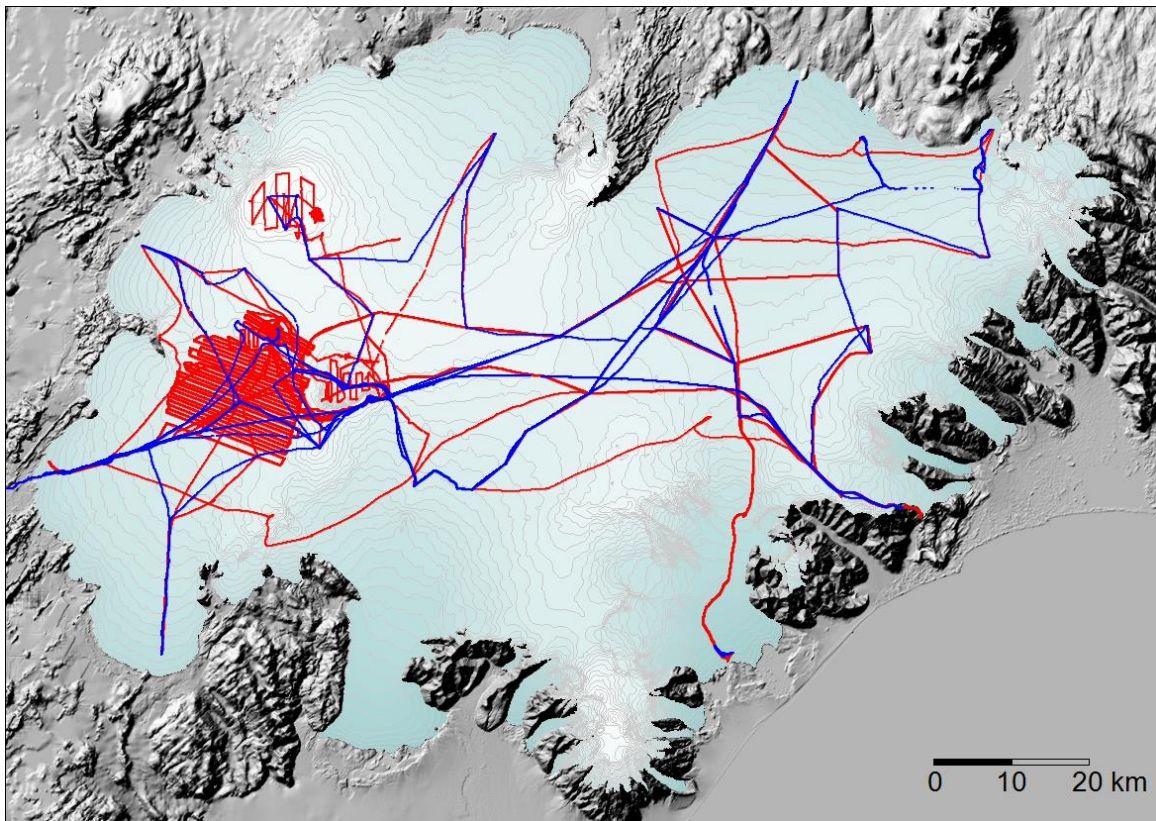
Elevation (m a. s. l.)		ΔS km ²	$\Sigma \Delta S$ km ²	ΔQ_s (10 ⁶ m ³)	$\Sigma \Delta Q_s$ (10 ⁶ m ³)
1650	1700	4,0	4,0	1,3	1,3
1600	1650	9,0	13,1	4,2	5,5
1550	1600	9,6	22,7	6,0	11,4
1500	1550	19,9	42,6	15,3	26,7
1450	1500	41,1	83,7	39,5	66,2
1400	1450	27,6	111,3	30,4	96,6
1350	1400	24,1	135,4	29,9	126,5
1300	1350	22,8	158,2	32,5	159,0
1250	1300	18,1	176,3	29,2	188,3
1200	1250	20,2	196,5	38,3	226,6
1150	1200	14,6	211,1	33,2	259,7
1100	1150	11,1	222,2	30,1	289,8
1050	1100	9,6	231,7	29,9	319,7
1000	1050	9,0	240,7	31,6	351,2
950	1000	8,9	249,6	33,5	384,7
900	950	8,6	258,1	33,7	418,4
850	900	7,8	265,9	31,6	450,0
800	850	7,3	273,2	30,6	480,6
750	800	10,1	283,2	44,2	524,8
700	750	12,1	295,3	56,9	581,6
650	700	10,5	305,8	53,9	635,6
600	650	6,2	312,0	33,7	669,3
550	600	1,0	313,1	5,7	675,0

Skaftá water drainage basin

Elevation (m a. s. l.)		ΔS km ²	$\Sigma \Delta S$ km ²	ΔQ_s (10 ⁶ m ³)	$\Sigma \Delta Q_s$ (10 ⁶ m ³)
1650	1700	2,2	2,2	1,1	1,1
1600	1650	15,6	17,8	8,6	9,7
1550	1600	22,7	40,4	15,2	24,9
1500	1550	30,8	71,2	24,5	49,4
1450	1500	24,5	95,7	22,1	71,5
1400	1450	22,3	118,0	23,5	95,0
1350	1400	20,5	138,5	25,3	120,3
1300	1350	22,5	161,0	32,1	152,4
1250	1300	15,6	176,6	25,7	178,1
1200	1250	21,0	197,6	41,8	219,9
1150	1200	22,7	220,2	56,2	276,1
1100	1150	23,7	243,9	69,5	345,6
1050	1100	24,2	268,1	80,3	425,8
1000	1050	26,2	294,3	94,9	520,7
950	1000	20,6	314,9	81,0	601,8
900	950	16,7	331,7	70,8	672,5
850	900	14,4	346,0	65,6	738,1
800	850	14,8	360,8	73,3	811,4
750	800	12,3	373,1	66,1	877,5
700	750	9,7	382,8	55,4	933,0
650	700	5,8	388,6	34,6	967,5
600	650	1,1	389,7	6,8	974,3

Appendix F: location of GPS surface profiles 2017.

During field trips, GPS L1,L2 land survey instruments mounted on snow track, cars or snowmobiles are used to collect data continuously. The collected data is kinematically postprocessed, usually with accuracy of a few centimeters for position of the antenna center, and surface elevation with an accuracy of few cm to few dm, depending on stability of the vehicle.



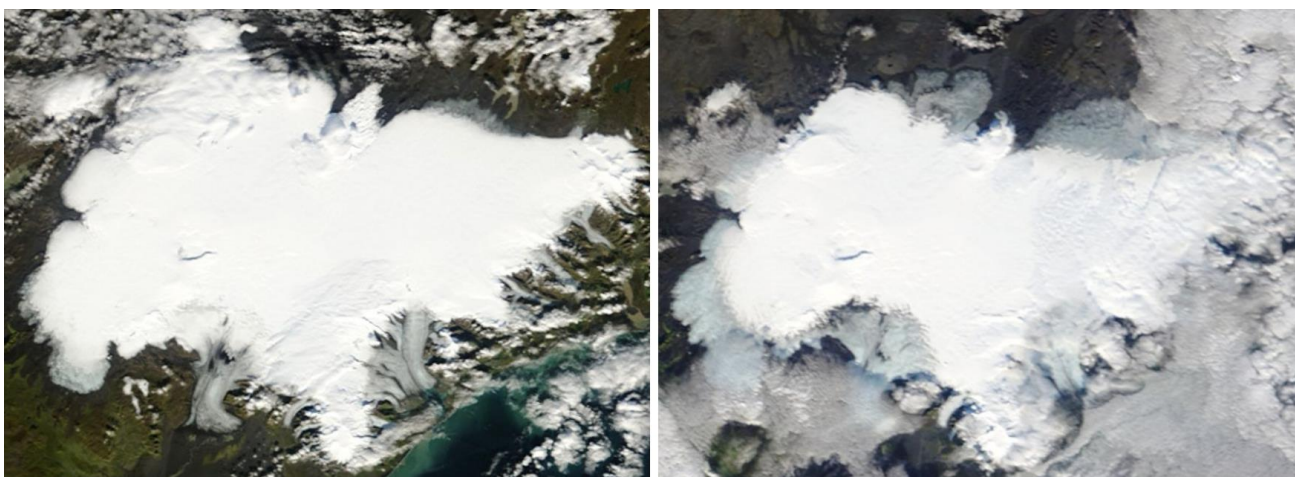
Location of GPS surface profiles 2017. Profiles surveyed in March, May and June shown in RED and surveyed in October and December in BLUE.

Appendix G: MODIS satellite images of Vatnajökull and vicinity 2016-2017.

The images are either from the MODIS Aqua or MODIS Terra satellites, visible light, 250 m resolution.

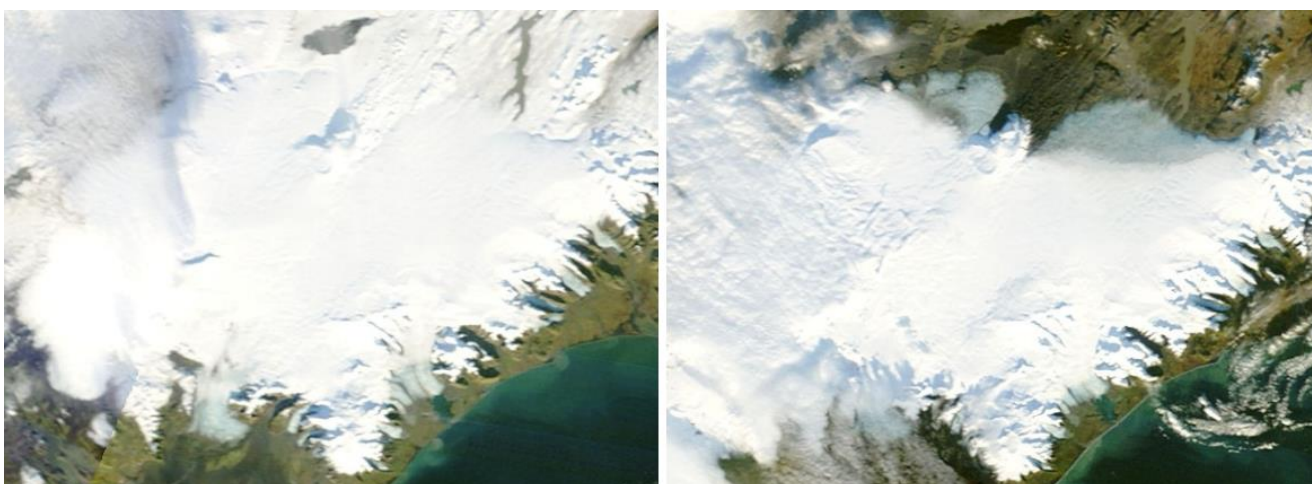
<http://rapidfire.sci.gsfc.nasa.gov/>

The Moderate Resolution Imaging Spectroradiometer (MODIS) flies onboard NASA's Aqua and Terra satellites as part of the NASA-centered international Earth Observing System. Both satellites orbit the Earth from pole to pole, seeing most of the globe every day. Onboard Terra, MODIS sees the Earth during the morning, while Aqua MODIS orbits the Earth in the afternoon.



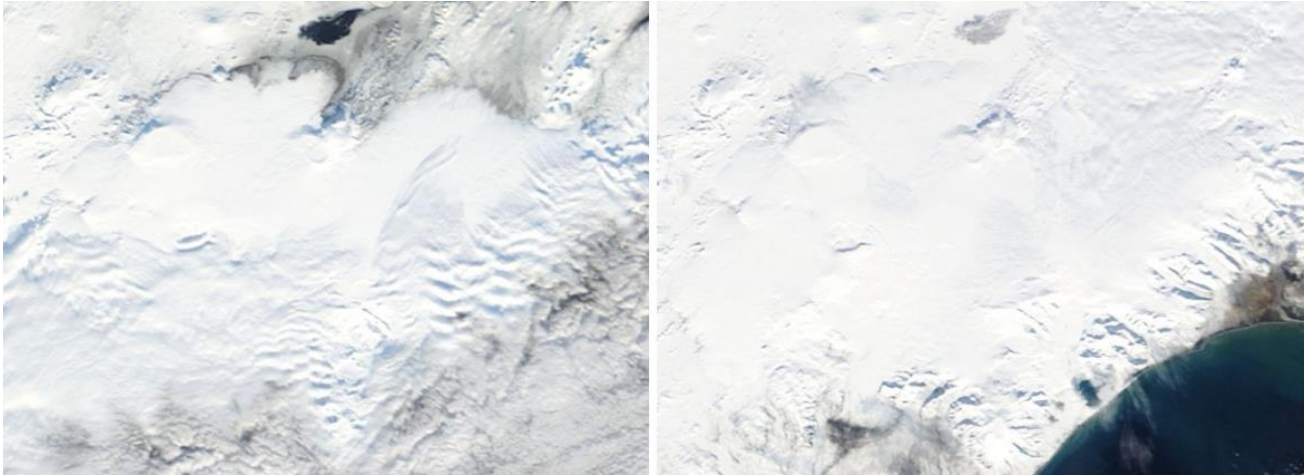
Left: September 26th, 2016. Since September 3rd there has been snowfall above ~800 m a.s.l..

Right: October 15th, 2016. Most of the autumn snow has melted from ablation zone of all visible outlets. When the image was acquired the summer balance expedition to glacier was ongoing. Autumn snow up to 2 m (at Háabunga) was measured in the accumulation zone, but bare ice in most of the ablation zone.

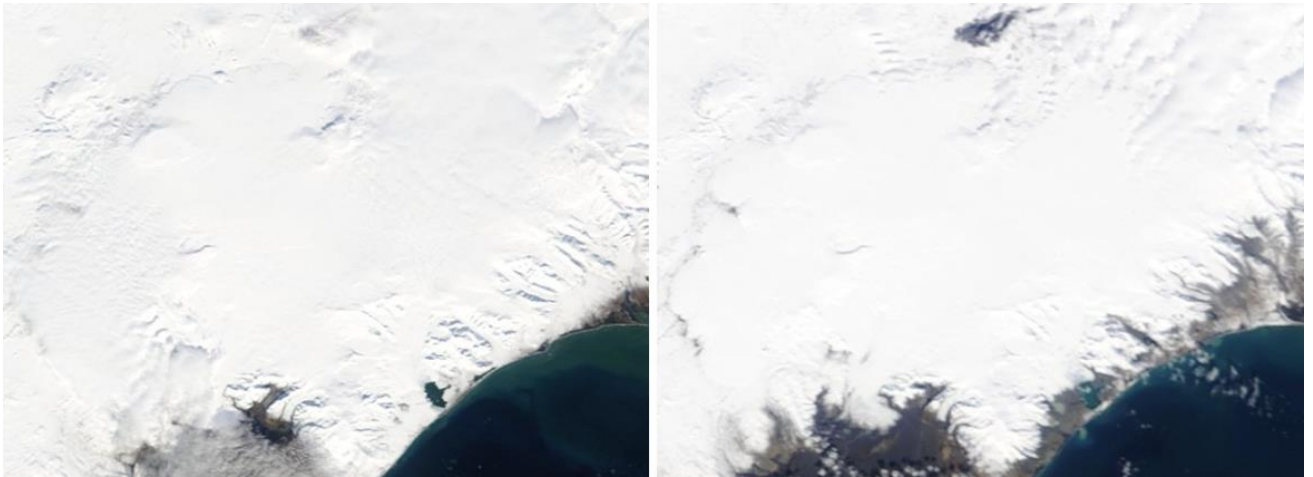


Left: November 5th 2016. Finally snow covers all of Vatnajökull except the lower areas of the SE-outlets.

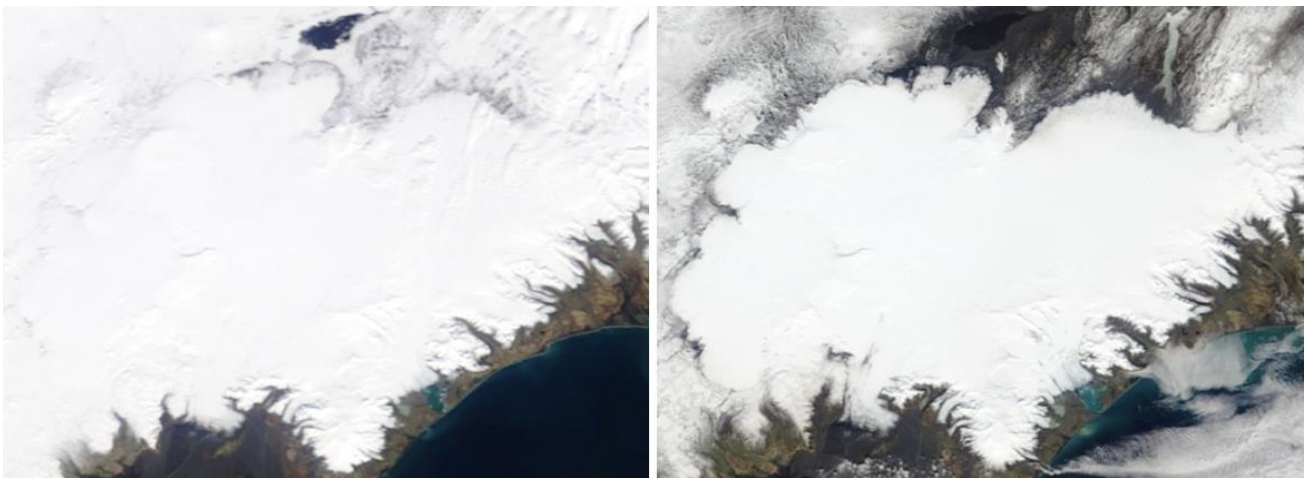
Right: November 10th. Snow in the ablation zone of the northern outlets and north highland has melted!; the autumn was extremely mild.



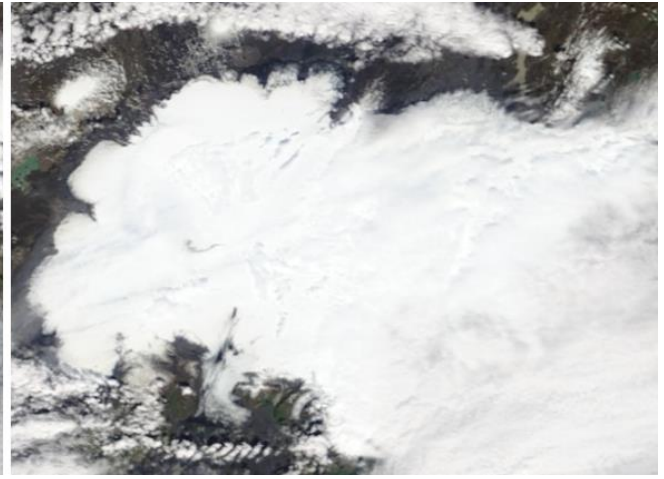
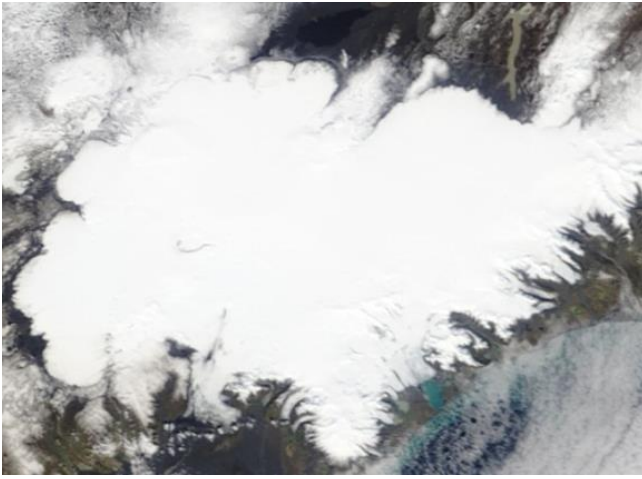
February 13th and March 3rd left and right respectively, height of winter. The snow cover of the south lowland and north highland is very thin, almost nothing in February.



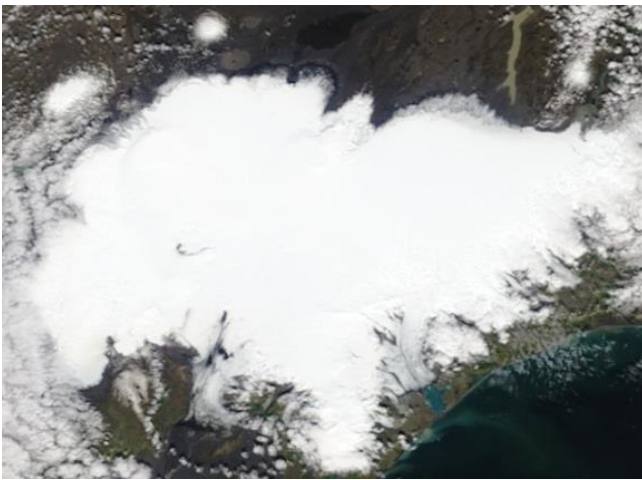
Left: March 21th, and April 16th. Not much has visibly changed since the first week of March.



*Left: May 21st. Melting has started.
Right: May 8th. Start of summer, most of the snow has melted in the western and northern highland, Hágöngulón is still frozen over.*



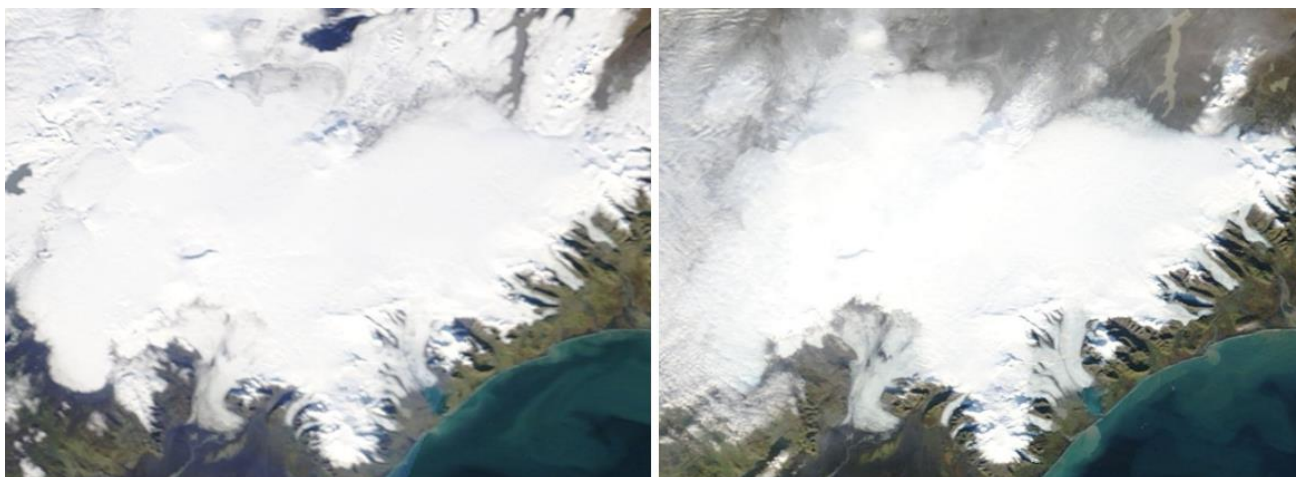
*Left: May 21st, not much has changed, the warm start of spring is halted. .
Right: June 14th. The snowline is still not visible on all outlet, June was neither warm or sunny.*



*Left: June 27th, slight change from the 14th, summer is stalling.
Right: July 24th. The snowline has migrating upwards all visible outlets. The thin snow on the snout of the northern outlets has melted, snowline is rising on all visible outlets. Some dust (brownish surface) is visible in areas just above the snowline.*



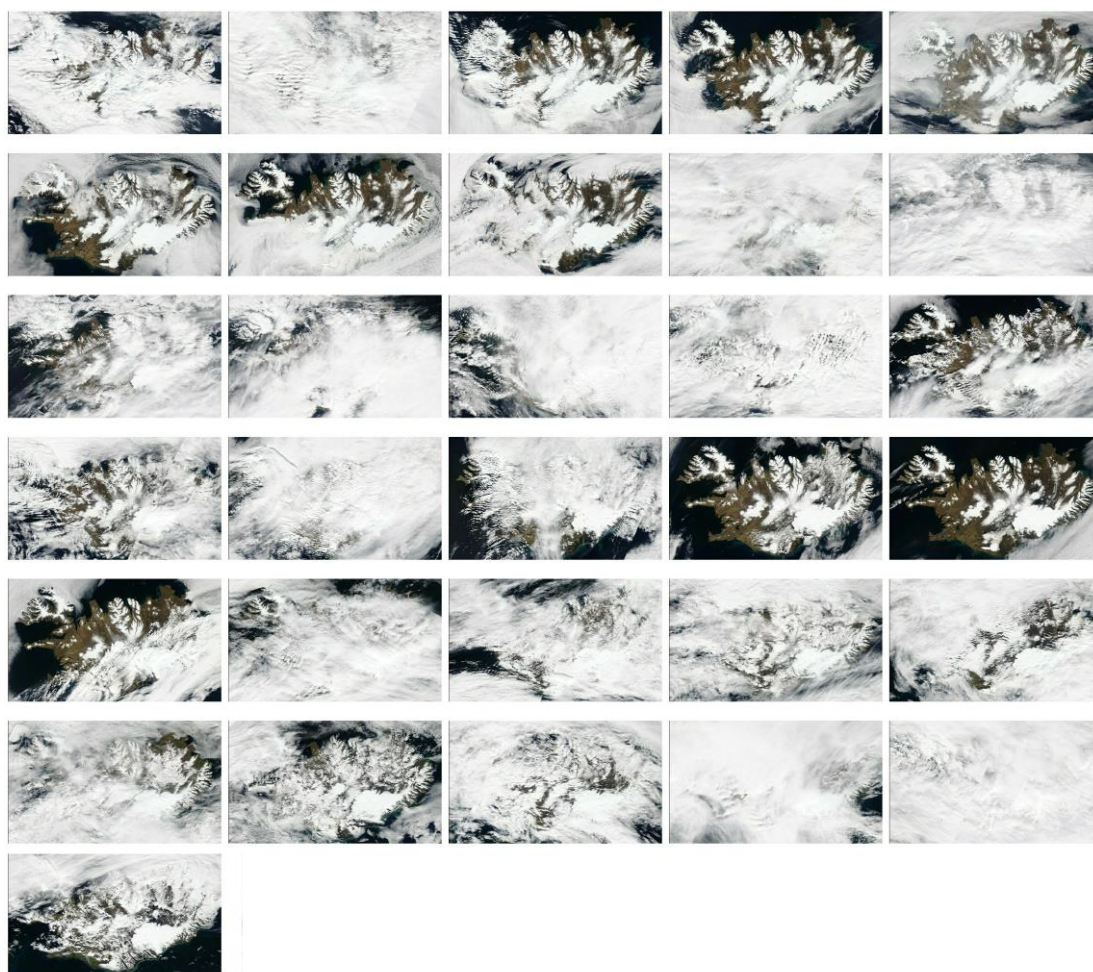
*Left: August 3rd. Snowline still rapidly migrating upward, it is high summer, and last week of July was extremely warm and sunny.
Right: August 30th, summer condition continue, still rapid meting upward and migration of the snowline.*



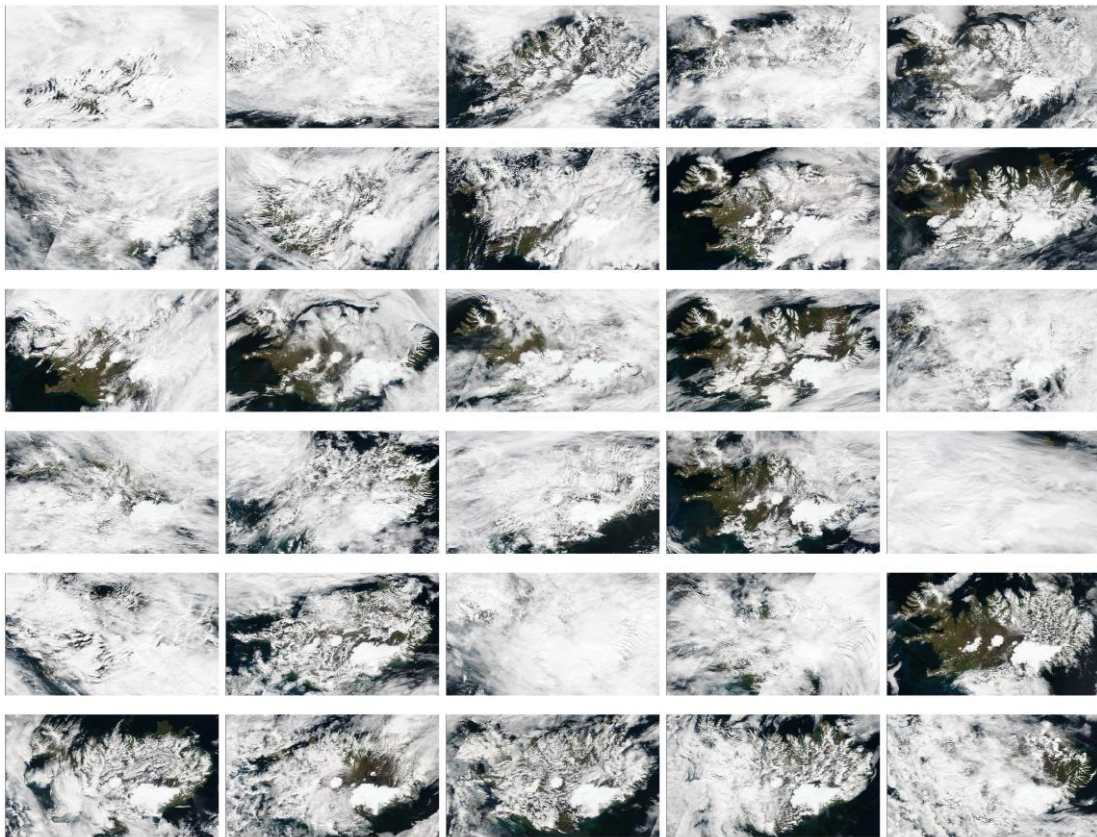
Left: October 16th. First snow below ~1000 m .

Right: October 26th. The autumn expedition people are on the glacier. Most of the autumn snow has melted from ablation zone of all visible outlets, and Tungnaárjökull and were bare ice in the ablation zone, and the ablation zone of Brúarjökull was impassable due to slush . Autumn snow up to 1.3 m (at Breiðabunga) was measured in the accumulation zone, but bare ice in most of the ablation zone.

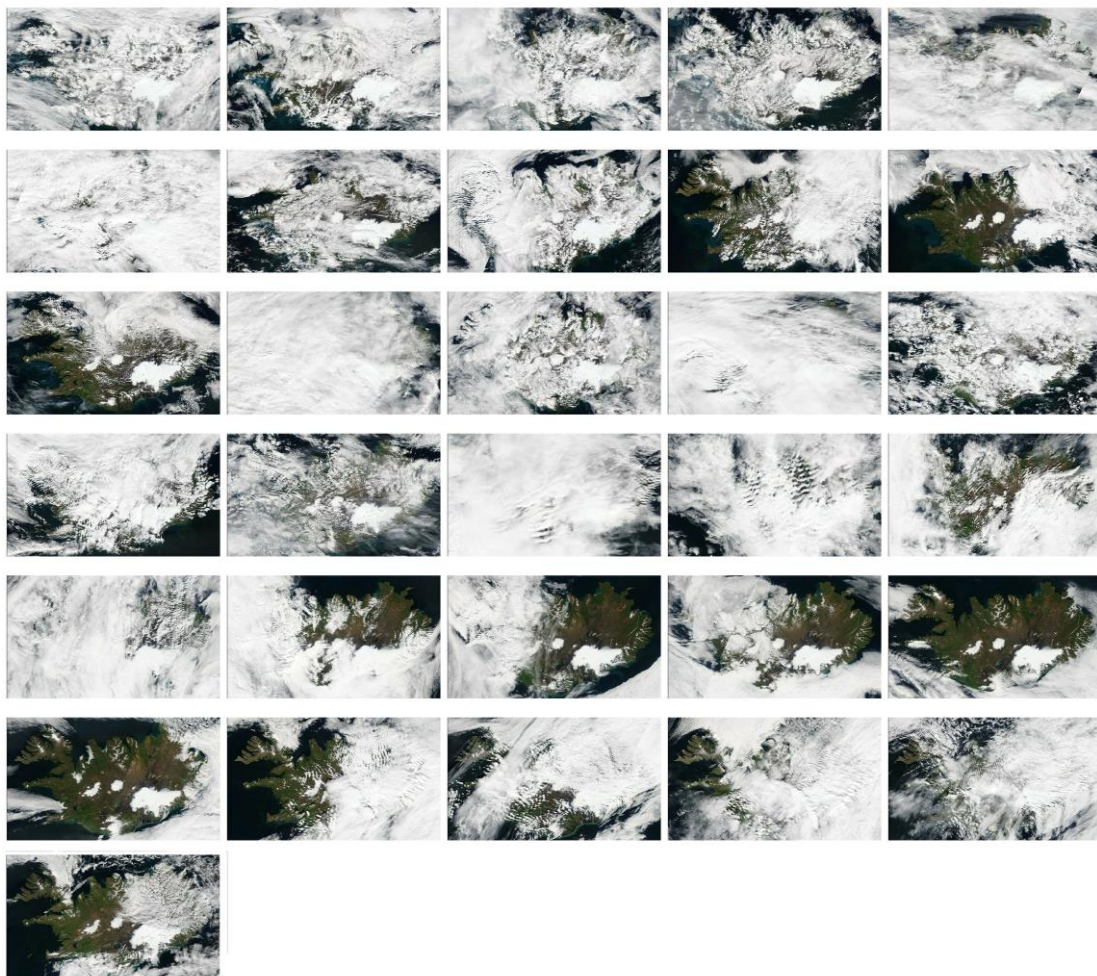
On the next pages MODIS images for all days of May, June, July, August and September 2017 are shown in 1km resolution.



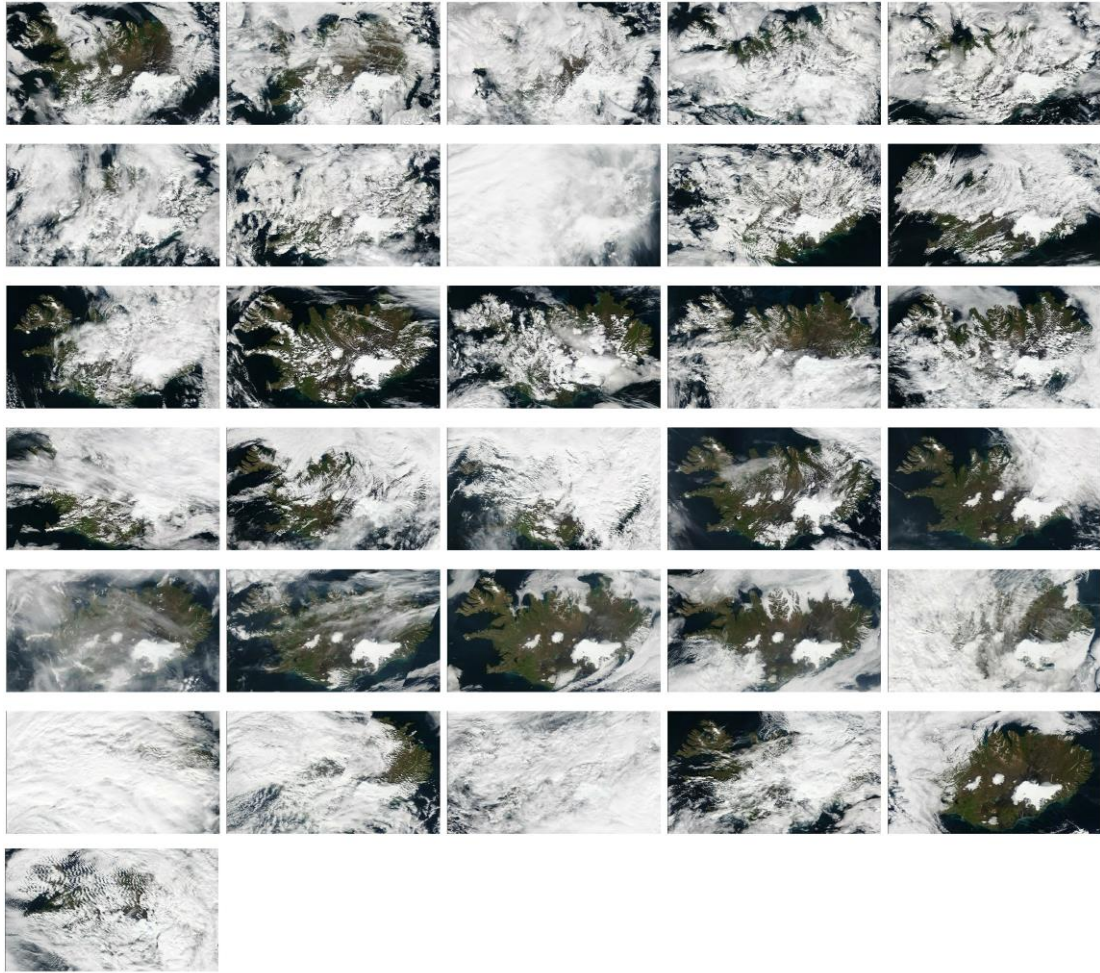
MODIS: May 2017 (read from left to right and downwards).



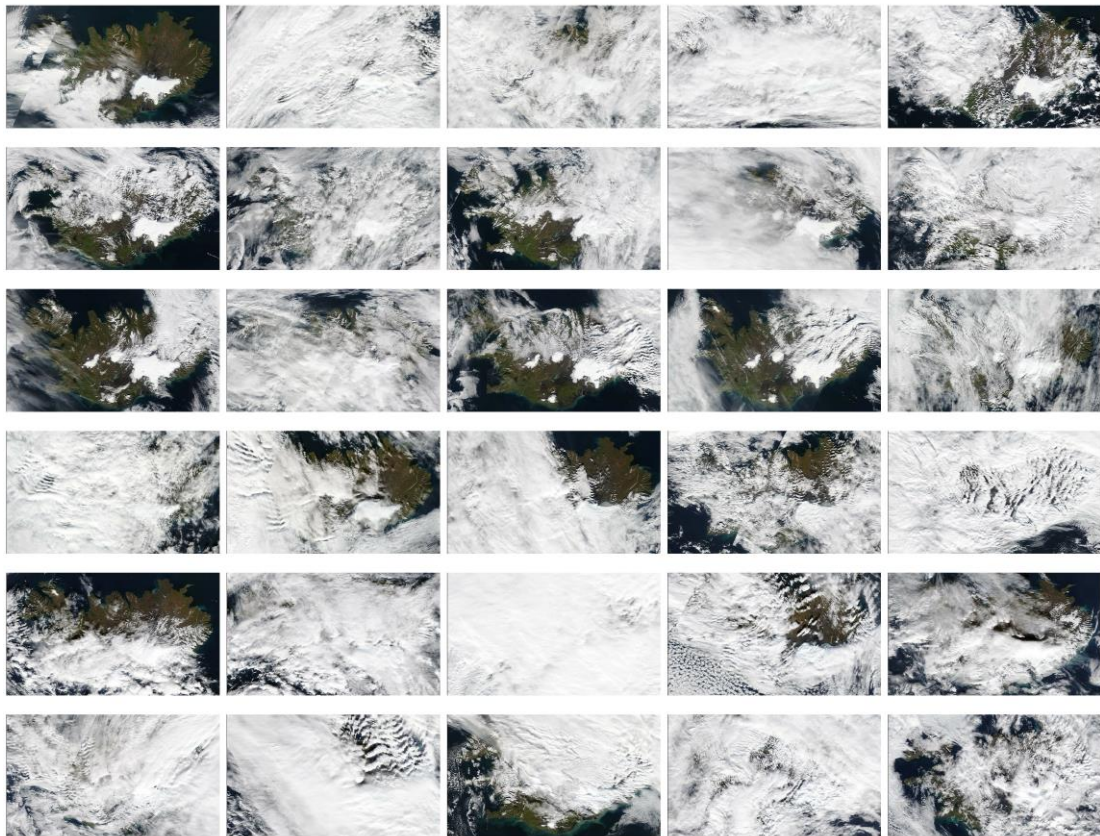
MODIS: June 2017 (read from left to right and downwards).



MODIS: July 2017 (read from left to right and downwards).



MODIS: August 2017 (read from left to right and downwards).



MODIS: September 2017 (read from left to right and downwards).